Annex 1

# Cashew Nut Shells Pyrolysis: Individual Gas Evolution Rates and Yields

***Tsamba, A. J.***, *Yang, W., Blasiak, W. and Wójtowicz, M.A.*

Published in
*Energy & Fuels* **2007**, *21*, 2357-2362


Royal Institute of Technology

School of Industrial Management and Engineering

Department of Materials Science and Engineering

Division of Energy and Furnace Technology

Brinellvägen 23

SE-100 44 Stockholm

SWEDEN

# Cashew Nut Shells Pyrolysis: Individual Gas Evolution Rates and Yields

A. J. Tsamba,*,† W. Yang,† W. Blasiak,† and M. A. Wójtowicz‡

*Division of Energy and Furnace Technology, Department of Materials Science and Engineering, School of Industrial Management and Engineering, Royal Institute of Technology, Brinellvägen 23, SE-100 44 Stockholm, Sweden, and Advanced Fuel Research, Inc., 87 Church Street, East Hartford, Connecticut 06108-3728*

*Received September 27, 2006. Revised Manuscript Received March 29, 2007*

Cashew nut shells are one type of the most abundant biomass tropical wastes, which can be used for energy generation. However, there is lack of data for the thermal conversion process of cashew nut shells such as pyrolysis individual gas products, yields, and reaction kinetics. In this research work, the pyrolysis processes of cashew nut shells at low heating rates (10, 30, and 100 K/min) were studied. Thermogravimetric analyzer coupled with a Fourier transform infrared spectrometer (TG-FTIR) was used. The pyrolysis product yields obtained were compared with the available data in the literature for wood and *Miscanthus Giganteus*. It was found that cashew nut shells have tars and volatiles at levels equivalent to those of wood pellets, both above the tar and volatile content of *M. Giganteus*. Further, kinetic parameters were obtained from the TG-FTIR results using an approach based on parallel independent first-order reactions with a Gaussian distribution of activation energies and following the $T_{max}$ method. The data obtained through this approach included the identification, kinetics, and yield of each gas product precursor. These results are then used as input files for a distributed activation energy model (DAEM) for biomass pyrolysis, based on a functional group analysis, which still does not include the devolatilization, cross-linking competitive reactions. The predicted evaluation data from this model were found to generally agree with that from TG-FTIR analysis. However, the model still demands improvement to accommodate secondary and cross-linking competitive reactions.

## Introduction

Renewable energy has been, for the last three decades, the main focus in energy research in the search of cleaner energy alternatives to support a sustainable development and cleaner environment. Cashew nut shells (CNS), found in a number of tropical countries, are biomass wastes and, as such, they constitute a great potential of renewable source for energy production.

Nonetheless, they are still poorly studied as such, especially regarding their intrinsic kinetics, whose role in thermochemical conversion processes for energy generation is of utmost importance. In fact, in his outstanding review on biomass studies, Yaman[1] presents about two hundred articles in biomass research studies and none of them is on CNS. A limited number of researchers that have dedicated their investigation to these biomasses are just a rare exception. Raveendran et al.[2] studied 14 different biomass samples in which CNS are included. However, not too much attention was given to this particular feedstock. In addition, Hoque and Battacharya[3] studied just the coconut shells gasification product (fuel) from fluidized and spouted bed gasifiers. In both studies, the only specific characteristics that are given are proximate and/or ultimate analysis.

To contribute to filling this gap, comprehensive research on intrinsic kinetics, profiles, and yields of tropical biomass thermal degradation has been in progress. Such research has already contributed to generate data on global kinetics of CNS and coconut shells pyrolysis.[4] The main focus of the present study is on the individual evolved gas species characterization.

Hence, the study reported in this article aimed at (i) determining the pyrolysis profiles and yields of the volatiles evolving from a non-isothermal pyrolysis of CNS, (ii) performing kinetic analysis, and (iii) generating heating rate independent kinetics input data files to be used for modeling the CNS pyrolysis.

In this work, pyrolysis of CNS at low heating rates (10, 30, and 100 K/min) was studied. A thermogravimetric analyzer coupled with Fourier transform infrared spectrometer (TG-FTIR) was used. It was assumed that each of the resulting evolution peaks is associated with the presence of the respective precursor in the original biomass sample (pool). Through the TG-FTIR system it was possible to determine the size (yield) of the pools for all the identified gas species. The shifts in the peak position were used to generate the kinetics of each devolatilization reaction associated with the evolution of all the species tracked through the peaks identification.

A similar approach has been successfully applied in different research works with coal as well as with biomass samples[5−7] with analogous objectives.

* Corresponding author. Fax: +46 8 207 681. Tel.: +46 8 790 6545 or (08) 205 204. E-mail: ajtsamba@zebra.uem.mz.
† Royal Institute of Technology.
‡ Advanced Fuel Research, Inc.

(1) Yaman, S. *Energy Convers. Manage.* **2004**, *45*, 651−71.
(2) Raveendran, K.; Ganesh, A.; Khilar, K. *Fuel* **1995**, *75*, 987−98.
(3) Hoque, M. M.; Battacharya, S. C. *Energy* **2001**, *26*, 101−10.
(4) Tsamba, A. J.; Yang, W.; Blasiak, W. *Fuel Process. Technol.* **2006**, *87-6*, 523−30.
(5) Bassilakis, R.; Carangelo, R. M.; Wójtowicz, M. A. *Fuel* **2001**, *80*, 1765−86.

10.1021/ef0604792 CCC: $37.00 
Published on Web 06/01/2007

## Methodology

**Experimental Setup.** Experimental tests were performed in a TG-FTIR system developed at Advanced Fuel Research, Inc. (AFR), for the study of the low heating rate pyrolysis of coal, which has also been successfully used with other kinds of feedstock. The setup, illustrated schematically in Figure 1, consists of a sample holder suspended from a balance in a gas stream within a furnace. As the sample is heated, the evolving volatile products are carried out of the furnace directly into a 5.1 cm diameter gas cell (heated to 428 K) where the volatiles are analyzed by the FTIR spectrometer.

The FTIR spectra are obtained every 30−40 s to determine quantitatively the evolution rate and composition of several compounds. The system allows the sample to be heated on a preprogrammed temperature profile, at heating rate intervals of 3−100 K/min, within 293 and 1373 K. The system continuously monitors: (i) the time-dependent evolution of volatile species; (ii) the heavy liquid (tar) evolution rate and its infrared spectrum with identifiable bands from functional groups; and (iii) weight of the nonvolatile material (residue). Further explanation on TG-FTIR as well as the species identification can be found in Bassilakis et al.[2]

In the experiments carried out in this research, helium carrier gas was passed through the oxygen trap to ensure an oxygen-free atmosphere during pyrolysis. The initial sample weight was 64−78 mg, and the flow rate of the carrier gas was 400 mL/min.

For each analysis, the sample material was heated in helium at 30 K/min, first from ambient temperature to 333 K for sample drying, and kept at this temperature for 30 min. The sample was then heated again to 1173 K, for thermal degradation or pyrolysis. Upon reaching 1173 K and holding the temperature for 3 min, the sample was immediately cooled to about 523 K in a 20 min period. After cooling, the helium flow was switched to a mixture of 21% $O_2$ and 79% He (simulating the atmospheric air composition), and the temperature was ramped to 1173 K at 30 K/min to combust the remaining char. Concentrations of all volatile species, except for tar, were determined using quantification routines obtained from calibration runs performed with pure compounds.

The volatile pyrolysis product species identified in this study are (i) carbon monoxide (CO); (ii) carbon dioxide ($CO_2$); (iii) tar (by difference using gravimetric data); (iv) water ($H_2O$); (v) methane ($CH_4$); (vi) ethylene ($C_2H_4$); (vii) formaldehyde ($CH_2O$); (viii) formic acid (HCOOH); (ix) carbon sulfide (COS); (x) acetic acid ($H_3CCOOH$); (xi) methanol ($CH_3OH$); (xii) ammonia ($NH_3$); (xiii) hydrogen cyanide (HCN); (xiv) isocyanic acid (HCNO); (xv) acetone ($H_3COCH_3$); (xvi) phenol ($C_6H_5OH$); and (xvii) acetaldehyde ($H_3CCHO$). Tar evolution patterns and yields were determined by difference, using the sum of gases quantified by FTIR and the balance curve obtained thermogravimetrically.

It is important to acknowledge that determining the tar yield by difference implies that all potential pyrolysis gas and condensing product species which cannot be identified by the FTIR will be integrated as being part of the tars. This is the case of some diatomic molecules, with special emphasis on hydrogen, which are not recognizable through FTIR and, for that reason, are included as tars in this method. But, as the main diatomic species expected to be part of biomass pyrolysis gas products is hydrogen, which is a lightweight molecule, its influence on tar and overall yields is assumed to be negligible in mass-based composition.

**Samples.** The biomass samples used in this study are CNS from *Annacardium Occidentale L.* The samples were obtained from a cashew nut processing plant where they are produced as waste from the main process. According to the processing stages, they might have already been roasted at about 400−470 K.

For testing purposes, the CNS used in these experiments were ground in a blender into a paste with reasonably consistent uniformity, although particles of about 1−3 mm size could still be found in the paste. The characteristics of this particular feedstock are given by the ultimate and proximate analysis provided in Table 1.

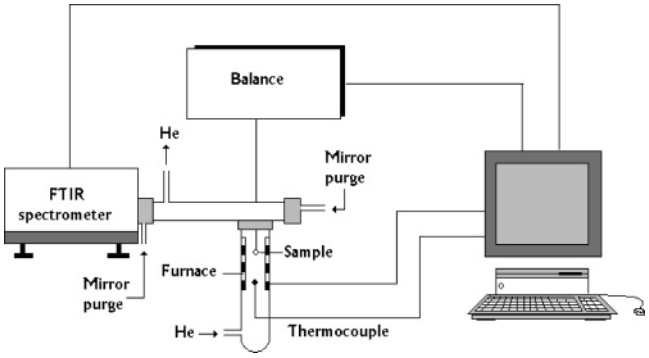


**Figure 1.** Schematic diagram of the TG-FTIR system.

**Table 1. Ultimate and Proximate Analysis of CNS (by BELAB AB-Sweden)**

| characteristic | unit | dry basis | dry, ash-free basis |
|---|---|---|---|
| ash | % (w/w) | 1.9 | |
| volatile matter | % (w/w) | 81.8 | 83.4 |
| fixed carbon | % (w/w) | 16.3 | 16.6 |
| C | % (w/w) | 58.3 | 59.45 |
| H | % (w/w) | 7.0 | 7.1 |
| N | % (w/w) | 0.7 | 0.7 |
| S | % (w/w) | 0.07 | 0.07 |
| Cl | % (w/w) | 0.02 | 0.02 |
| O | % (w/w) | 32.02 | 32.64 |
| LHV | MJ/kg | 22.539 | 22.975 |
| HHV | | 24.051 | 24.517 |

**Pyrolysis Intrinsic Kinetics Analysis.** In this study, it is implicitly assumed that the reaction rates to be determined follow a parallel-first-order independent kinetics mechanism, which is a reasonable starting assumption for biomass.[1] This means that each volatile species can evolve as one or more time/temperature resolved peak(s), independently. Each one of these evolution peaks is associated with the existence of respective precursor material in the original biomass sample, known as pool. Additionally, the shifts in shape and position of the peak as a function of the heating rate provides information on the intrinsic kinetics of the pyrolysis associated with a given peak. A Gaussian distribution of activation energies is assumed, with the mean value $E_0$ and the width of the distribution function $\sigma$, for each peak.

The mathematical description of the above-mentioned theory is summarized below.

For a single reaction $i$, the following expression is then written

$$\frac{dV_i}{dt} = k_i(V_i^* - V_i) \quad (1)$$

where $V_i$ is the amount of volatile matter evolved, $V_i^*$ is the volatile-matter content (at infinite time), $t$ is time, and $k_i$ is the reaction-rate constant, defined as

$$k_i = A_i \exp[-E_i/(RT(t))] \quad (2)$$

In this equation, $A$ is the pre-exponential factor, $E$ is the activation energy, $T(t)$ is temperature in kelvin, and $R$ is the gas constant. It should be noted that at constant heating rates, the temperature is time-dependent through the expression $T(t) = T_0 + \beta T$, in which $T_0$ is the initial temperature and $\beta$ is the heating rate.

Integrating over time and over all reactions with different activation energies and using the Arrhenius kinetics for $k_i$ indicated

(6) De Jong, W.; Pirone, A.; Wójtowicz, M. A. *Fuel* **2003**, *82*, 1139−47.

(7) Holstein, A.; Bassilakis, R.; Wójtowicz, M. A.; Serio, M. A. *Proc. Combust. Inst.* **2005**, *30*, 2177−85.

**Table 2. Pyrolysis Yields of CNS Compared with Those of *M. giganteus* (MG) and Wood Pellets (WP), All in a Dry-Ash-Free Basis[3]**

| | | 10 K/min heating rate | | | 30 K/min heating rate | | | 100 K/min heating rate | | |
|---|---|---|---|---|---|---|---|---|---|---|
| sample | | WP | MG | CNS | WP | MG | CNS | WP | MG | CNS |
| volatiles (TG) | | 86.20 | 80.20 | 82.21 | 86.20 | 79.40 | 83.16 | 86.20 | 81.90 | 83.69 |
| char | | 13.80 | 19.80 | 17.79 | 13.80 | 20.60 | 16.84 | 13.80 | 18.10 | 16.31 |
| tar | | 37.20 | 18.10 | 34.00 | 38.80 | 21.90 | 39.00 | 48.40 | 28.30 | 37.88 |
| methane | $CH_4$ | 1.27 | 1.18 | 3.24 | 1.30 | 1.14 | 2.34 | 1.15 | 1.16 | 1.93 |
| pyr−water | $H_2O$ | 10.60 | 17.70 | 22.09 | 16.00 | 18.50 | 20.31 | 13.60 | 20.60 | 16.33 |
| carbon monoxide | CO | 7.48 | 8.55 | 3.05 | 6.77 | 7.15 | 2.43 | 5.10 | 5.56 | 2.75 |
| carbon dioxide | $CO_2$ | 5.90 | 10.40 | 12.27 | 5.08 | 9.43 | 12.12 | 4.88 | 9.11 | 18.92 |
| ethylene | $CH_2CH_2$ | 0.15 | 0.52 | 0.14 | 0.23 | 0.27 | 0.13 | 0.09 | 0.13 | 0.13 |
| hydrogen cyanide | HCN | 0.09 | 0.22 | 0.13 | 0.09 | 0.14 | 0.08 | 0.05 | 0.11 | 0.09 |
| ammonia | $NH_3$ | 0.00 | 0.13 | 0.09 | 0.02 | 0.10 | 0.11 | 0.03 | 0.11 | 0.06 |
| isocyanic acid | HCNO | 0.11 | 0.20 | 0.03 | 0.02 | 0.11 | 0.03 | 0.05 | 0.07 | 0.02 |
| formaldehyde | $CH_2O$ | 3.66 | 1.12 | 0.48 | 2.93 | 1.12 | 0.18 | 3.15 | 1.16 | 0.20 |
| acetaldehyde | $CH_3CHO$ | 9.28 | 10.20 | 2.18 | 8.11 | 9.02 | 2.35 | 3.97 | 7.70 | 1.98 |
| methanol | $CH_3OH$ | 0.98 | 1.42 | 0.52 | 0.74 | 1.13 | 0.47 | 0.64 | 1.07 | 0.49 |
| formic acid | HCOOH | 2.68 | 2.12 | 0.26 | 1.73 | 1.66 | 0.16 | 0.82 | 0.37 | 0.23 |
| acetic acid | $H_3CCOOH$ | 2.78 | 4.24 | 1.92 | 2.37 | 3.59 | 1.99 | 2.28 | 3.35 | 1.76 |
| carbonyl sulfide | COS | 0.18 | 0.31 | 0.00 | 0.11 | 0.16 | 0.04 | 0.00 | 0.11 | 0.02 |
| phenol | $C_6H_5OH$ | 1.46 | 2.31 | 0.84 | 0.65 | 1.83 | 0.88 | 0.73 | 1.99 | 0.50 |
| acetone | $H_3COCH_3$ | 2.05 | 1.80 | 0.59 | 2.15 | 1.86 | 0.53 | 1.63 | 2.10 | 0.43 |

in eq 2 and a Gaussian distribution of activation energies, the following expression is obtained:

$$\frac{V^* - V}{V^*} = \frac{1}{\sigma\sqrt{2\pi}}\int_0^\infty \exp\left[-A\int_{t_0}^{t}\exp\left(-\frac{E}{RT(t)}\right)\mathrm{d}t - \frac{(E-E_0)^2}{2\sigma^2}\right]\mathrm{d}E \quad (3)$$

This derivation is discussed in detail by Anthony et al.[8]

While isothermal techniques are useful to determine kinetic parameters, their implementation is time-consuming. Unlike isothermal techniques, non-isothermal techniques provide faster means for obtaining the same kinetic information. The most common non-isothermal technique is the so-called Friedman method,[9] where the logarithm of the rate constant, *k*, is plotted at each point as a function of the inverse temperature. The rate constant, *k*, is calculated from the equation

$$\frac{\mathrm{d}w}{\mathrm{d}t} = k(w^* - w) \quad (4)$$

where $w$ is the sample mass at time $t$ and $w^*$ is the final sample mass.

Plotting $\ln(k)$ versus $1/T$, from the Arrhenius expression in eq 2, the parameters $A$ and $E$ can be determined from the linear region(s) of the plot. A drawback of this method is that it introduces a bias in the values of $A$ and $E$ when the reaction has a distribution of activation energies.[10] In such a case, the Friedman method is not able to differentiate between the effect of the distribution and the effect of the magnitude of the mean activation energy and gives an erroneous value for $E_0$. This value is usually lower than the "true" value.[7]

One of the non-isothermal methods for the determination of kinetic parameters is through the measurement of the temperature at which the devolatilization rate is the maximum ($T_{max}$). As commonly found, in a typical sequence of experiments, thermal-decomposition rates are measured at different heating rates. Thus, the relationship between the heating rate $\beta$ and the value of $T_{max}$ is given by the following equation:

$$\ln\left(\frac{\beta}{T_{max}^2}\right) = \ln\left(\frac{AR}{E_0}\right) - \frac{E_0}{RT_{max}} \quad (5)$$

Equation 5 is the formula used for the determination of the kinetic parameters $A$ and $E_0$.[11] While the value of $E_0$ is accurately determined even for wide distributions, the value of $A$ usually requires a slight adjustment (typically within a factor of 2).[7] The width of the assumed Gaussian distribution, $\sigma$, can then be determined from the width of the peak representing the rate of species evolution (or weight loss). In the $T_{max}$ method, some difficulties arise when peaks are not well resolved. In such cases, substantial shifts in $T_{max}$ may occur. However, unless peak deconvolution is attempted,[12] the same problem arises when using the Friedman method. Another limitation is associated with the presence of small, multiple maxima superimposed on a broader peak, that is, when the assumption of first-order kinetics is not fully supported. In this case, again, the applicability of both the $T_{max}$ and the Friedman methods is reduced. The exact value of $T_{max}$ may also be difficult to determine for large and wide peaks.

Once the $A$ and $E_0$ values are determined, the sizes of the precursor pools for individual species and $\sigma$ are determined by adjusting the simulated peak heights so that they best fit the TG-FTIR data.

At the end of the above procedure and for the evolution of each precursor pool (peak), $A$, $E_0$, $\sigma$, and the pool size, that is, the concentrations of the precursor species, are determined. In general, each volatile species (light gases, tars, etc.) may evolve as one or more peaks, and accordingly, a single or multiple precursor pools are used in the simulations.

The above-described $T_{max}$ method is often difficult to utilize as the limited data resolution. Especially at 100 K/min, it causes significant uncertainty in $T_{max}$ determination. Another reason to be considered as constraining the determination of $T_{max}$ is the size of the sample, which definitely plays an important role in mass and heat transfer between the sample surface and its core. For this reason, it is sometimes advantageous to fit $A$, $E_0$, and $\sigma$ values to experimental data using a trial-and-error approach. Non-unique solutions are usually found as a result of the fitting exercise, which is due to the so-called *compensation* effect. In other words, different pairs of kinetic parameters ($A$, $E_0$) provide equally good fits to experimental data. For this reason, the values of pre-exponential factors are often fixed and selected in such a manner that they are consistent with the transition-state theory ($A \approx 10^{11}-10^{16}$ s$^{-1}$).[13]

(8) Anthony, D. B.; Howard, J. B.; Hottel, H. C.; Meissner, H. P. *Proceedings of the 15th Symposium (Int) on Combustion*; The Combustion Institute: Pittsburgh, 1975; pp 1303−17.

(9) Friedman, H. L. *J. Polym. Sci., Part C* **1963**, *6*, 183−192.

(10) Braun, R. L.; Burnham, A. K. *Energy Fuels* **1987**, *1*, 153−61.

(11) Teng, H.; Serio, M. A.; Wójtowicz, M. A.; Bassilakis, R.; Solomon, P. R. *Ind. Eng. Chem. Res.* **1995**, *34*, 3102−11.

(12) Kim, S.; Park, J. K.; Chun, H. D. *J. Environ. Eng.* **1968** (*July*), 507.

**Table 3. Kinetic Parameters and Precursor-Pool Sizes (Yields) in Pyrolysis of CNS (with $A = 2.2 \times 10^{13}$ s$^{-1}$)**

| species | pool no. | yield (% (w/w) daf) | $E_0/R$ ($10^4$ K) | $\sigma/R$ (K) |
|---|---|---|---|---|
| carbon monoxide | 1 | 0.430 | 2.01 | 390 |
| | 2 | 1.080 | 2.25 | 520 |
| | 3 | 1.230 | 2.73 | 2300 |
| carbon dioxide | 1 | 2.600 | 1.74 | 450 |
| | 2 | 5.200 | 1.92 | 1280 |
| | 3 | 3.700 | 2.26 | 600 |
| | 4 | 2.900 | 2.61 | 2500 |
| tars | 1 | 31.000 | 1.99 | 600 |
| | 2 | 6.300 | 2.28 | 100 |
| water | 1 | 3.870 | 1.50 | 1000 |
| | 2 | 6.050 | 1.98 | 1500 |
| | 3 | 5.000 | 2.26 | 500 |
| | 4 | 4.650 | 2.60 | 3500 |
| methane | 1 | 0.280 | 2.08 | 1980 |
| | 2 | 2.220 | 3.02 | 2800 |
| ethylene | 1 | 0.134 | 2.77 | 2200 |
| phenol | 1 | 0.120 | 2.05 | 800 |
| | 2 | 0.618 | 2.74 | 3900 |
| acetone | 1 | 0.515 | 2.17 | 1800 |
| methanol | 1 | 0.490 | 1.87 | 500 |
| hydrogen cyanide | 1 | 0.089 | 2.23 | 4200 |
| ammonia | 1 | 0.004 | 1.58 | 1100 |
| | 2 | 0.007 | 2.18 | 100 |
| | 3 | 0.060 | 2.42 | 2800 |
| | 4 | 0.030 | 3.39 | 2400 |
| formaldehyde | 1 | 0.288 | 2.08 | 1200 |
| formic acid | 1 | 0.216 | 2.20 | 1000 |
| acetic acid | 1 | 1.100 | 2.05 | 600 |
| | 2 | 0.918 | 2.28 | 400 |
| acetaldehyde | 1 | 0.470 | 2.09 | 1 |
| | 2 | 1.700 | 2.27 | 200 |
| isocyanic acid | 1 | 0.028 | 2.55 | 2200 |

In most cases, a value of $A = 2.2 \times 10^{13}$ s$^{-1}$ is assumed to be adequate. This is the approach used in this study.

## Results and Discussion

**Experimental Yields.** Yields of pyrolysis products determined through TG-FTIR experiments are shown in Table 2, in which a summary of the weight loss and gas yields for all the runs are given. From these TG-FTIR yields, a good mass balance closure is noticeable. The volatile matter data are generally consistent with the values reported in Table 1, and char-yield variation with the heating rate is observed and decreases as the heating rates increases. Under the experimental conditions used in this work, tar yields were found to be in the range 34−39 wt % in a dry-ash-free (daf) basis, and the yield of pyrolytic water was 16−20 wt % daf. Relatively high yields of acetaldehyde (2.0−2.4 wt % daf) and acetic acid (1.8−2.3 wt % daf) were observed at all heating rates.

Comparing the yields from the three samples presented in Table 2, it was found that CNS are richer in (i) volatiles and tars than *Miscanthus Giganteus* (however, they are still poorer compared to wood pellets yields for both products); (ii) tars and N-species compared to wood pellets; and (iii) noncombustible gases such as $CO_2$, $NH_3$, and pyrolytic water. Regarding methane, CNS are the richest among the three samples.

(13) Benson, S. W. *Thermochemical Kinetics*; John Wiley & Sons: New York, 1968.

**Table 4. Relative Deviation between TG-FTIR Yields and Model-Predicted Yields**

| pyrolysis product species | 10 K/min, $\epsilon_i$, % | 30 K/min, $\epsilon_i$, % | 100 K/min, $\epsilon_i$, % |
|---|---|---|---|
| carbon monoxide | −11.66 | +11.52 | −0.26 |
| carbon dioxide | +14.77 | +15.81 | −31.50 |
| tars | +8.88 | −4.67 | −1.30 |
| water | −12.91 | −3.77 | +16.15 |
| methane | −29.44 | +6.52 | +20.74 |
| ethylene | −7.46 | +1.49 | +5.22 |
| phenol | −13.41 | −21.53 | +27.95 |
| acetone | −13.98 | −2.91 | +17.28 |
| methanol | −5.92 | +3.67 | +0.41 |
| hydrogen cyanide | −41.57 | +7.95 | +29.55 |
| ammonia | +11.00 | −9.90 | −7.92 |
| formaldehyde | −67.71 | +36.11 | +31.25 |
| formic acid | −21.30 | +25.93 | −5.56 |
| acetic acid | −13.78 | +1.19 | +12.83 |
| acetaldehyde | −0.60 | −8.25 | +8.48 |
| isocyanic acid | −14.29 | −14.29 | +28.57 |
| average $\lvert\epsilon\rvert_{HR}$ | 12.17 | 6.62 | 12.22 |

**Kinetic Parameters.** Assuming each volatile species as being released independently from other species and each peak (or shoulder) obtained in the derivative thermogravimetry profiles (mass change rate patterns) as a product of a distinctive pool of precursor material in the original CNS sample, the TG-FTIR system was applied for the identification of the individual gas species evolution peaks.

As discussed earlier, all the reaction rates were considered as obeying a parallel-first-order independent kinetics mechanism. This assumption is consensually considered as the most acceptable approach for the biomass devolatilization process as indicated by Tsamba et al.[4] The same hypotheses were applied successfully by other authors in the same field.[5−7] Results obtained through these assumptions are given in Table 3, for $A = 2.2 \times 10^{13}$ s$^{-1}$, as previously suggested.

It should be noted, however, that the identification and determination of pool sizes as well as its kinetics is influenced by the restrictions mentioned previously to determine the exact $T_{max}$.

**Comparison of Model-Predicted and Experimental Results.** TG-FTIR data obtained through experimental procedures were used to perform the kinetic analysis described previously. The kinetic parameters at low heating rates as well as the pool sizes obtained experimentally from the TG-FTIR system were used to generate input files for the code FG-Biomass. Then, by using this code to predict the yields at the same heating rates as the experimental program, the curves given in Figure 2 were obtained. In all these figures, the black and blue curves represent TG-FTIR experimental results while red and green curves resulted from predicted data obtained through curve-fitting exercise with the code developed.

In general, the model was found to correctly simulate the locations of evolution peaks for individual species (CO, $CO_2$, etc.). For several species, yet, it was difficult to fit model-predicted yields to experimental data at all heating rates. Probable reasons for these deviations can be attributed to the following factors:

(a) The used code does not include the cross-linking competitive reactions which influences the yields.

(b) The mass samples used in all tests (including repetitive checking tests) were in the same range. This might have influenced the transport phenomena patterns.

(c) The assumed first-order parallel-independent reaction mechanism can be inappropriate for this not well-known biomass.

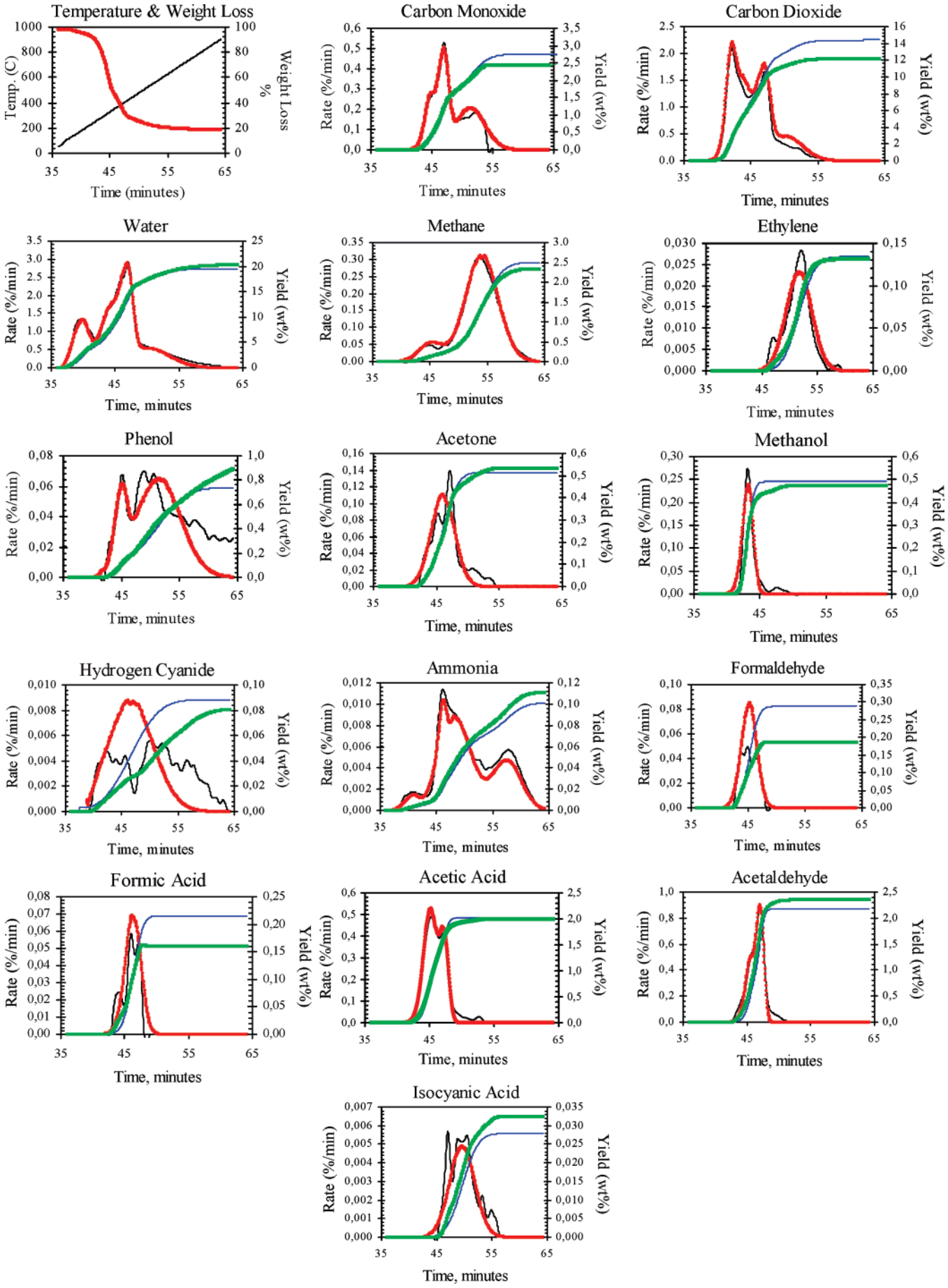


**Figure 2.** Product evolution rates and mass change from experimental TG-FTIR (black and blue) and from model prediction (red and green), at 30 K/min.

In view of these deviations, a compromise had to be made by having the fits underpredicting experimental data at one heating rate and overpredicting at another (Table 4).

To assess the accuracy of the model to actual data, relative deviation (shown in Table 4) between the experimental and predicted yields at the same heating rate ($|\epsilon_{HR}|$, %) was determined through eq 6.

$$|\epsilon_{HR}| = \left[\frac{\sum|\epsilon_i Y_i|}{\sum Y_i}\right]_{HR} = \left\{\frac{\sum\left|\left(\frac{\Delta Y_{TG-FTIR}^{FG-DVC}}{Y^{TG-FTIR}}\right)_i Y_i\right|}{\sum Y_i}\right\}_{HR} \quad (6)$$

In this equation, $Y^{FG-DVC}$ is the model-predicted yield of a given component (in %) and $Y^{TG-FTIR}$ is the experimental yield of component $i$ (in %), at the same heating rate (HR).

In general, for individual components, the model fits better the experimental data at 30 K/min. In particular, the model worked better to predict the yields of tars, methane, and acetaldehyde whose deviation is below 10% at all heating rates. The predicted and experimental results were highly divergent for carbon dioxide, phenol, formaldehyde, and isocyanic acid, independently of the heating rate.

## Conclusions

TG-FTIR was successfully used to determine and identify individual CNS pyrolysis products and respective gas precursors (pools) at low heating rates (10, 30, and 100 K/min) and to generate the respective intrinsic kinetics data. Individual yields from CNS pyrolysis were compared to those of wood pellets and *M. Giganteus*, obtained under the analogous conditions, found in the literature.

This comparison showed that CNS pyrolysis yields (i) more char; (ii) more volatiles and tars than *M. Giganteus* but less than wood pellets; (iii) less combustible volatiles (more carbon dioxide and water), and (iv) more N-species than wood pellets (and less than *M. Giganteus*).

Further, intrinsic kinetic parameters (reaction order, activation energy, and frequency factor) were obtained from the TG-FTIR results using a model based on a parallel independent first-order reaction mechanism with a Gaussian distribution of activation energies. On the basis of these kinetic results, input files for the distributed activation energy model (DAEM) biomass pyrolysis code were prepared. Then, the model was used for predicting yields under the same experimental temperature program as the experiments. In general, the model-predicted results were found to agree with that from TG-FTIR analysis, with minor deviations. A further improvement in the study is required to address the sample mass influence and the cross-linking reactions (responsible for partial conversion of the tars into volatiles and char coking and, thus, influencing the yields of volatiles, char, and tar), as well as the appropriate reaction mechanism.

EF0604792

Annex 2

# Pyrolysis characteristics and global kinetics of coconut and cashew nut shells

*Tsamba, A. J., Yang, W. and Blasiak, W.*

Published in
*Fuel Processing Technology* **2006**, *87*, *523-530*


Royal Institute of Technology

School of Industrial Management and Engineering

Department of Materials Science and Engineering

Division of Energy and Furnace Technology

Brinellvägen 23

SE-100 44 Stockholm

SWEDEN

ELSEVIER

Fuel Processing Technology 87 (2006) 523 – 530

FUEL PROCESSING TECHNOLOGY

www.elsevier.com/locate/fuproc

# Pyrolysis characteristics and global kinetics of coconut and cashew nut shells

Alberto J. Tsamba *, Weihong Yang, Wlodzimierz Blasiak

*Royal Institute of Technology, School of Industrial Engineering and Management, Department of Materials Science and Engineering, Division of Energy and Furnace Technology; Brinellvägen 23, SE-100 44, Stockholm Sweden*

Received 26 September 2005; received in revised form 5 November 2005; accepted 12 December 2005

**Abstract**

Coconut and cashew nut shells are two typical biomass wastes abundant in most of the tropical countries. However, despite their enormous potential as energy sources, they are hardly studied and their thermal characteristics are still not well known. In this study, both biomasses are thermally degraded through thermogravimetry and their characteristics such as devolatilisation profiles and kinetics are analyzed, from 250 to 900 °C, in an inert atmosphere, at two different heating rates, and compared with wood pellets. The results show that their pyrolysis profiles are different from that of the commonly studied woody biomass. In fact, they present two different peaks instead of the one overlapping peak, for hemicellulose and cellulose. In addition, they present activation energies ranging from that are slightly above the commonly known maximum for biomass. At 10 and 20 °C/min the activation energy varied from about 130 to 174 and 180 to 216 kJ/mol, for cashew and coconut shells, respectively.


*Keywords:* Coconut shells; Cashew nut shells; Pyrolysis; Kinetics

## 1. Introduction

Biomass, defined as any hydrocarbon material mainly consisting of carbon, hydrogen, oxygen, nitrogen and some other components in small proportions [1], includes wood and its derived wastes, different organic wastes (including biodegradable MSW), agricultural and crop wastes, animal wastes, energy plantations, among others. Cashew nut (CNS) and coconut shells (CcNS) are part of this family. They are abundant in tropical countries in Latin America, Africa and Asia, occurring as biomass wastes from different agro-industrial processes. These two biomasses represent a grand potential as renewable energy sources for power generation [2–6] for different end-uses, especially for household rural energy, in the developing countries where they occur.

In biomass energy technologies, pyrolysis process is of key importance as this thermal degradation of solid fuels is present in both combustion and gasification. It has a key influence over the quality of the char that is either gasified or burned. As it is known, biomass thermo-conversion technologies are strongly influenced by the reactivity char produced in the pyrolysis phase [7]. Therefore, for the design of any technology conversion system that suits specific characteristics of the biomass to be converted, pyrolysis process of such material is to be fully characterised. However, although many studies in biomass have already been performed in different aspects, CcNS and CNS are rarely found in such studies. In fact, in his outstanding review on biomass studies, Yaman [1] presents about two hundreds articles in biomass research studies and none of them is on CNS or CcNS. However, there are a limited number of researchers that have dedicated their investigation to these biomasses. In Raveendran et al. [5] studies of 13 different biomass samples in which CNS and CcNS are included. However, not too much attention was give particularly to these materials. In addition, Hoque and Battacharya [8] studied just the CcNS gasification product (fuel) from fluidised and spouted bed gasifiers. In both studies, the only specific characteristics that are given are proximate and/or ultimate analysis.

In the other side, lignocellulosic biomass basic components are hemicellulose, cellulose and lignin. Researchers have already confirmed that lignin starts decomposing at low temperatures (160–170 °C) and continues to decompose at low rate until approx. 900 °C. Hemicellulose is the second component to start

* Corresponding author. Tel.: +46 8 790 6545; fax: +46 8 207 681.
*E-mail address:* ajtsamba@zebra.uem.mz (A.J. Tsamba).

0378-3820/$ - see front matter © 2006 Elsevier B.V. All rights reserved.
doi:10.1016/j.fuproc.2005.12.002

decomposing, followed by cellulose, in a narrow temperature interval from about 200 to 400 °C. This is the interval in which the main decomposition takes place and accounts for the greatest decomposition in the biomass pyrolysis process consisting of degradation reactions. Beyond 400 °C, the most important reaction leads to the aromatisation process, at low mass loss rate [9].

Given the fact that biomass fuels differ extremely according to many factors [10] such as the type of biomass, species, the climate in which they are grown, the way each biomass species is cultivated (if this is the case) and other factors, the question on how different or similar the thermal characteristics of these tropical biomasses would be from the wood material that are quite well known is to be responded.

In this study, CcNS and CNS pyrolysis are investigated using thermogravimetry with the endeavour of characterising their thermal decomposition process, particularly, pyrolysis profiles and kinetics. For comparison, wood pellets are also submitted to the same analysis under identical circumstances.

Kinetics parameters were determined through the use of Coats and Redfern model, considering the pyrolysis mechanism of independent first order parallel reactions [10–13] and assuming that intra-particle heat transfer and diffusion effects are negligible, given the fine size of the sample particles used.

## 2. Experimental

The samples of CNS (from *Annacardium occidentale* L. tree) and CcNS (from *Coccos nucifera* L. tree) were collected in Mozambique (Africa) and were grinded to a small particle-size of less than 15 mg each (irregular size). It is important to mention that CNS were roasted beforehand as one of the cashew nut processing steps.

This study was performed using SETARAM 92 (TG), with Pt-crucible and a vertical hung-down thermobalance. Scientific argon was used as protective/inert carrier gas at 50 ml/min. The following temperature program was used:

i. From ambient temperature to 110 °C, at a heating rate of 10 °C/min, for sample drying (moisture removal);
ii. Isothermal drying at 110 °C, for 10 min (until constant mass is reached);
iii. Temperature raising from 110 to 900 °C (for pyrolysis and subsequent release of volatiles) at different heating rates (5, 10, 20, 40 and 50 °C/min), and
iv. Isothermal transformation at 900 °C for 10 min (to enhance the devolatilisation process and production of char).

From the ambient temperature to 900 °C, argon at a flow rate of 50 ml/min was used to maintain the reacting atmosphere inert. The mass loss and mass loss rate were recorded online by specific software designed by SETARAM, as functions of time and temperature.

In order to determine the pyrolysis kinetics parameters obtained through thermal analytical techniques, different methods are available [14–17], and are based in different assumptions made to simplify the complexity of the several reactions that occur during the devolatilisation process.

In this study, it is assumed that, given the smaller size of the sample particles, intra-particle heat transfer and diffusion phenomena are negligible and that a parallel first order reactions model is valid. These assumptions allow the use of Coats and Redfern method, one of the most commonly used methods and regarded as giving a good approach in thermal kinetics determination [17]. As it is required in this method, the reaction order had to be fixed in advance to allow the determination of the activation energy ($E_{act}$) and the pre-exponential factor ($A$), essential for characterising the pyrolysis kinetics.

Coats and Redfern method can be derived from the following chemical kinetics basic equations:

$$\frac{dx}{d\tau} = k(T)\Psi(x) \tag{1}$$

$$k = A\exp\left(\frac{-E_{act}}{RT}\right) \tag{2}$$

$$x = \frac{w_0 - w_\tau}{w_0 - w_f} \tag{3}$$

$$\Psi(x) = (1-x)^n \tag{4}$$

$$T = \xi\tau + T_0 \tag{5}$$

$$\xi = \frac{dT}{d\tau} \tag{6}$$

$$\int_0^x \frac{dx}{\Psi(x)} = \frac{A}{\xi}\int_0^T \exp\left(-\frac{E_{act}}{RT}\right)dT \tag{7}$$

$$F(x) = \int_0^x \frac{dx}{\Psi(x)} \approx \frac{ART^2}{\xi E_{act}}\left(1-\frac{2RT}{E_{act}}\right)\exp\left(-\frac{E_{act}}{RT}\right) \tag{8}$$

$$\ln\frac{F(x)}{T^2} = \ln\frac{AR}{\xi E_{act}}\left(1-\frac{2RT}{E_{act}}\right) - \frac{E_{act}}{RT} \tag{9}$$

$\Psi(x)$ is a function that depends on the reaction mechanism and the conversion rate as indicated in Eq. (4); $\xi$ is the heating rate; $k$ is the chemical reaction kinetics Arsenics constant, dependent on the reaction temperature ($T$), as indicated in Eq. (2); $w_0$, $w_f$ and $w_\tau$ are the initial, final and actual weight of the sample being thermally decomposed; $A$ is the Arrhenius pre-exponential factor; $R$ is the universal gas constant; $\tau$ is the time; $T$ is the absolute temperature that is a function of the heating rate and time [Eq. (5)]; $T_0$ is the initial absolute temperature; $n$ is the order determined by the chemical reaction mechanism.

Eqs. (1)–(7) are generally derived from chemical reactions kinetics theory. Eqs. (8) and (9) are dependent on different assumption made in each specific method. Hence, in Coats and Redfern Method, the equations given below follow:

$$F(x) = -\ln(1-x) \text{ for } n = 1;$$
$$F(x) = \frac{-\ln[1-(1-x)^{1-n}]}{1-n} \text{ for } n \neq 1 \tag{10}$$

Table 1
Proximate and ultimate analysis of the biomass samples studied in the present work

| Biomass type | Ultimate analysis (db, % w/w) | | | | | | | Prox. analysis (db, % w/w) | | | HHV, MJ/kg | Density, kg/m$^3$ |
|---|---|---|---|---|---|---|---|---|---|---|---|---|
| | C | H | N | O | S | Cl | Tr. El | Volat. | Fix-C | Ash | | |
| Coconut shells | 53.9 | 5.7 | 0.1 | 39.44 | 0.02 | 0.12 | 0.72 | 74.9 | 24.4 | 0.7 | 20.515 | 1090 |
| Cashew nut shells | 58.3 | 7 | 0.7 | 32.05 | 0.06 | 0.03 | 1.86 | 81.8 | 17.3 | 0.9 | 24.051 | 1012 |
| Wood pellets | 50.9 | 6.2 | 0.2 | 42.06 | 0.01 | 0.02 | 0.61 | 81.3 | 18.1 | 0.6 | 20.265 | 584 |

Since for the pyrolysis of the lignocellulosic biomasses activation energy reported in the literature is in the range of 100–250 kJ/mol [15], the approximation is made as given in Eq. (11), then Eq. (9) turns to Eq. (12).

$$\frac{RT}{E_{act}} \approx 0 \tag{11}$$

$$\ln\frac{F(x)}{T^2} = \ln\frac{AR}{\xi E_{act}} - \frac{E_{act}}{RT} \tag{12}$$

Eq. (12) is transformed into linear function, as follows:

$$F_T(X) = B - cX \tag{13}$$

Where $F_T(X) = \ln\frac{F(x)}{T^2}$, $B = \ln\frac{AR}{\xi E_{act}}$, $c = \frac{E_{act}}{R}$ and $X = \frac{1}{T}$.

Plotting thermogravimetric data by applying Eq. (13), pre-exponential ($A$) and activation energy ($E_{act}$) are determined and the Arrhenius constant obtained.

From Eq. (2), Arrhenius constant can be plotted against temperature as:

$$\ln k = \ln A - \frac{E_{act}}{R}\frac{1}{T} \tag{14}$$

This equation is used in the present study to assess the influence of temperature intervals and heating rate factors.

## 3. Results and discussion

### 3.1. Pyrolysis profiles

Table 1 presents the proximate and ultimate analysis of the three biomass samples that have been studied in this work.

The high hydrocarbons and less oxygen content are to be highlighted, together with high heating value and density of both tropical biomasses, compared to wood pellets. The carbon and hydrogen contents are a good indicative of hydrocarbons content that are to be released during pyrolysis. Additionally, it is well known that fuels that are rich in oxygen are poor in energy content (HHV). These differences play an important role in the pyrolysis of these materials and respective gases and char yields, as Figs. 1 and 2 show.

Fig. 1 shows the mass loss observed for dried samples of CNS, CcNS and wood pellets, above 100 °C, at a heating rate of 10 °C/min. The volatiles yield is greater in CNS compared to both wood pellets and CcNS. Wood pellets have comparably much volatile matter content than CcNS but lower than CNS. The char yield is inversely proportional to the volatiles yield. The temperature interval in which each biomass sample experiences the greater mass loss is different from one to another. From the thermograms showed in Fig. 1, these intervals are 247–420, 280–415 and 260–450 °C, where about 77%, 75% and 70% of the total volatiles weight are released in CNS, CcNS and wood pellets, respectively.

Fig. 2 shows the mass loss rate (derivative thermograms) for the three samples. A clear difference between wood pellets thermogram and the other two tropical biomass samples thermograms is noticeable. In fact, the two distinct DTG peaks found in CNS and CcNS, from 250 to 450 °C, differ clearly from the typical overlapping derivative thermogram found in woody biomass and in the vast majority of biomass species in this interval. The last is found in almost all biomass thermogravimetry studies and presents a shoulder at lower temperatures and an outstanding point at higher temperatures [5,6,12,18,19].

According to the previous studies in different biomass materials, the shoulder at left hand side corresponds to the hemicellulose decomposition while the higher temperature peak in the right hand side represents the degradation of cellulose [12,14,18,20]. This difference has never attracted any special attention of any biomass researcher so far, at the knowledge of the authors of this study, although the two-peak thermogram is also presented by Siddhartha and Reed [14] for CcNS.

Based in the precedent studies of biomass pyrolysis, the first peaks in CcNS and CNS represent hemicellulose decomposition and the second pair of peaks shows the mass loss rate change during thermal degradation of cellulose. Therefore, it is to mention that the peaks for hemicellulose and cellulose are at about 340 and 395, 329 and 400, and 380[1] and 420 °C, for CNS, CcNS and wood pellets, respectively.

Although it cannot be concluded right from the thermograms, it is known that lignin decomposition is distributed along a wide range of temperature interval and its peak is not commonly distinguishable [12,18]. However, it is believed that the long flat tail observed at high temperatures is caused by lignin decomposition. Fig. 2 shows a low peak at about 500 °C for CNS which must be indicative of lignin decomposition peak. Wood pellets and CcNS lignin decomposition behave as expected, without any perceptible peak.

According to Vamvuka et al. [12] the DTG peak height is directly proportional to reactivity and the correspondent temperature is inversely proportional to this chemical activity parameter. Applying this theory, it can be concluded that reactivity of CNS is similar to that of CcNS but higher than that of wood pellets. Concerning cellulose, the wood pellets still contain the

[1] Difficult to distinguish with precision, given the peak shape.

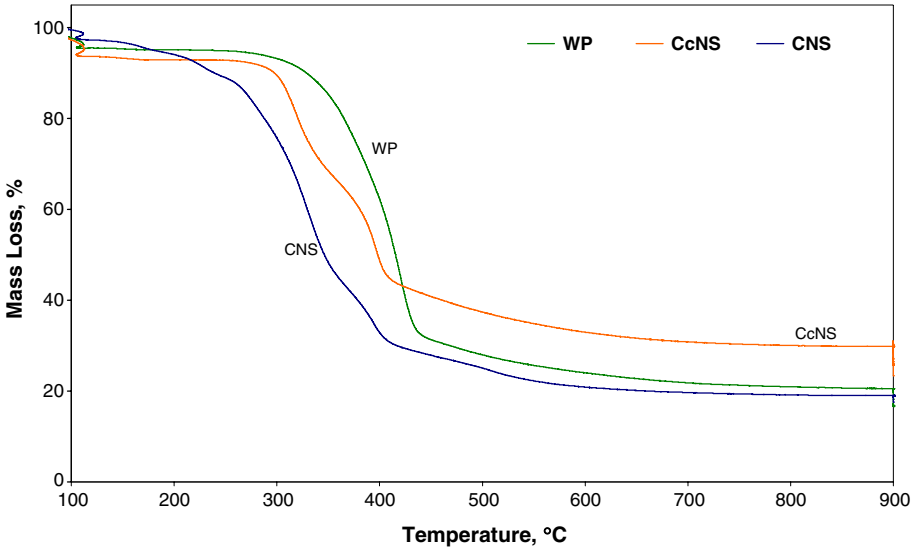


Fig. 1. Mass loss from the thermal decomposition of CNS, CcNS and wood pellets at 10 °C/min.

less reactive (high temperature) but fast reacting cellulose. CNS presents the slow reacting cellulose, despite being as reactive as that of CcNS.

### 3.2. Global kinetics

For kinetics parameters determination, the interval from 250 to 450 °C was used based in the fact that this is the interval in which the most pyrolysis for the three components takes place, as observed from the thermograms in Figs. 1 and 2.

As mentioned before, Coats and Redfern method is applied and first order parallel reaction mechanism is followed.

As seen in Fig. 1, the two different reactions in the temperature interval where the main pyrolysis process in both biomass species takes place, from 250 to 450 °C, are evident, suggesting that different lignocellulosic components, first, hemicellulose and then cellulose, are degraded [14,12,21,22]. These stages are approximately from 250 to 380 °C and from 380 to 450 °C, respectively. This subdivision is observed in both biomass samples at both heating rates considered in the study. These two intervals are the main focus of the present study.

The results obtained indicate the following reactions rate equations:

For CNS, at 10 °C/min

$$\frac{dx}{d\tau} = -r^{CNS}_{hem,10} = 7.18*10^{8} e^{(-15{,}416.8/T)}(1-x) \text{ and}$$

$$\frac{dx}{d\tau} = -r^{CNS}_{cell,10} = 1.20*10^{10} e^{(-18{,}694.7/T)}(1-x)$$

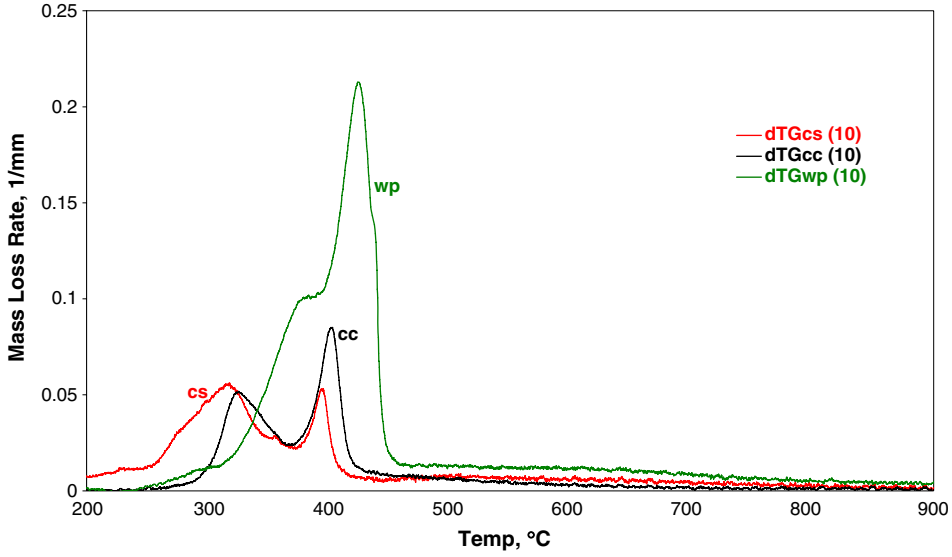


Fig. 2. Mass loss rate from the thermal decomposition of CNS, CcNS and wood pellets at 10 °C/min.

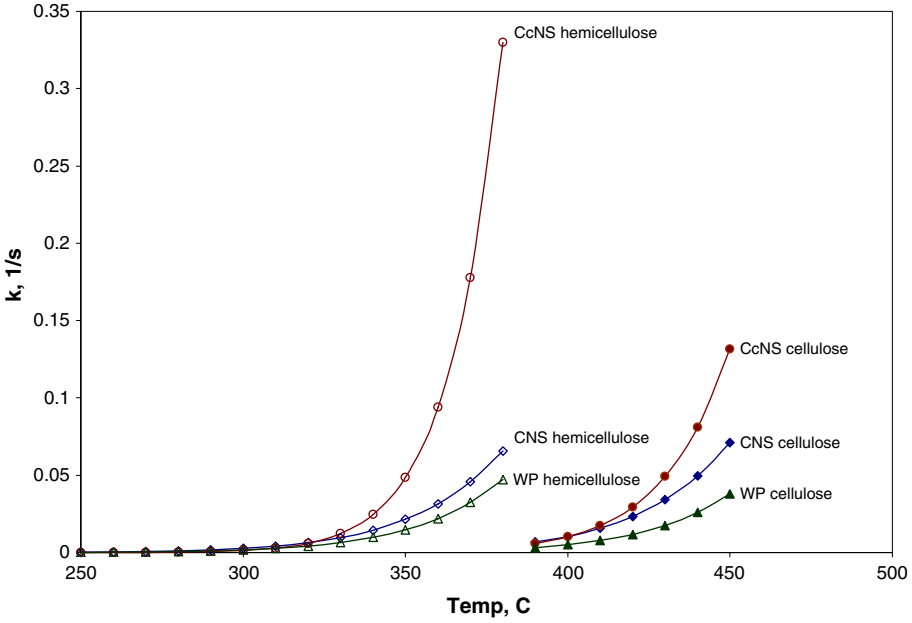


Fig. 3. Arrhenius constant vs temperature for CNS and CcNS pyrolysis at 10 °C/min.

For CNS at 20 °C/min

$$\frac{dx}{d\tau} = -r^{CNS}_{hem,20} = 4.17*10^{09} e^{(-15{,}660.5/T)}(1-x) \text{ and}$$

$$\frac{dx}{d\tau} = -r^{CNS}_{cell,20} = 2.89*10^{11} e^{(-20{,}396.5/T)}(1-x)$$

For CcNS at 10 °C/min

$$\frac{dx}{d\tau} = -r^{CcNS}_{hem,10} = 6.25*10^{16} e^{(-25{,}985.1/T)}(1-x) \text{ and}$$

$$\frac{dx}{d\tau} = -r^{CcNS}_{cell,10} = 1.31*10^{14} e^{(-24{,}973.2/T)}(1-x)$$

For CcNS at 20°C/min

$$\frac{dx}{d\tau} = -r^{CcNS}_{hem,20} = 1.15*10^{15} e^{(-23{,}216.3/T)}(1-x) \text{ and}$$

$$\frac{dx}{d\tau} = -r^{CcNS}_{cell,220} = 1.54*10^{12} e^{(-21{,}600.4/T)}(1-x)$$

These kinetics parameters, in each of these intervals, are expected to be mainly determined by the nature of the lignocellulosic component being degraded and, in minor proportion, of the biomass sample from which it comes, as the plot below shows.

Fig. 3 shows the influence of temperature interval (and hence of the component being decomposed) over the Arrhenius kinetics constant. Clearly the first interval, where hemicellulose thermal degradation is the most predominant, $k$, for all samples, changes slightly within 250 and 300 °C. Above 300 °C, CcNS hemicellulose constant shows a sharp increase, followed by CcNS. In the temperature interval where cellulose decomposition is the most important, the change is greater right from 390 °C, with CcNS showing the highest change with the temperature increase, followed by CNS. In both intervals, wood pellets showed the slowest change. Thus, it can be concluded

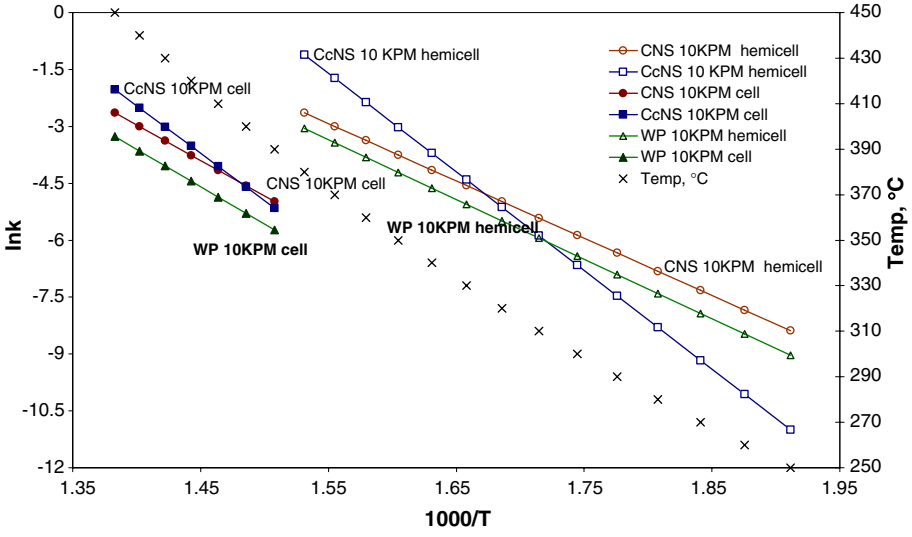


Fig. 4. The influence of the lignocellulosic component and type of biomass on the Arrhenius constant at 10 °C/min.

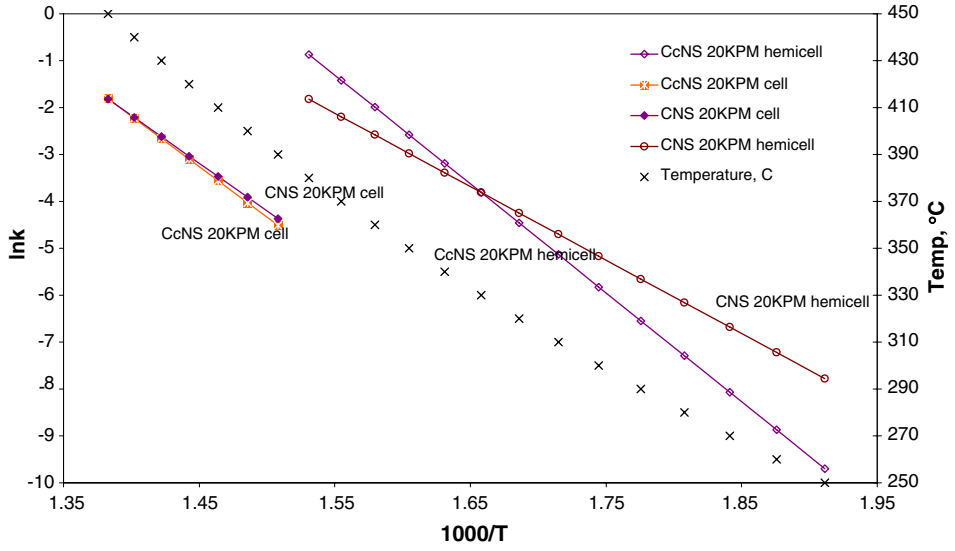


Fig. 5. The influence of the lignocellulosic component and type of biomass on the Arrhenius constant at 20 C/min.

that CNS hemicellulose and cellulose decomposition rate is greater than that of CNS.

Figs. 4 and 5 give the linearization of the relationship between kinetics constant and temperature (given in Fig. 2) based in Eq. (9) for both samples at 10 and 20 °C/min, respectively.

The heavier dependence on the component being decomposed is clearly noticeable from these two graphics. Indeed, although the biomass samples are different, Arrhenius constants are found in the same range for hemicellulose, in one hand, and for cellulose, in the other hand, for all three samples. However, there are some little differences such as the fact that CcNS constants are more sensitive to temperature change than that of CNS, as earlier noticed from Fig. 3. This is due to the global-activation energy of each reaction. The higher the activation energy, the higher is the sensitivity of Arrhenius constant to temperature. This is in line with the observed fact that activation energy changes from about 130,206 to 174,373 kJ/kmol, for CNS, and from 179,599 to 216,048 kJ/kmol, for CcNS. It is the activation energy that is high for CcNS than for CNS thermal decomposition. Such behaviour is found at both heating rates.

The influence of the heating rate can be viewed from Fig. 6, below.:

Using just one sample (CcNS) to illustrate how the Arrhenius kinetics constant is influenced by the heating rate, it can be seen that the higher the heating rate, the higher the value of the kinetic constant will be. Indeed, from Eqs. (2) and (5) it stands that the higher the heating rate, the lesser the influence of the activation energy over the kinetic constant. However, this influence tends to be smaller in cellulose than in hemicellulose decomposition. These findings were also observed in CNS pyrolysis, and wood pellets. They are in agreement with chemical kinetics reaction theory.

The figure above (Fig. 7) compares different activation energies from different studies [9,11,12,14,15,17,18,23–27],

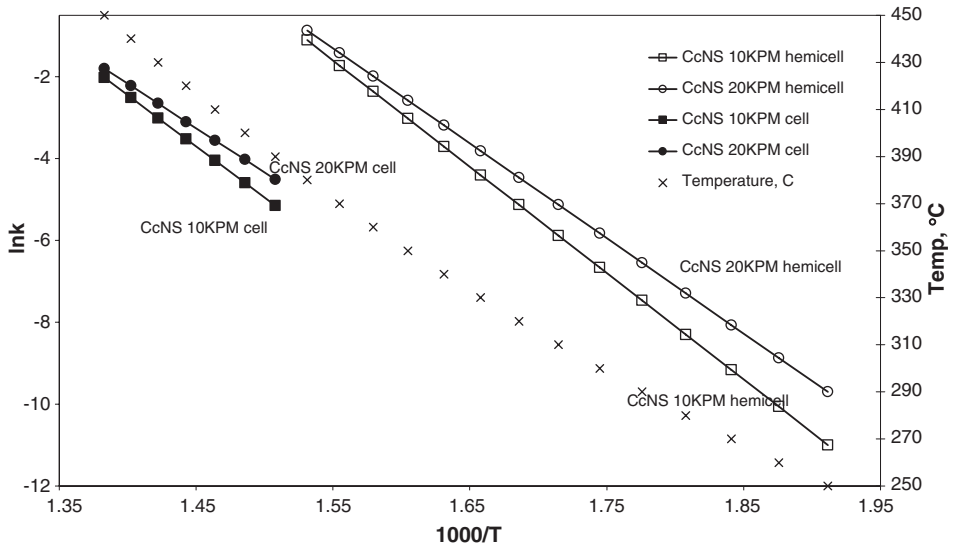


Fig. 6. The influence of the heating rate on the Arrhenius constant.

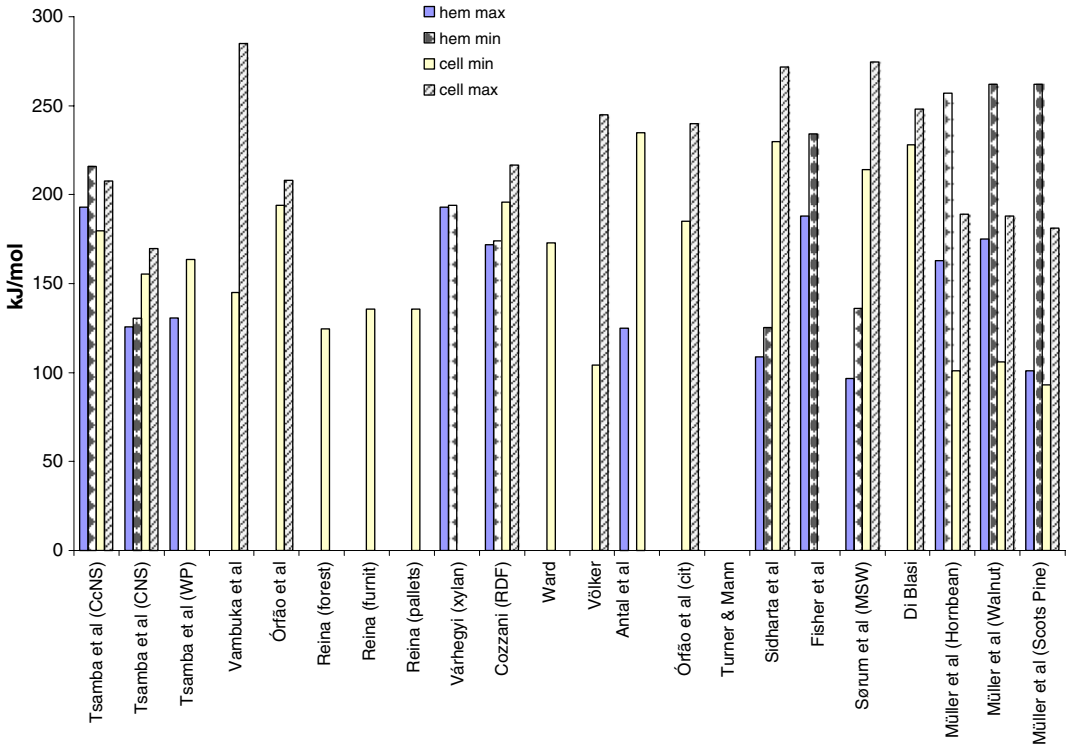


Fig. 7. Comparative activation energies results from different authors.

including from the present study. The figure clearly shows how diversified are the results, although they can be assumed to be in a fairly limited range. Excluding the results of the present study and Müller-Hagedorn et al.[2] [18] values, the activation energies from the other studies can be summarized as follows:

$$E_{act,hem}^{min} = 147.24 \pm 38.52 \text{ kJ/mol and}$$
$$E_{act,hem}^{max} = 172.75 \pm 39.44 \text{ kJ/mol}$$

$$E_{act,cell}^{min} = 176.92 \pm 42.41 \text{ kJ/mol and}$$
$$E_{act,cell}^{max} = 248.64 \pm 25.75 \text{ kJ/mol}$$

Results from the present study fall in the range given above for all the samples studied in the present work. Comparably, CNS and CcNS present moderate activation energies and, consequently, relatively most reactive than the average woody biomass. In fact, the higher the activation energy, the lowest will the reactivity be, according to the chemical concept of both parameters.

In general, differences are to be expected due to the different techniques, methodologies and models used as well as the nature of the samples studied. Nevertheless, the difference between the rest of the biomasses samples and coconut is manifest. This difference can only be attributed to the nature of hemicellulose and cellulose present in this kind of lignocellulosic materials. In fact, as discussed by different researchers, hemicellulose or cellulose represent different series of related macromolecular compounds that differ according to various factors as the type of biomass, the species and the geo-climatic conditions in which they are grown, among other factors. Indeed, these factors play an important role in characteristics such as the kind of hemicellulose (*glucomannans*, *arabinogalactans* and *xylans*) as referred by Siddhartha and Reed [14], and cellulose (α and β-*glucopyranosides*), as well as in ash content which play a catalytic effect in the biomass thermal decomposition.

[2] They used a very wide range of reactions order, all different from 1 (one).

## 4. Conclusions

CNS and CcNS pyrolysis was successfully characterised. Differences and similarities between these tropical biomass wastes and wood pellets were found and discussed.

It was found that, definitely, CcNS and CNS are different from the ordinary woody biomass in some important aspects. They are richer in hydrocarbons than wood, which leads to a poor char yield. Additionally, their main pyrolysis presents clearly different and distinct peaks for hemicellulose (first) and for cellulose (second) differing from the ordinary one overlapping peak normally found in most of the woody biomass pyrolysis.

The kinetics parameters obtained for CcNS and CNS, although they can be assumed to be in conformity with the data range obtained by previous researchers, still they show some dissimilarities, compared to woody biomass, as follows:

- High hydrocarbon content in and less char CNS;
- Moderate activation energies (130 to 216 kJ/mol) which enable the respective reactivity to be high.

*Symbols and abbreviations*

| | |
|---|---|
| CcNS | Coconut shell |
| cell | Cellulose |

| | |
|---|---|
| CNS | Cashew nut shell |
| cnsl | Cashew nut shell liquid |
| daf | Dry-ash-free basis |
| db | Dry basis |
| dTG | Derivative thermogravimetry |
| hem, hemicell | Hemicellulose |
| KPM | Kelvin per minute |
| max | Maximum |
| min | Minimum |
| min | Minute |
| °C | Degrees Celsius |
| $-r$ | Reaction rate |
| TG | Thermogravimetry (thermogravimetric analyser) |

## References

[1] S. Yaman, Energy Conversion and Management 45 (2004) 651–671.
[2] P. Das, A. Ganesh, Biomass and Energy 25 (2003) 113–117.
[3] P. Das, T. Sreelatha, A. Ganesh, Biomass and Bioenergy 27 (2004) 265–275.
[4] K. Prabhakar, R.C. Maheshwari, O.P. Vimal, Agricultural Wastes 17 (1986) 313–317.
[5] K. Raveendran, A. Ganesh, K.C. Khilar, Fuel 74 (1995) 1812–1822.
[6] K. Raveendran, A. Ganesh, K. Khilar, Fuel 75 (1995) 987–998.
[7] E. Cetin, B. Moghtaderi, R. Gupta, T.F. Wall, Fuel 83 (2004) 2139–2150.
[8] M.M. Hoque, S.C. Battacharya, Energy 26 (2001) 101–110.
[9] T. Fisher, M. Hajaligol, B. Waymack, D. Kellog, Journal of Analytical and Applied Pyrolysis 62 (2002) 331–349.
[10] J.J.M. Órfão, F.J.A. Antunes, J.L. Figueiredo, Fuel 78 (1999) 349–358.
[11] C. Di Blasi, Journal of Analytical and Applied Pyrolysis 47 (1998) 43–64.
[12] D. Vamvuka, E. Karakas, P. Grammelis, Fuel 82 (2003) 1949–1960.
[13] P. Stolarek, S. Ledakowicz, Thermochimica Acta 433 (2005) 215–223.
[14] G. Siddhartha, T.B. Reed, Thermal Data for Natural and Synthetic Fuels, Marcel Dekker, Inc.0-8247-0070-8, 1998.
[15] R. Capart, L. Khezami, A.K. Burnham, Thermochimica Acta 417 (2004) 79–89.
[16] M.J. Safi, I.M. Mishra, B. Prasad, Thermochimica Acta 412 (2004) 155–162.
[17] L.T. Vlaev, I.G. Markovska, L.A. Lyubchev, Thermochimica Acta 406 (2003) 1–7.
[18] M. Müller-Hagedorn, H. Bockhorn, L. Krebs, U. Müller, Journal of Analytical and Applied Pyrolysis 68–69 (2003) 231–249.
[19] L. Sørum, M.G. Grønli, J.E. Hustad, Fuel 80 (2001) 1217–1227.
[20] J.M. Heikkinen, J.C. Hordjik, W. de Jong, H. Spliethoff, Journal of Analytical and Applied Pyrolysis 71 (2004) 883–900.
[21] M. Stenseng, A. Jensen, K. Dam-Johansen, Journal of Analytical and Applied Pyrolysis 58–59 (2001) 765–780.
[22] J. Reina, L. Puigjaner, E. Velo, Thermocimica Acta 320 (1998) 161–167.
[23] S. Völker, Th. Rieckmann, Journal of Analytical and Applied Pyrolysis 62 (2002) 165–177.
[24] S.M. Ward, J. Braslaw, Combustion and Flame 61 (1985) 261–269.
[25] V. Cozzani, L. Petarca, L. Tognotti, Fuel 74 (1995) 903–912.
[26] G. Várhegyi, M.J. Antal, E. Jakab, P. Szábo, Journal of Analytical and Applied Pyrolysis 42 (19973) 73–87.
[27] K.G. Mansaray, A.E. Ghaly, Biomass and Bioenergy 17 (1999) 19–31.

Annex 3

# Determining the global kinetics of cashew nut and coconut shells pyrolysis by combining model-free and model-fitting methods

***Tsamba, A. J.***, *Yang, W. and Blasiak, W.*

Submitted for publicashion to
*Thermochimica Acta*
October, 2007


Royal Institute of Technology

School of Industrial Management and Engineering

Department of Materials Science and Engineering

Division of Energy and Furnace Technology

Brinellvägen 23

SE-100 44 Stockholm

SWEDEN

# Determining the Global Kinetics of Cashew Nut and Coconut Shells Pyrolysis by Combining Model-Free and Model-Fitting Methods

*Alberto J. Tsamba*[*]*, Weihong Yang and Wlodzimierz Blaziak*
Division of Energy and Furnace Technology
Department of Materials Science and Engineering
School of Industrial Engineering and Management
Royal Institute of Technology
SE-100 44 Stockholm, SWEDEN

## Abstract

Thermal characterisation of unique tropical biomass, as coconut (CcNS) and cashew nut shells (CNS) has been the main focus of a research being conducted by the authors of this study. In this work, the objective was to combine model-free methods and model fitting procedures for the determination of pyrolysis global kinetic parameters of these two tropical biomasses. Thus, thermogravimetric analysis was performed at 10, 30 and 100 K/min in an inert atmosphere. Data analysis was primarily performed using model-free methods. Then, results from these analyses were used as reference for the determination of the reaction order. The results were then compared with those obtained previously through Coats-Redfern method. A good agreement between all the results was achieved and the experimental data were predicted with high precision.

The average frequency factor and activation energy for CcNS pyrolysis were 3.16E14 1/s and 195.73±8.29 kJ/mol, respectively. For CNS, they were 1.66E08 1/s and 122.34±18.48 kJ/mol, respectively. The averaged deviation was 12.39 1/s for A and 15.233kJ/mol for $E_{act}$, in CNS pyrolysis, while for CcNS was 9.33 1/s for A and 12.661kJ/mol for Eact. It had been proved that model-free methods are reliable auxiliar tools for the determination of apparent kinetics especially, as input data in modelling techniques.

Key words: *pyrolysis, kinetics, isoconversional, model-free, model-fitting methods*

[*] Corresponding author: Phone +46 8 7906545; Fax: +46 8 207 681 E-mail address: ajtsamba@zebra.uem.mz (Alberto Júlio Tsamba)

## 1. Introduction

Biofuels are being increasingly appreciated as sustainable alternative to fossil fuels. Indeed, apart from being renewable they are carbon dioxide free fuels, therefore, playing an important role in the mitigation of Climate Change that is believed to be driven by the enhanced greenhouse gas (GHG) effect. International global statistics, indicate the use of fossil fuels for energy generation as the most important source GHG and carbon dioxide as the main GHG.

Consequently, the switch to biomass as an alternative fuel is increasing worldwide. This increasing demand brings new challenges to the R&D related to biomass fuels and pressure over the natural biomass resources. Coconut shells (CcNS) as well as cashew nut shells (CNS), which are abundant in a number of tropical countries, are among the so-called biomass wastes which have been so far neglected as potential renewable energy sources. In fact, these types of biomass are not as popular as other crop residues such as residues from rice, maize or cotton. Thus, research studies foccusing in this kind of biomass are scarce if existent.

Previous reviews have identified this gap [1]. As a result, the authors of this study have been studying these two tropical biomass wastes aiming at generating thermal data that can be used for technology sellection as well as technical design of energy conversion technologies to fit the specific characteristics of these materials. Hitherto, this work has generated pyrolysis profiles and (semi)global kinetics of both CNS and CcNS pyrolysis, following Coats and Redfern method [1], individual yields and kinetics of the evolved gas products from the pyrolysis of CNS [2] and CNS [3], which allows modelling of pyrolysis at high heating rates.

As it is known, model-free analytical methods for kinetic parameters determination have the advantage of allowing the determination of the activation energy as well as the frequency factor without the need of establishing the reaction mechanism. The most popular are the analytical methods are the isoconversional Ozawa-Flynn-Wall (OFW) and the Friedman analyses as well as ASTM E698.

This study intends to combine the model fitting technique and model-free (with focus on isoconversional) methods to determine the global kinetics of the CcNS and CNS pyrolysis.

As above indicated, in a previous work, semiglobal kinetics were determined following the independent parallel decomposition reactions for the three lignocellulosic components (hemicelluloses, cellulose and lignin). In this work, the thermal decomposition will be considered as global. No distinction between the three main lignocellulosic pyrolysis products precursors will be made.

### 1.1. Isoconversional Model-Free Methods

The use of an isoconversional analysis implies assuming that each conversion degree corresponds to one and only one point in the reaction course.

The application of an isoconversional method is only compatible with a single step reaction mechanism, as given in equation (1). From that equation, it is concluded that the Arrhenius

constant is a function of temperature, k(T), while the mechanism of the reaction is just a function of the conversion degree, f(α).

It is:

$$\frac{d\alpha}{dt}(T,\alpha) = k(T)\,f(\alpha) \qquad \textbf{Eq. 1}$$

As the reaction takes place under a constant heating rate, ξ (in a thermogravimetric analyzer), the relationship between temperature (T) and time (t) follows the formula $T=T_0+\xi t$.

Therefore, Eq.1 can be rewritten as:

$$\frac{d\alpha}{dT} = \frac{k(T)}{\xi} * f(\alpha) \qquad \textbf{Eq. 2}$$

Hence, after separating the variables, equation (2) turns into:

$$\frac{d\alpha}{dT} = \frac{A}{\xi}\exp\left(-\frac{E_{act}}{RT}\right)f(\alpha) \qquad \textbf{Eq. 3}$$

From this relationship, by applying natural logarithm the equation given bellow is valid:

$$\ln\left(\frac{d\alpha}{dT}\right) = \ln\left(\frac{A}{\xi}\right) + \ln\left[f(\alpha)\right] - \frac{E_{act}}{RT} \equiv \ln\left(\frac{d\alpha}{dt}\right) \qquad \textbf{Eq. 4}$$

Directly from this equation, Ozawa as well as Flynn and Wall, working independently, suggested the function through which the activation energy can be calculated as a function of the heating rate and the inverse of temperature:

$$\ln\xi = \ln\left[\frac{A}{\frac{d\alpha}{dT}}f(\alpha)\right]_{\alpha} - \frac{E_{act}}{R}\frac{1}{T} \qquad \textbf{Eq. 5}$$

In the other hand, from integration of equation (3) can be indicated as:

$$F(\alpha) = \int_0^{\alpha}\frac{d\alpha}{f(\alpha)} = \int_0^{T_{\max}}\frac{A}{\xi}\exp\left(-\frac{E_{act}}{RT}\right)dT \qquad \textbf{Eq. 6}$$

Doyle's approximation [4], helps obtaining the final equation from equation (6), which is, for $-20<[-E_{act}/(RT)]<-60$:

$$\log \xi \approx -\log F(\alpha) + \log \frac{AE_{act}}{R} - 2.315 - 0.457 \frac{E_{act}}{R} \quad or$$
$$\ln \xi \approx \ln F(\alpha) + \ln \frac{AE_{act}}{R} - 5.3515 - 1.502 \frac{E_{act}}{R} \qquad \textbf{Eq. 7}$$

Therefore, the slope in a logξ vs 1/T or lnξ vs 1/T plot, is either (-0.457$E_{act}$/R) or (-1.052$E_{act}$/R), respectively.

In the other side, the Friedman method, based in equation (1) relates the logarithm of the reaction rate to the inverse temperature at a given constant conversion degree and heating rate, as follows:

$$\left(\frac{d\alpha}{dt}\right)_{\xi} = A_{\alpha} \exp\left(-\frac{E_{act}}{RT}\right)_{\alpha,\xi} f(\alpha_{\xi}) \qquad \textbf{Eq. 8}$$

And,

$$\ln\left(\frac{d\alpha}{dt}\right)_{\xi} = \ln\left[A\alpha * f(\alpha_{\xi})\right] - \left(\frac{E_{act}}{RT}\right)_{\xi,\alpha} = \ln\left[A_{\alpha} * f(\alpha_{\xi})\right] - \frac{E_{act}}{R}\frac{1}{T_{\xi,\alpha}} \qquad \textbf{Eq. 9}$$

In this equation, the first right-side member is constant, at a given heating rate and conversion degree. Thus, the correspondent plot gives straight lines whose slopes are directly proportional to the activation energy and, therefore, it can be derived from there.

In both OFW and Friedman analyses, as it is implicit that the reaction follows a single step mechanism, the respective activation energies are expected to be equal or similar. That means that it should not change considerably with the conversion degree. In other words, the lines should be parallel, therefore, having the same slope. A great change in the magnitude of these values with the change of the conversion degree (α) indicates the occurrence of a multi-step reaction(s) that definitely do not fit the single step reaction mechanism and, consequently, cannot be analysed solely by equation (1) [5].

Discussion on isoconversional methods as well as their respective interpretation can be found somewhere else [4]-[16]

It must be noted that these methods are valid only and solely if the assumption of a constant activation energy is implied, which is unavoidable for the separation of variables of the equation 10 (integral of eq. 9) in the derivation of equation 5.

$$\int_0^{\alpha} \frac{d\alpha}{f(\alpha)} = A_{\alpha} \int_0^{t_{\alpha}} \exp\left(\frac{-E_{act}}{RT}\right) dt \qquad \textbf{Eq. 10}$$

Therefore, any dependence of the activation energy on the degree of conversion will nullifies equation 11 and all related formulas become mathematically false [13].

### 1.2. The ASTM E698 or Kissinger's Method

ASTM E698 method is between the model-free and model fitting methods. In fact, it also does not demand the reaction mechanism for the determination of activation energy. However, for the determination of the frequency factor, it assumes first order reaction mechanism [17].

This method is based in the so-called Kissinger's equation, which relies on the DTG peak temperature ($T_{max}$), as it represent the temperature at which the maximum reaction rate is achieved, and therefore, the following relation is valid:

$$\left[\frac{d}{dt}\left(\frac{d\alpha}{dt}\right)\right]_{T=T_p} = 0 \qquad \textbf{Eq. 11}$$

Approximations from this method give the following equation:

$$\ln\left(\frac{\xi}{T_{\max}^2}\right) = -\frac{E_{act}}{RT_{\max}} + M \qquad \textbf{Eq. 12}$$

In which M is a constant, according to the equation:

$$M = \ln\frac{AR}{E_{act}^0} \qquad \textbf{Eq. 13}$$

$E^{\circ}_{act}$ is the activation energy at $T_o$.
The plotting of $ln(\xi/T^2_{max})$ versus $(1/T)$ results in a straight line whose slope is $(-E_{act}/R)$, as well.

For the determination of the frequency factor, the equation bellow is used:

$$A = \frac{\xi}{T_{\max}} \frac{E_{act}}{RT_{\max}} = \frac{\xi E_{act}}{R T_{\max}^2} \qquad \textbf{Eq. 14}$$

## 2. Methodology

### 2.1. Experimental

The study was carried using thermogravimetry in a TGA SETARAM 92 Thermoanalyzer (Fig.1). The analyzer consisted of an electronic microbalance, a graphite furnace, a gas system, a CS 92 controller and a computer fully operated by a Setaram software (version 1.54 a).

The electronic thermal microbalance is a beam balance (detection limit of 1$\mu$g)[1]. The furnace is cylindrical and is heated by a graphite tube located concentrically to the furnace and cooled by a water circuit. The mass loss was recorded at intervals of 0.5-1.0 min, depending on the heating rate.

Argon was used as inert atmosphere and carrier gas while nitrogen was the protective gas. The following temperature program was used:

- From ambient temperature to 110°C: sample drying (moisture removal) at a heating rate of 10 K/minute (all runs);
- Isothermal drying at 110°C, for 10 minutes: ensuring complete moisture removal;
- Temperature raise at different heating rates (10, 30, 100 K/minute), from 110°C to 900°C: thermal degradation of the sample and subsequent release of volatiles (for all runs); and,
- Isothermal process at 900°C for 10 minutes: enhancing the devolatilisation process and consolidation of char.

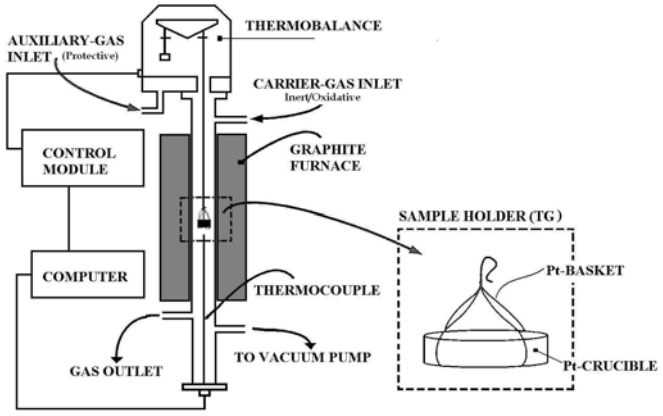


Figure 1. Schematic view of the TG SETARAM 92 assembly [1]

The sample was placed in a Pt-crucible supported by a Pt-wire basket and suspended centrally in the furnace tube. The temperature measurements were taken by an S-type thermocouple located right at the bottom of the crucible.

### 2.2. Experimental Data Processing

The data generated experimentally consisted of the fractional mass loss as a function of the temperature change and the elapsed time. This information was processed using different analytical methods to determine the global kinetic parametres of the pyrolysis.

As the first approach, model-free methods were used to ensure the type of the chemical reaction involved: if single or multiple steps, as well as the approximate frequency factor and activation energy. In the case where the single step is confirmed, the activation energy and frequency factor are determined and used as reference for the determination of the most probable reaction order through model fitting iteractive procedures.

Where the reaction path appeared incompatible with single step reaction, the model fitting procedure was applied to determine the most apropriate reaction model as well as the frequency factor and activation energy, using the average from isoconversional results as indicators. In fact, as noted by Šimon[13], the kinetic parameters determined through isoconversional methods are apparent. Thus, they should be considered as being only adjustable parameters in the fitting temperature function k(T) from equation (1) that assumes the frequency factor to be independent from the temperature.

For comparison, the ASTM E698 model is also used to determine the kinetic parameters. All these model-free methods had already been discussed in previous sections of this article.

The model fitting was done through the NETZSCH Thermokinetics Advanced software, a tool that has been in use by a number of researchers for thermal decomposition of solid materials ([6], [18]).

## 3. Results and Discussion

### 3.1. Coconut Shells Pyrolysis

Pyrolysis of coconut shells presented a mass loss corresponding approximately to 80-83%. This measn that 17-20% of this material remained as char (fixed carbon and ash). The mass loss plots for the three heating rates are shown in Fig.2

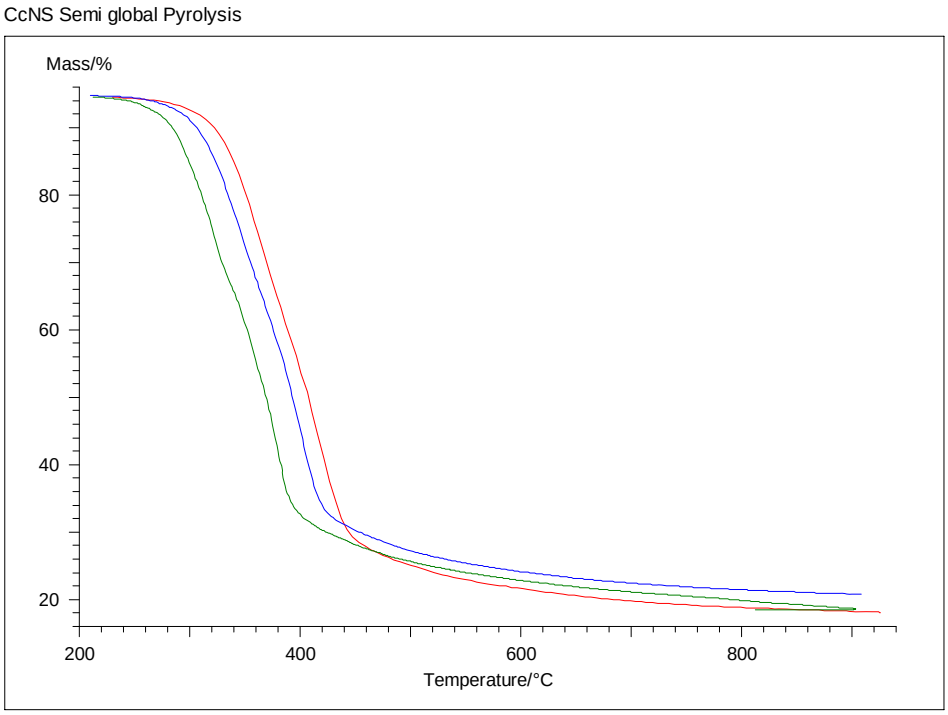


Figure 2. Mass Loss during CcNS Pyrolysis (green: 10K/min; blue: 30 K/min and red: 100 K/min)

Analysis of these data through Friedman, Ozawa-Flynn-Wall and ASTM E698 methods, gives the results showed in Figs.3-7. The results from Friedman and OFW methods are very similar and they confirm a single step reaction that goes till 80% mass loss. Above this mass loss percentage, the reaction is either multi-step or catalysed, therefore, does not fit any of the model-free methods. In fact, this can be clearly seen in both Friedman and OFW analyses plots. Indeed, the regular and similar slope of the activation energies lines in activation energy plots as well as the regular zero-slope in energy plots (plateau) indicate similar activation energies and frequency factors at different conversion degrees, which confirms a single step feature for the pyrolysis of coconut shells.

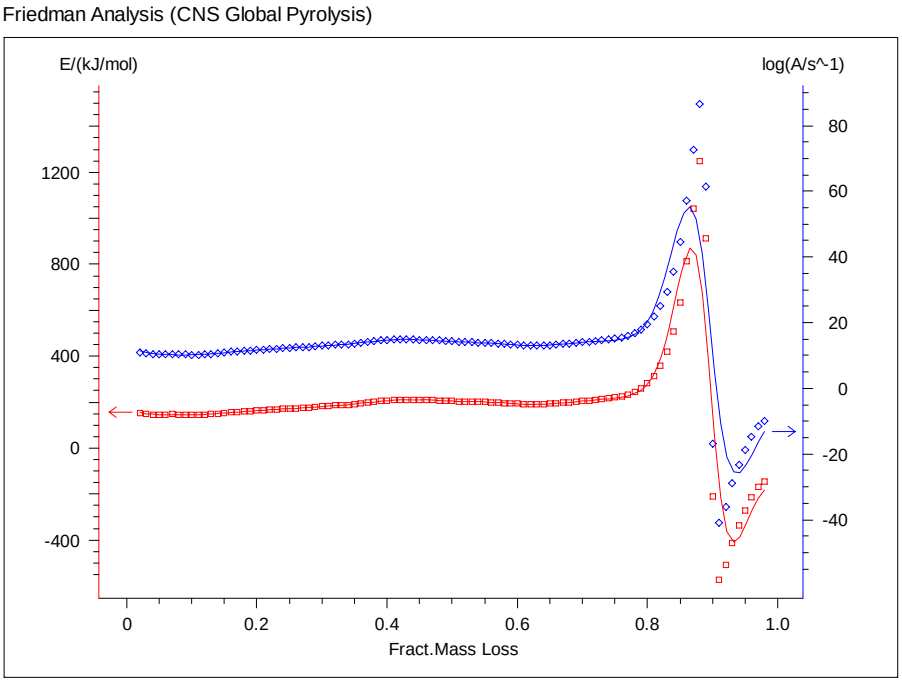


Figure 3. Friedman Analysis for CcNS Pyrolysis (Energy Plot)

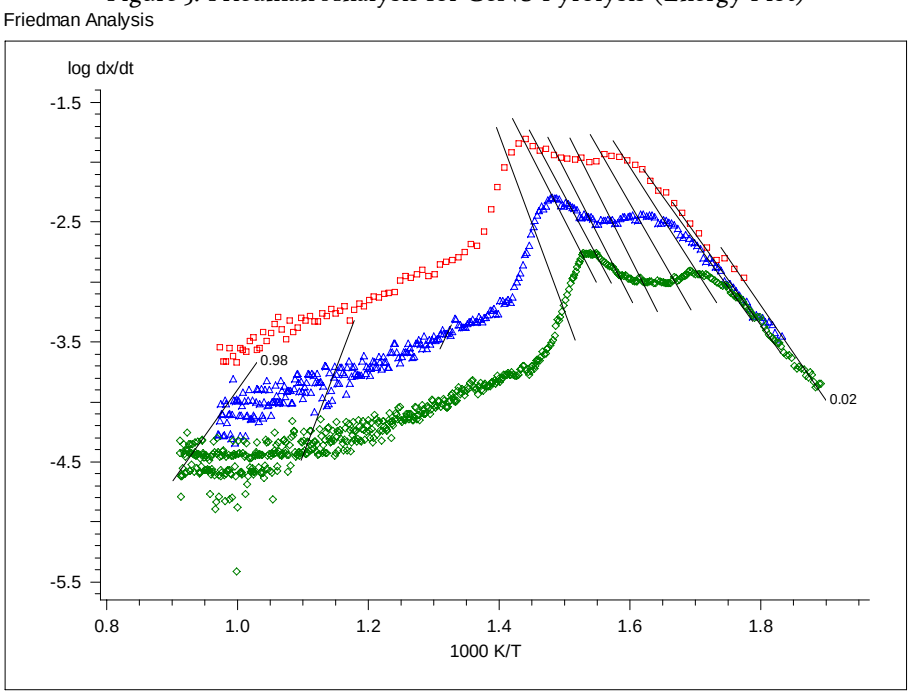


Figure 4. Friedman Analysis for CcNS Pyrolysis (Activation Energy Plot)

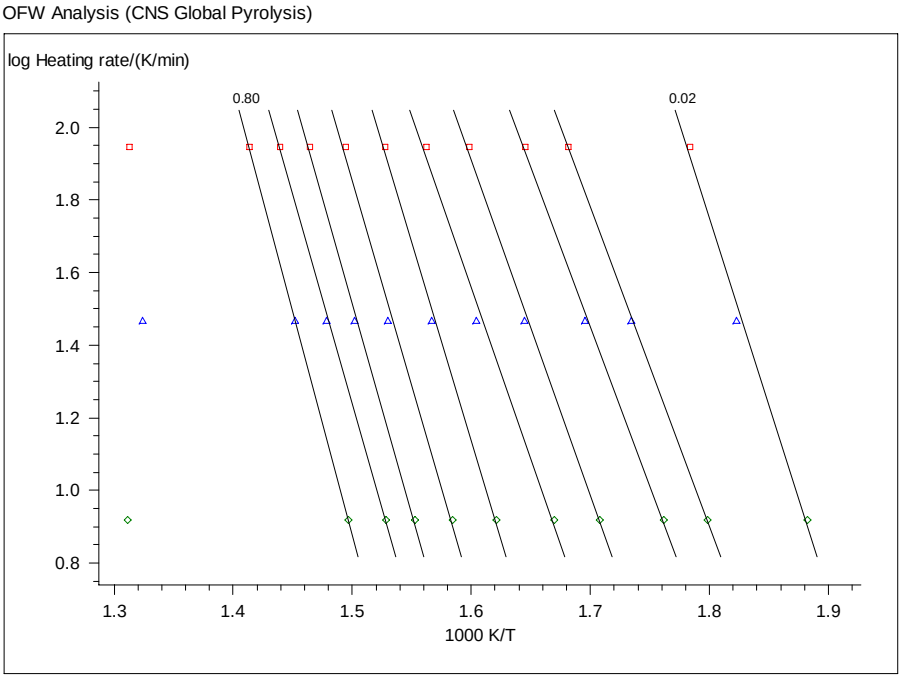


Figure 5. OFW Analysis for CcNS Pyrolysis (Activation Energy Plot)

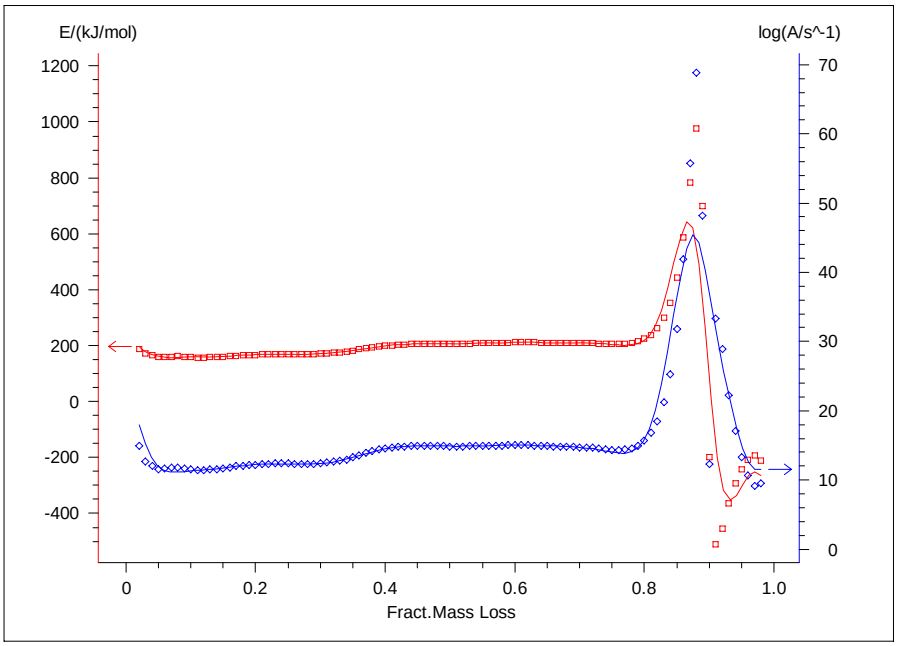


Figure 6. OFW Analysis for CcNS Pyrolysis (Energy Plot)

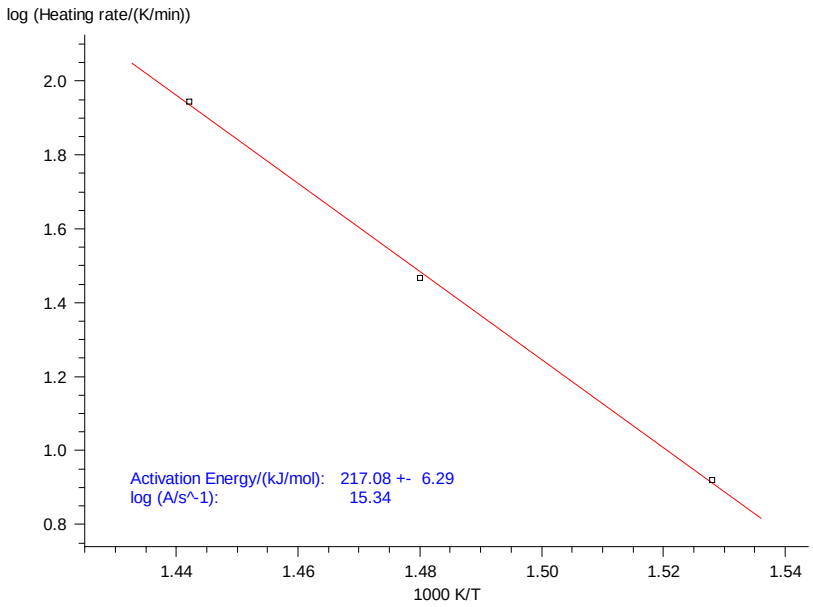


Figure 7. ASTM E698 Analysis for CcNS Pyrolysis

Therefore, the validity of the isonversional methods are restricted, in the present case, to $0 \leq x \leq 80\%$, which corresponds to $T \leq 459.47^{o}C$, in a reaction following the single step mechanism. According to the experimental conversion degree at different heating rates, that corresponde to $T_{100} \leq 426.7^{o}C$, $T_{30} \leq 415.3^{o}C$ or $T_{10} \leq 387.2^{o}C$, as shown in Figs. 8-9.

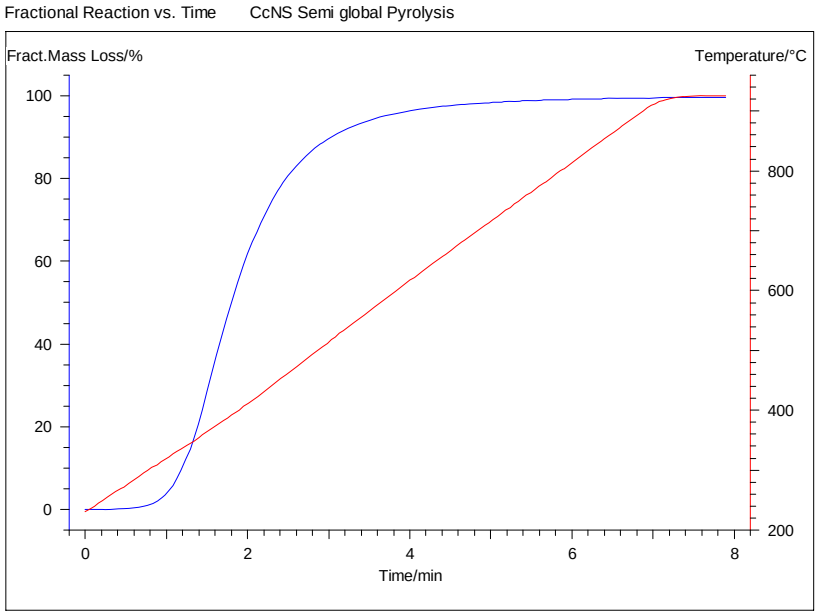


Figure 8. Temperature Program and Fractional Mass Loss (x=80%, T=460°C)

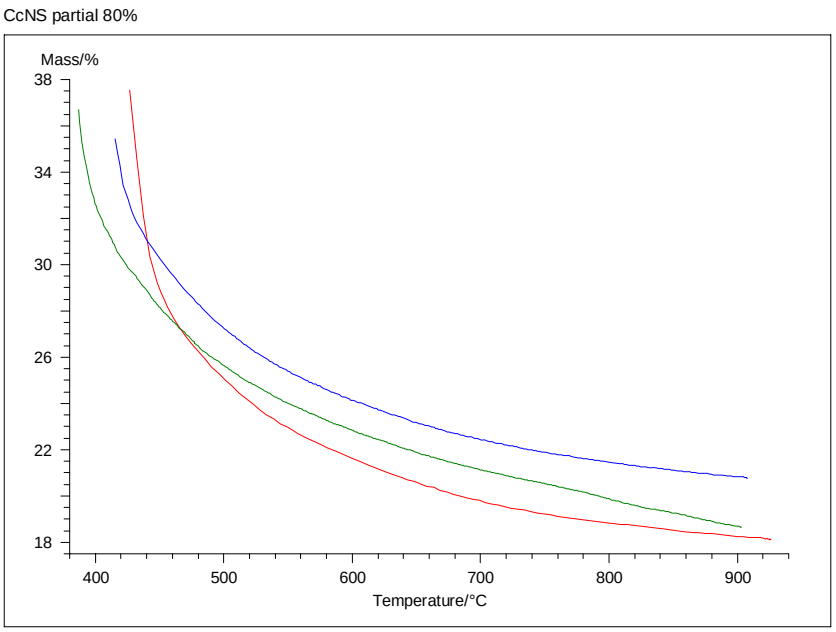

Figure 9. Mass Loss above 80% for CcNS Pyrolysis (only)

The kinetic parameters from these three model-free methods are summarized as shown in Table 1:

**Table 1. Summary of model-free kinetic parameters**

| Analytical Method | Activ. Energy (kJ/mol) | | | lg A |
|---|---|---|---|---|
| | E | | ΔE | |
| Friedman | 187.58 | ± | 15.23 | 13.2 |
| OFW | 189.54 | ± | 9.02 | 13.75 |
| ASTM E698 | 217.08 | ± | 6.29 | 15.34 |

In table 1, the values from Friedman and OFW methods represent the average from the analysis. Using the isoconversional figures as reference, the model-fitting approach was the applied to find the reaction order correspondent to these model-free kinetic parameters, through the use of the NETZSCH Advanced Software for Kinetics (2007).

The results are presented in Figs. 10-11. The set of kinetic parameters determined is the closest and provides the best fit to the mass loss curve for the three experimental heating rates as shown in the graphic (full lines correspond to model predicted mass loss). The corresponding values are n=4.31 (reaction order), $A=3.981x10^{13}s^{-1}$ (frequency factor) and $E_{act}=181.50\pm5.02$ kJ/mol (activation energy), and a correlation factor of 0.997319.

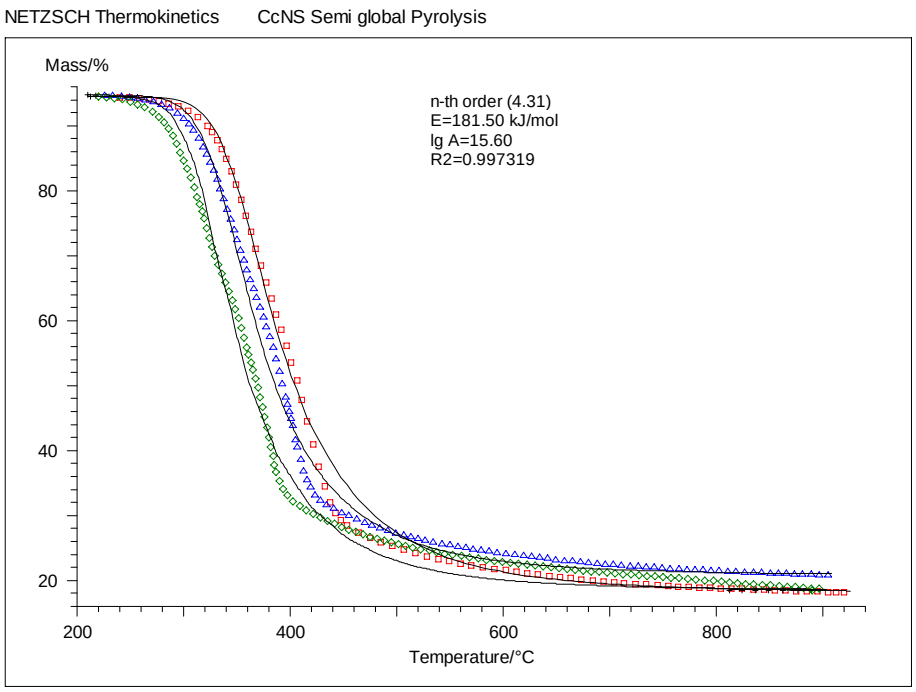


Figure 10. Model-fitting plot (prediction in full lines): conv, degree vs temperature

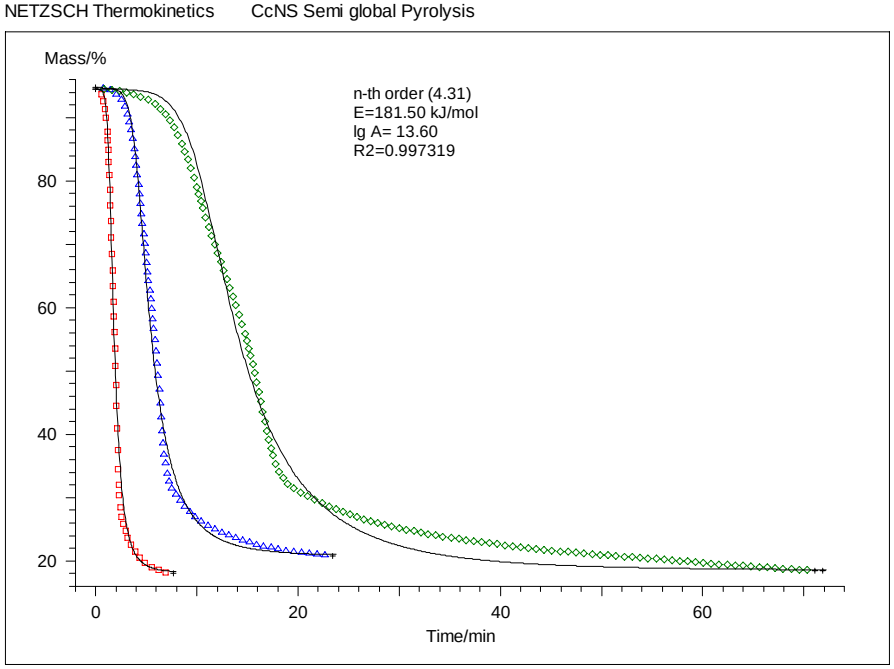


Figure 11. Model-fit plot (prediction in full lines): conv, degree vs time

Through Figs. 10-11, the fine fit of modelled data over the experimental results is confirmed even for the mass loss fraction over 80%, the interval that was found to be outside the single step mechanism range.

Comparing the results from model-free with those generated through model-fitting procedures, as shown in Fig. 12, only the parameters from ASTM E698 show a substantial deviation. The OFW and Friedman results agree satisfactorily with the modell-fitting results.

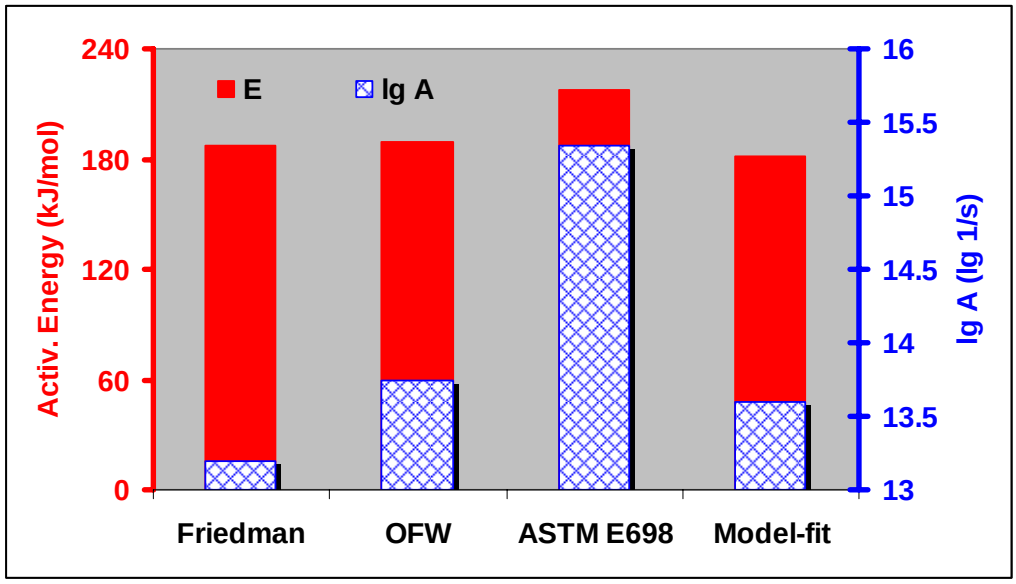


Figure 12. Summary of the Kinetic (Energy) Parameters for CcNS using four different methods

Although the agreement between experimental and model predicted results is good, main authors have been applying first order as the most approriate reaction order[[1]]. Hence, for comparison, first order is used in the model fitting technique and checked against the results given in Fig. 12. The data from this procedure gives a poor agreement with the experimental results($R^2$=0.979391), as Fig. 13 shows.

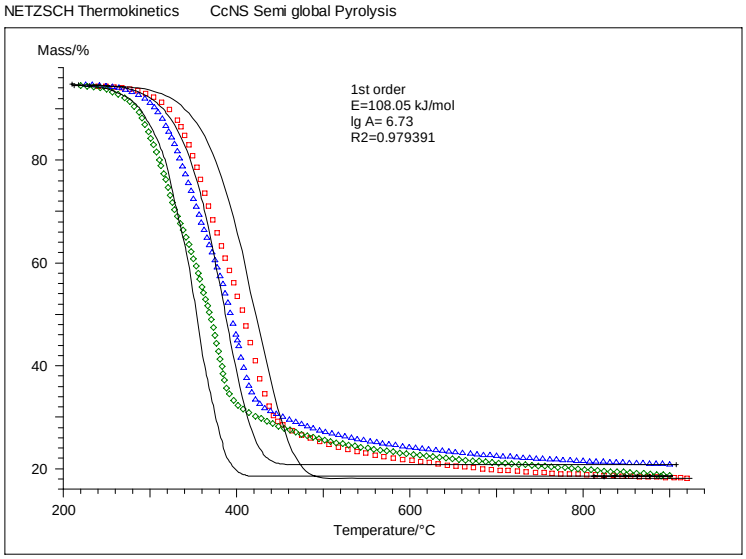


Figure 13. Experimental vs Predicted Mass Loss assuming first order for CcNS Pyrolysis

### 3.2. Cashew Nut Shells

For the pyrolysis of cashew nut shells (Fig. 14), the same approach was followed. The results showed that the mechanism of CNS pyrolysis does not follow a single step mode. Indeed, Friedman as well as OFW analyses do not show any regular values neither for the activation energy nor for the frequency factor, in any range. This evidence is shown through Figs 14-17.

The values obtained through any of these two isoconversional methods are very similar and, despite being different from one conversion degree to another, they still represent the calculated values under the given conditions (conversion degree) for the process under analysis, and they have to be interpreted as such. Hence, these values were still used as indicators for the determination of the reaction model. By folowing this methodology, the most probable reaction mechanism were determined based on the average values from Friedman as well as from OFW methods.

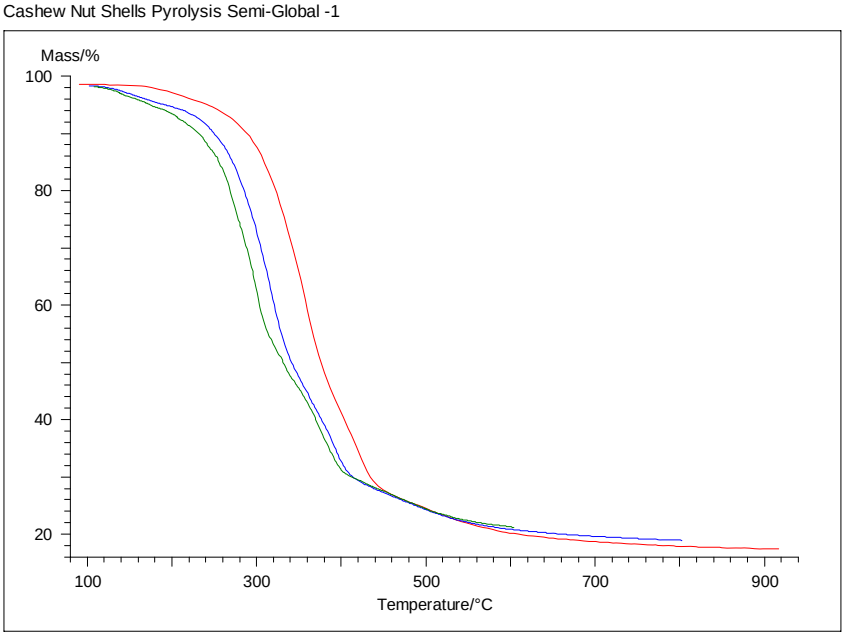


Figure 14. Mass Loss during CNS Pyrolysis

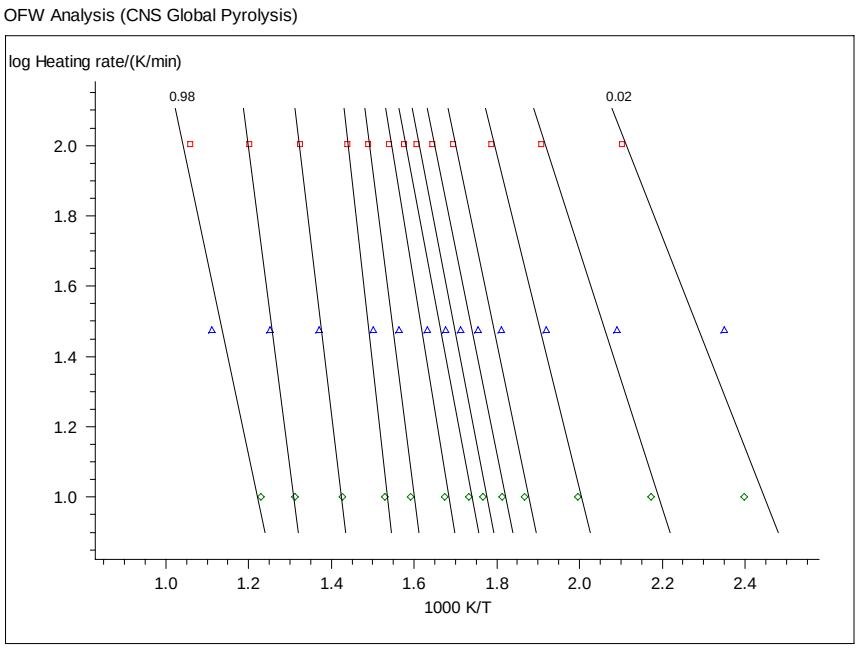


Figure 15. OFW Analysis for CNS Pyrolysis

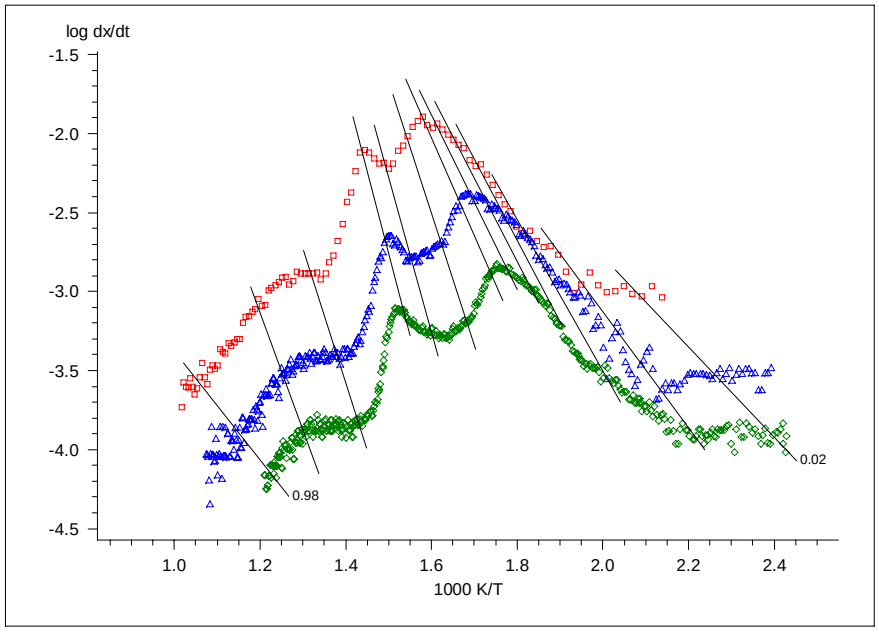


Figure 16. Friedman Analysis Plot for CNS Pyrolysis

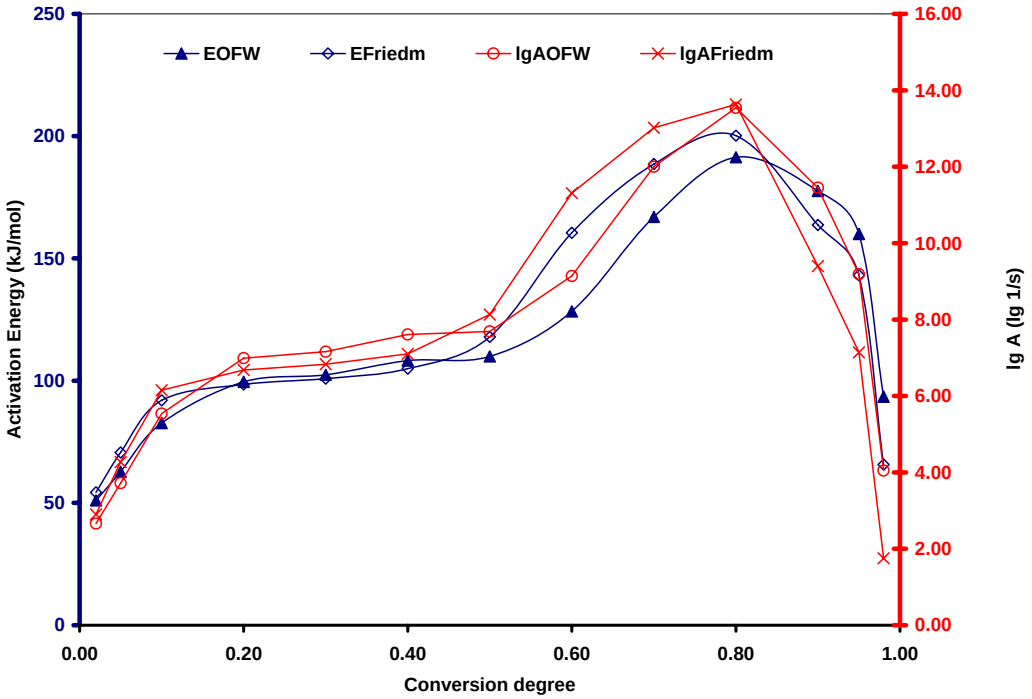


Figure 17. Friedman and OFW Energy Plots for CNS Pyrolysis

The average activation energy and frequecy factor from both the Friedman and the OFW methods are $E_{act}$=120.07±23.89 kJ/mol; A=5.623x10$^{7}$s$^{-1}$ and $E_{act}$=118±19.16 kJ/mol; A=3.631x10$^{7}$s$^{-1}$, respectively.

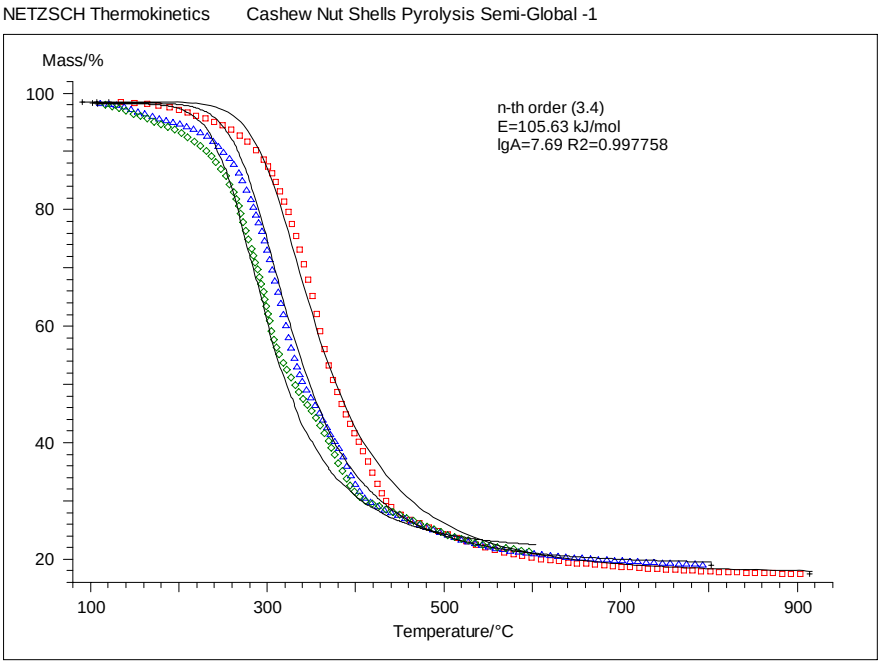


Figure 18. Model-fitting plot for CNS Pyrolysis (conv. degree vs temperature)

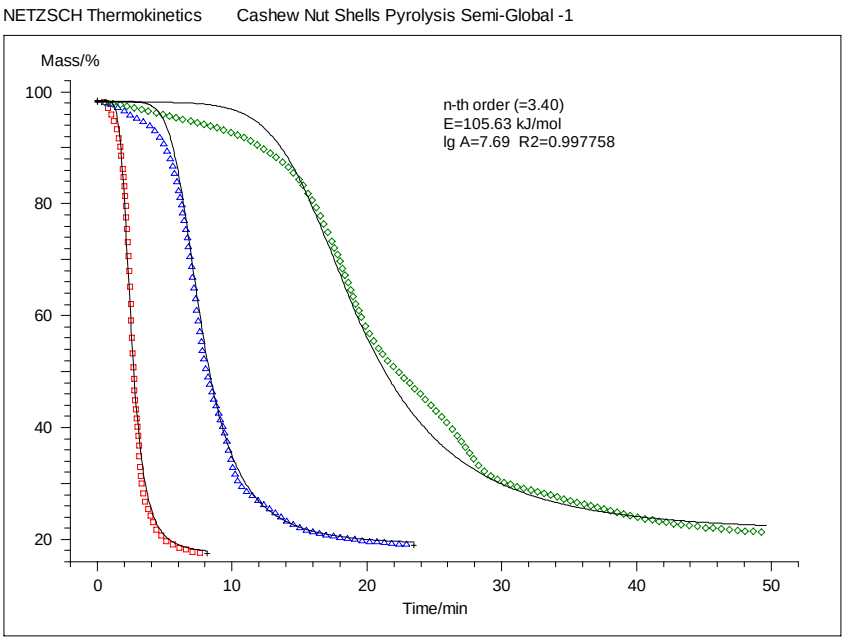


Figure 19. Model-fitting plot for CNS Pyrolysis (conv. degree vs time)

Using these averages as indicators, the reaction mechanism was determined through model fitting technique as it was done with coconut shells pyrolysis. The results are shown in Figs. 18-19. The two plots show an acceptable agreement between the experimental and the model predicted results. The set of kinetic parameters found through this calculalations is: n=3.40, $E_{act}$=105.63 kJ/mol and A= $4.898x10^{7}s^{-1}$, with a correlation coefficient of 0.997758.

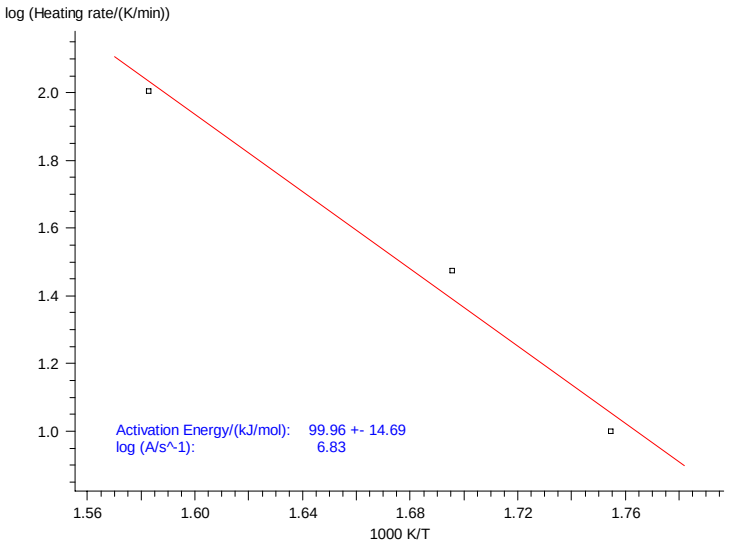


Figure 20. ASTM E698 for CNS Pyrolysis

Again, for comparison, the ASTM E698 method plot is used and the results are displayed in Fig. 20.

The summary of these kinetic parameters is given in Fig 21, and the results can be clearly regarded as being in the same range.

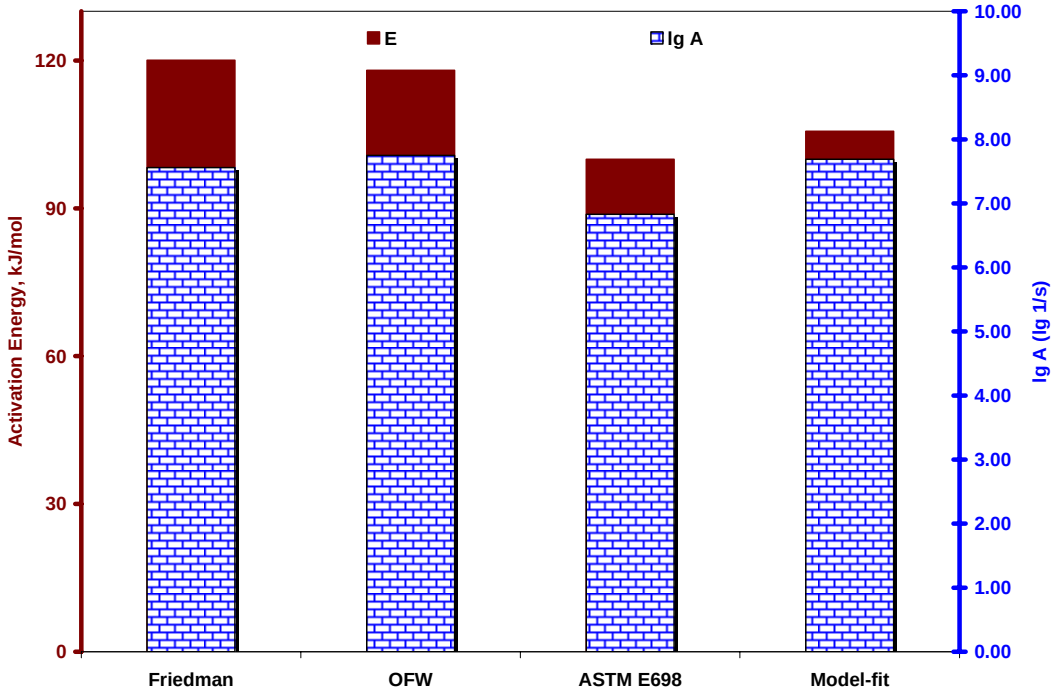


Figure 21. Summary of the Kinetic (Energy) Parameters for CcNS using four different methods

Again, as it happened with coconut shells pyrolysis kinetics, the assumption of a first order global reaction (shown in Figs 22-23) does not agree with the experimental data. Therefore, first order is not considered in this study.

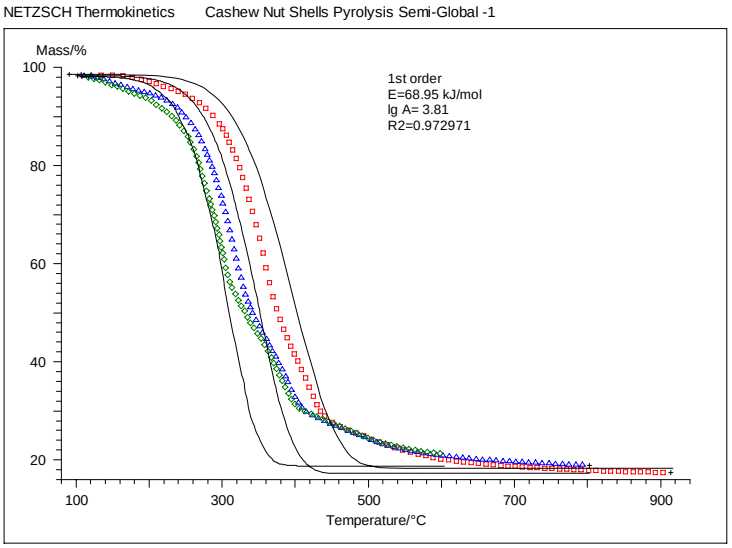


Figure 22. The prediction level achieved when applying first order approach (mass loss vs temperature)

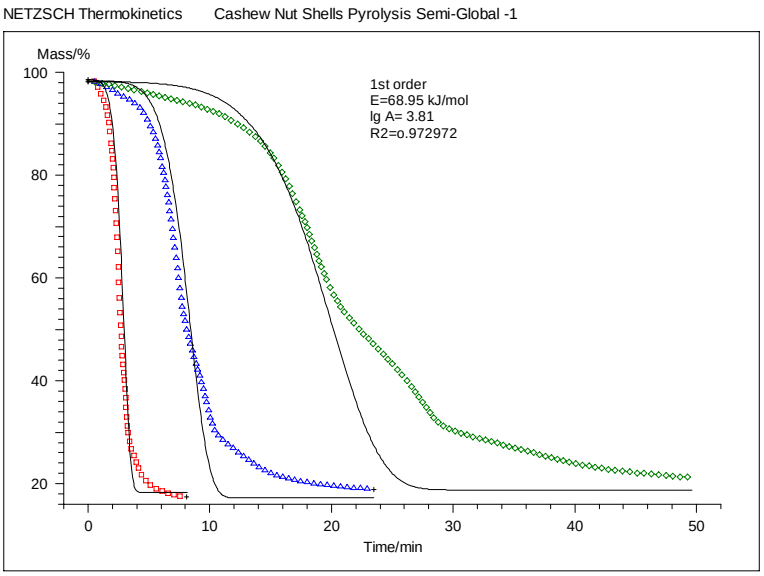


Figure 23. The prediction level achieved when applying first order approach (mass loss vs time)

## 3.3. Comparison with Coats and Redfern Results

Comparison of the results from this reserach work with those obtained in the previous research works is given in the following figs 24-26. The results from Tsamba et al [[1]] were obtained at 10 K/min and 20 K/min using Coats & Redfern method, assuming parallel independent reaction mechanism . As in such study, at each heating rate two temperature intervals were considered, one for hemicelluloses and another for celluloses, for the present purpose, the average at each heating rate is generated.

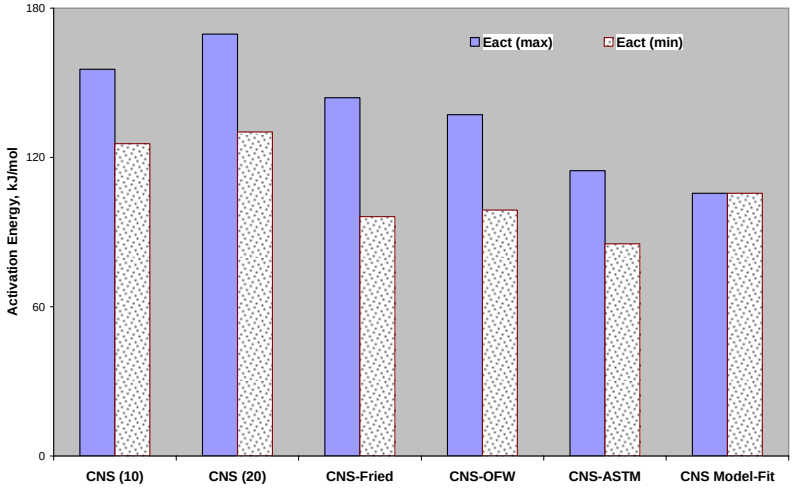


Figure 24. CNS pyrolysis minimum and maximum Eact by different methods

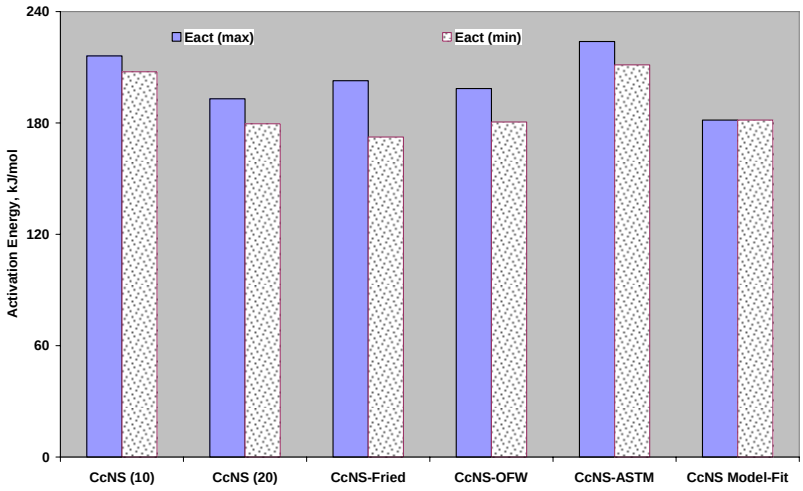


Figure 25. CcNS pyrolysis minimum and maximum Eact by different methods

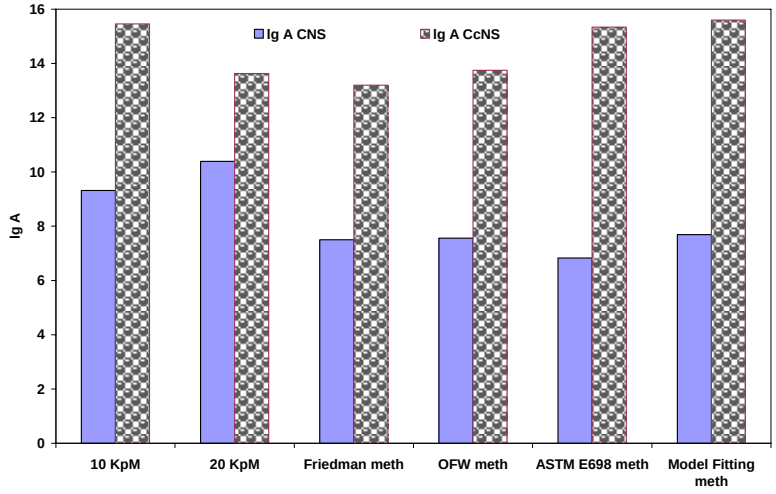


Figure 26. Frequency factor logari thm for CcNS and CNS pyrolysis by different methods

All the results from the five different methods can be considered, with enough confidence, as being in the same range, with similar magnitude. Indeed, the averaged deviation (AVDEV) for activation energy and frequency factor is just 12.661 kJ/mol and 9.33 1/s (CcNS pyrolysis) and 15.233 kJ/mol and 12.39 1/s, respectively (CNS pyrolysis).

However, it is important to note that although the results are good, the right interpretation of these data must be taken into account. As discussed earlier, isonconversional methods treat multi-step complex reactions as single-step processes. Hence, the activation energies obtained through these methods are apparent and do not have any mechanistic meaning. On the other hand, according to Šimon[[13]], the principal merit of the model-free methods relies on the fact that they provide reliable kinetic data for the modelling of a process without a deeper insight into its mechanism.

As it is known, the determination of kinetic parameters is a complex and problematic issue. Indeed, the so-called compensation effect induces multiple pairs of activation

energy and frequency factors as sollutions that, in a model-fitting procedure, can be interpreted as good. This leads to biased estimates of the pair activation energy-frequency factor, principally.

On the other hand, modelling any chemical reaction is a procedure that can only be underatken if the input parameters are unbiased and free from systematic errors. Imprecisions linked with analytical approximations in the determination of input data are prejudicial to modelling procedures. Thus, model-free methods are, comparably, useful tools for the genaration of unbiased kinetic parameters, given the simplicity and error-avoidance approach that otherwise would be linked to the sellection of a kinetic model.

## 4. Conclusions

Different model-free methods were succesfully combined with model fitting method to generate global kinetic parameter for the pyrolysis of coconut shells and of cashew nut shells. In fact, the results achieved through different model-free methods, such as Friedman, Ozawa-Flynn-Wall and ASTM E698 analyses, provided activation energies and frequency factors well comparable with similar parameters determined through global model fitting method, in one side, and with the Coats and Redfern method, in the other side.

Using the kinetic parameters determined through model-free methods as reference, it was possible to determine the specific reaction order through the use of model-fitting method for an assumed multi-step model for the pyrolysis of coconut and cashew nut shells. The comparison of the results from the methods used in both works referred above, provided averaged deviation of, respectively, 12.39 $s^{-1}$ and 15.233 kJ/mol for the frequency factor and activation energy in cashew nut shells pyrolysis while, for coconut shells the same parameters were 9.33 $s^{-1}$ and 12.661 kJ/mol, respectively.

It was, therefore, confirmed that modell-free methods can be used as auxiliar tools to model-fitting techniques for the determination of the kinetic triplet for the solid reactions.

## 5. References


[1] Tsamba A.J., Weihong, Y. and Blasiak, W.; *Fuel Processing Technology* 87-6 (**2006**) 523-530

[2] Tsamba, A.J.; Weihong, Y.; Blasiak, W. and Wójtowicz, M.; Energy & Fuels, 21(2007) 2357-2362

[3] Tsamba A.J., Weihong, Y. and Blasiak, W.; *Modelling Evolved Gas Yields From Cashew Nut and Coconut Shells Pyrolysis;* 9th International Conference on Energy for a Clean Environment (CleanAir-2007); Póvoa de Varzim, Portugal, July 2-4, 2007

[4] Flynn, J. H.; Thermal Analysis, 27 (1983) 95-102

[5] Hong, J.; Guo, G. and Zhang, K.; J. Anal. Applied Pyrolysis 77-2 (2006) 111-115

[6] Padhi, S. K.; Thermochimica Acta 448 (2006) 1-6

[7] Alonso, M.V.; Oliet, M.; García, J.; Rodrígiez, F and Echeverría, J.; Chemical Eng. Journal 122 (2006) 159-166

[8] Jankovic, B.; Adnadevic, B. and Menthus, S.; Thermochimica Acta 456 (2007) 48-55

[9] Baitalow, F. Schmidt, H.G: and Wold, G; Thermochimica Acta 337 (1999) 111-120

[10] Zorba, T.; Chrissafis, K.; Paraskevopoulos, K. M. and Bikiaris, D. N.; Polymer Degradation and Stability 92 (2007) 222-230

[11] Mamleev, V.; Bourbigot, S.; Le Bras, M. And Lefebver, J.; J. Thermal Anal. Calorimetry, 78 (2004) 1009-10027

[12] Ozawa, T.; J. Thermal Analysis, 31 (1986) 547-551

[13] Šimon, P.; J. Therm. Anal. Calorimetry, 76 (2004) 123-132

[14] Choudbury, D.; Borah, R.C.; Goswamee, R.L.; Sharmah, H. P. and Rao, P.G.; J. Therm. Anal. Calorimetry, 89 (2007) 3, 965-970

[15] Mamleev, V.; Bourbigot, S.; Le Bras, M.; Duquesne, S. And Šesták, J.; Phys. Chem. Chem. Phys., 2 (2000) 4708-4716

[16] Burnham, A. K. and Braun, R. L.; Energy & Fuels, 13-1(1999) 1-22

[17] Saha, B and Ghoshal, A.K.; Chem. Eng. J., 111 (2005) 39-43

[18] Yu, H-M.; Zhang, Q-H.; Qi, L-J.; Lu, C-W.; Xi, T-G. and Luo, L.; Termochimica Acta 451 (2006) 10-15

Annex 4

# Modelling evolved gas yields from cashew nut and coconut shells pyrolysis

*Tsamba, A. J., Yang, W. and Blasiak, W.*

Presented to
*9th Conference on Energy for Clean Environment*
sellected (and submitted) for publicashion in
*Clean Air International Journal*
July, 2007


Royal Institute of Technology

School of Industrial Management and Engineering

Department of Materials Science and Engineering

Division of Energy and Furnace Technology

Brinellvägen 23

SE-100 44 Stockholm

SWEDEN

# MODELLING INDIVIDUAL EVOLVED GAS YIELDS FROM CASHEW NUT AND COCONUT SHELLS PYROLYSIS

**A.J.Tsamba [*©], W.Yang[#] and W. Blasiak[#]**

*UNIVERSIDADE EDUARDO MONDLANE (UEM)
FACULDADE DE ENGENHARIA, Departamento de Engenharia Química
Av. de Moçambique km 1.5 Cx. Postal, 257 Maputo, MOZAMBIQUE

[#]ROYAL INSTITUTE OF TECHNOLOGY (KTH), School of Industrial Engineering and Management,
Department of Materials Science and Engineering, Energy and Furnace Technology Division
Brinellvägen 23, SE-100 44 Stockholm, SWEDEN

## Abstract

Coconut and cashew nut shells are some of the biomass wastes typically available in many tropical countries. As renewable resources, they are eligible as important green sources for energy generation. Despite this evident fact, they are not yet commonly studied as such. In fact, while coconut shells are commonly known as activated carbon raw material, cashew nut shells are mostly known as cnsl precursors. Both products are of great importance commercially. In this research study, a non-isothermal pyrolysis of these two biomass wastes is performed using TG-FTIR, at moderate heating rates (10, 30 and 100 K/min) with the objective of identifying the evolved gases and determine the respective intrinsic kinetics. This TG-FTIR system continuously monitors i) the time dependent evolution of volatiles, ii) the tars evolution rate, and iii) the weight of char. FT-IR spectra were obtained every 30 seconds and quantification of all volatiles (except tars) was done from quantification routines obtained from calibration runs with pure compounds. The data are used to generate input files that are used in a code based on the distributed activation energy model (DAEM). Using the code and the input files generated, the gas yields were predicted for comparison with the experimental results, at the same conditions. The prediction results showed a good agreement with the experimental data. Thus, the code was extended to very high heating rates (1000 and 10,000 K/s). The results at low heating rates are compared to the literature available data obtained under analogous conditions.

Key words: *biomass wastes, pyrolysis, kinetics, yields*

[©] Corresponding author: ajtsamba@zebra.uem.mz (Alberto Júlio Tsamba)
Fax: +46 8 20 76 81 Ph: +46 8 790 6545

# INTRODUCTION

The demand for biomass as biofuel for energy production has been increasing in the last decades. Although different reasons can be listed to justify this sharp increase, it is to emphasize the need for sustainable and $CO_2$-neutral fuels or energy sources. With the Kyoto Protocol first commitment period approaching, many industrialized countries committed to meet their GHG reduction targets by 2012 will be investing more in renewable energy sources and pushing for touchable results.

In the developing countries, the need for generating energy from local as well as renewable resources has also become a great apprehension. Hence, new energy sources are encouraged to be promoted. Under this scope, coconut shells (CcNS) as well as cashew nut shells (CNS), abundant in most of the tropical countries, were found to be poorly known as energy source. Just to illustrate, an outstanding review on biomass studies by Yaman et al [1] presents about two hundreds articles in biomass research studies and none of them is on CNS or CcNS. Notwithstanding this evidence, few studies were found from a very limited number of researchers that have dedicated their investigation to these biomasses. Raveendrani et al [2] studies of 14 different biomass samples include CNS and CcNS. Though, not too much attention was given particularly to these feedstocks. Hoque et al [3] studied just the CcNS gasification product (fuel) from fluidised and spouted bed gasifiers. In both studies, the only specific characteristics that are given are proximate and/or ultimate analysis.

This study is part of a more comprehensive research on tropical biomass wastes, with focus on CNS and CcNS. The aim of this research is to generate data on tropical biomasses, such as CNS and CcNS, in order to fill in the gap identified concerning data that would allow the design or selection of an appropriate energy conversion technology for these feedstocks. Through such research, important data have been generated and published, hitherto. Such data include i) global kinetics of CNS and CcNS pyrolysis at low and moderate heating rates [4], [5]; ii) individual evolution rates and yields for the CNS pyrolysis products [6]; and, iii) identification of pyrolysis gas-precursors, respective sizes and kinetics[6].

The primary objective of the study presented in this article is to model pyrolysis of both CNS and CcNS at high heating rate, from 1,000 to 10,000K/s and compare the product yields with those obtained at lower and moderate heating rates, such as 10, 30 and 100K/min.

The modeling is performed with a FG-code based in distributed activation energy model (DAEM) that allows the prediction of individual gas products at high heating rates.

As indicated in previous studies, two computer codes based in DAEM are known, namely the FG-DVC and FLASHCHAN [7]. Each of this is a standalone model for pyrolysis that can be applied as long as the kinetic parameters (including the activation energy standard deviation) as well as the heating rate are known.

DAEM has been extensively and successfully used to analyze complex reactions such as pyrolysis of both biomass and coals, thermal regeneration reaction of activated carbon [8]. To apply this model effectively, the reactions must be considered as being parallel, independent and irreversible and to be following first-order reaction mechanism.

# METHODOLOGY AND EXPERIMENTAL SETUP

## Biomass samples

The biomass samples used in this study are cashew nut shells from *Annacardium Occidentale L.* and coconut shells from *Cocos nucifera L*. The CNS samples were obtained from a cashew nut processing plant where they are produced as waste from the main process. According to the processing stages, they might have already been roasted at about 400-470K. The CcNS samples were obtained directly from a palm field.

For testing purposes, the CNS used in these experiments were ground in a blender into a paste with reasonably consistent uniformity, although particles of about 1-3mm-size could still be found in the paste. The CcNS were milled into a very fine and uniform powder.

Characteristics of these important feedstocks are given by the ultimate and proximate analysis provided in table 1.

Table 1. Ultimate and Proximate Analysis of CNS and CcNS (by BELAB AB-Sweden)

| Characteristic | unit | dry basis | | dry, ash-free basis | |
|---|---|---|---|---|---|
| | | CNS | CcNS | CNS | CcNS |
| Ash | | 1.9 | 0.7 | | |
| Volatiles | %w/w | 81.8 | 74.9 | 83.4 | 75.3 |
| Fixed carbon | | 16.3 | 24.4 | 16.6 | 28.6 |
| C | %w/w | 58.3 | 53.9 | 59.45 | 54.7 |
| H | | 7.0 | 5.7 | 7.1 | 5.8 |
| N | | 0.7 | 0.1 | 0.7 | 0.1 |
| S | | 0.07 | 0.02 | 0.07 | 0.02 |
| Cl | | 0.02 | 0.12 | 0.02 | 0.12 |
| O | | 32.02 | 39.44 | 32.64 | 40.0 |
| *LHV*<br>*HHV* | MJ/kg | *22.539*<br>*24.051* | *19.265*<br>*20.515* | *22.975*<br>*24.517* | *16.726*<br>*19.265* |

## Experimental Setup

Experimental pyrolysis tests were performed in a TG-FTIR system at three different low heating rates. The setup adopted, illustrated schematically in Figure 1, consists of a sample-holder suspended from a balance in a gas stream within a furnace. As the sample is heated, the evolving volatile products are carried out of the furnace directly into a 5.1cm-diameter gas cell (heated to 428K) where the volatiles are analysed by FTIR spectrometer.

The FTIR spectra are obtained every 30–40 seconds to determine quantitatively the evolution rate and composition of several compounds. The system allows the sample to be heated on a pre-programmed temperature profile, at heating rate intervals as 3–100K/min, within 293 and 1373K. The system continuously monitors: (i) the time-dependent evolution of volatile species; (ii) the heavy liquid (tar) evolution rate and its infrared spectrum with identifiable bands from functional groups; and (iii) weight of the non-volatile material (residue). Further explanation on TG-FTIR as well as the species identification can be found in Bassilakis et al [12].

In the experiments carried out in this research, helium carrier gas was passed through oxygen trap to ensure an oxygen-free atmosphere during pyrolysis. The initial sample weight was 64–78 mg, and the flow rate of the carrier gas was 400 mL/min.

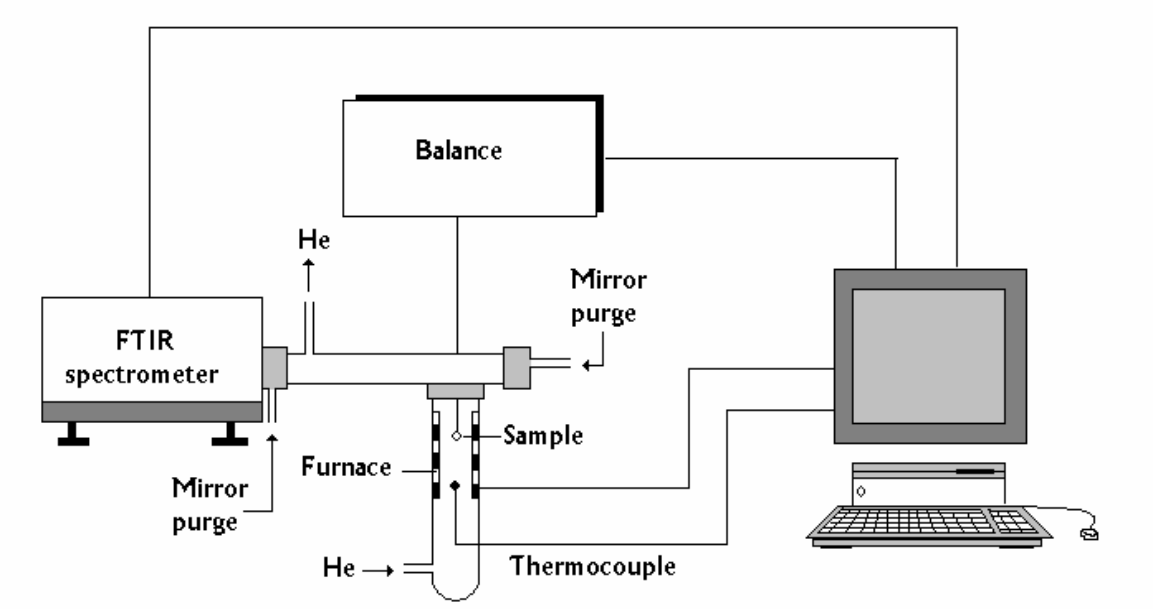


Figure 1. Schematic diagram of the TG-FTIR system

For each analysis, the sample material was heated in helium at 30K/min, first from ambient temperature to 333K for sample drying, and kept at this temperature for 30 minutes. The sample was then heated again to 1173K, for thermal degradation or pyrolysis. Upon reaching 1173K and holding the temperature for 3 minutes, the sample was immediately cooled to about 523K in a 20-minute period. After cooling, the helium flow was switched to a mixture of 21% O2 and 79% He (simulating the atmospheric air composition), and the temperature was ramped to 1173K at 30K/min to combust the remaining char. Concentrations of all volatile species, except for tar,

were determined using quantification routines obtained from calibration runs performed with pure compounds. Tar yields were determined by difference.

The volatile pyrolysis products species identified in this study are i) carbon monoxide (CO); ii) carbon dioxide ($CO_2$); iii) tar (by difference using gravimetric data); iv) water ($H_2O$); v) methane ($CH_4$); vi) ethylene ($C_2H_4$); vii) formaldehyde ($CH_2O$); viii) formic acid (HCOOH); ix) carbonyl sulphide (COS); x) acetic acid ($H_3CCOOH$); xi) methanol ($CH_3OH$); xii) ammonia (NH3); xiii) hydrogen cyanide (HCN); xiv) isocyanic acid (HCNO); xv) acetone ($H_3COCH_3$); xvi) phenol ($C_6H_5OH$) and xvii) acetaldehyde ($H_3CCHO$). Evolution patterns and yields of tars were determined by difference, using the sum of gases quantified by FTIR and the balance curve obtained thermogravimetrically.

## Methodology for Kinetic Parameters Determination

As already referred in this study, it was implicitly assumed that all the reactions followed a parallel-first-order independent kinetics mechanism, which is the most consensual assumption for biomass. This implies that each volatile species evolves as one or more time/temperature resolved peak(s), independently. Each one of these evolution peaks is associated with the existence of a respective precursor material in the original biomass sample, known as pool. Additionally, the shifts in shape and position of the peak as a function of the heating rate provide information on the intrinsic kinetics of the pyrolysis associated with a given peak. A Gaussian distribution of activation energies is assumed, with the mean value E0 and the width of the distribution function σ, for each peak.

For each of such reactions (i), the following reaction rate equation must be valid:

$$\frac{dV_i}{dt} = k_i\left(V_i^* - V_i\right) \qquad (1)$$

Where $V_i$ is the amount of volatile matter evolved, $V_i^*$ is the volatile-matter content (at infinite time), t is time, and $k_i$ is the reaction-rate constant.

By integrating equation (1) for several reactions and considering that the temperature, at constant heating rate, is time-dependent an follows the expression $T(t)=T_0+\beta T$, in which $T_0$ is the initial temperature and β is the heating rate; *t* is the time elapsed since the reaction started and $t_0$ is the time at which the temperature started, the final DAEM equation for non-isothermal process becomes:

$$\frac{V^* - V}{V^*} = \frac{1}{\sigma\sqrt{2\pi}}\int_0^{\infty}\exp\left[-A\int_{t_0}^{t}\exp\left(-\frac{E}{RT(t)}\right)dt - \frac{\left(E-E_0\right)^2}{2\sigma^2}\right]dE \qquad (2)$$

In this equation, A is the pre-exponential factor, E is the activation energy; $E_o$ is the mean activation energy; T(t) is temperature in degrees Kelvin, R is the universal gas constant and σ is the standard deviation of the activation energy. The details on the assumptions and restrictions to

use the DAEM are expansively discussed in the literature [7],[9]-[11] and do not constitute the aim of this article.

The code used in this study is derived from FG-DVC (functional group, devolatilization, cross-linking) code for coal. This code was adopted for biomass without the DVC component. To run this code, as already indicated somewhere in this document, one needs the kinetic parameters for each component evolving from pyrolysis process, such as the mean activation energy, the exponential factor, the standard deviation of the activation energy, and define the heating rates at which the model is to be applied for yields prediction.

In order to generate these data, experimental tests were performed at three different heating rates and the process monitored through a TG-FTIR system. The results obtained from this system are analyzed using $T_{max}$ approach for the determination of the kinetic parameters. This approach has been applied extensively and successfully by other researchers [12]- [19].

One of the non-isothermal methods for the determination of kinetic parameters is through the measurement of the temperature at which the devolatilization rate is the maximum ($T_{max}$). As commonly found, in a typical sequence of experiments, thermal-decomposition rates are measured at different heating rates. Thus, the relationship between the heating rate *ß* and the value of $T_{max}$ is given by the following equation:

$$\ln\left(\frac{\beta}{T_{\max}^2}\right) = \ln\left(\frac{AR}{E_0}\right) - \frac{E_0}{RT_{\max}} \qquad (3)$$

Equation (3) is the formula used for the determination of the kinetic parameters $A$ and $E_0$ [20]. While the value of $E_0$ is accurately determined even for wide distributions, the value of $A$ usually requires a slight adjustment (typically within a factor of two). The width of the assumed Gaussian distribution, σ, can then be determined from the width of the peak representing the rate of species evolution (or weight loss). In the $T_{max}$ method, some difficulties arise when peaks are not well resolved. In such cases, substantial shifts in $T_{max}$ may occur. However, unless peak deconvolution is attempted [21], the same problem arises when using the Friedman method. Another limitation is associated with the presence of small, multiple maxima superimposed on a broader peak, i.e., when the assumption of first-order kinetics is not fully supported. In this case, again, the applicability of both the $T_{max}$ and Friedman methods is reduced. The exact value of $T_{max}$ may also be difficult to determine for large and broad peaks.

Once $A$, $E_0$, values are determined, the sizes of different precursor pools for individual species and σ are determined by adjusting the simulated peak heights so that they best fit the TG-FTIR data.

At the end of the above procedure and for the evolution of each precursor pool (peak), $A$, $E_0$, σ and the pool size, i.e., the concentrations of the different precursor species are determined. In general, each volatile species (light gases and tars) may evolve as one or more peaks, and, consequently, a single or multiple precursor pools will be used in the simulations, correspondingly.

The above-described, $T_{max}$ method is often difficult to utilize with limited data resolution. Especially at 100K/min, there is a significant uncertainty in $T_{max}$ determination. Another reason to be considered as constraining the determination of $T_{max}$ is the size of the sample, which definitely

plays an important role in mass and heat transfer between the sample surface and its core. For this reason, it is sometimes advantageous to fit $A$, $E_0$ and σ values to experimental data using a trial-and-error approach. Non-unique solutions are usually found as a result of this fitting exercise, which is due to the so-called *compensation* effect. In other words, different pairs of kinetic parameters (A, $E_0$) provide equally good fit to experimental data. For this reason, the values of pre-exponential factors are often fixed, and selected in such a manner that they are consistent with the transition-state theory ($A \approx 10^{11}$–$10^{16}$ $s^{-1}$) [22]. In most cases, as it happened in this study, a value of $A = 2.2 \times 10^{13}$ $s^{-1}$ can be assumed as adequate.

## Results and Discussion

### Experimental Individual Gas Yields

Under the experimental conditions given in the previous section the following pyrolysis products were detected and the respective yields determined: carbon monoxide, carbon dioxide, tar (by difference), pyrolytic water, ethylene, methane, formaldehyde, acetaldehyde, formic acid, methanol, ammonia, hydrogen cyanide, isocyanic acid, sulphur dioxide, acetone, phenol and carbonyl sulphide.

Tables 2 and 3 give a summary of the results (yields) obtained from the experimental pyrolysis at 10, 30 and 30 K/min, for CNS and CcNS, respectively.

**Table 2. Cashew nut shells pyrolysis yields for each individual product[23]**

| Sample | ***Cashew nut shells*** | | | | | |
|---|---|---|---|---|---|---|
| Sample mass, mg | | | | | | |
| Heating rate, K/min | 10 | | 30 | | 100 | |
| Basis | a.r. | daf | a.r. | daf | a.r. | daf |
| Moisture | 1.41 | | 1.58 | | 1.48 | |
| ash | 1.92 | | 2.41 | | 1.69 | |
| volatiles (TG) | 79.47 | 82.21 | 79.84 | 83.16 | 81.04 | 83.69 |
| char (TG) | 17.20 | 17.79 | 16.17 | 16.84 | 15.79 | 16.31 |
| gas (FTIR) | 46.60 | 48.21 | 42.40 | 44.16 | 44.36 | 45.82 |
| tar (by difference) | 32.87 | 34.00 | 37.44 | 39.00 | 36.68 | 37.88 |
| pyrolytic water | 21.35 | 22.09 | 19.50 | 20.31 | 15.81 | 16.33 |
| carbon monoxide | 2.95 | 3.05 | 2.33 | 2.43 | 2.66 | 2.75 |
| carbon dioxide | 11.86 | 12.27 | 11.64 | 12.12 | 18.32 | 18.92 |
| methane | 3.13 | 3.24 | 2.24 | 2.34 | 1.87 | 1.93 |
| ammonia | 0.09 | 0.09 | 0.11 | 0.11 | 0.09 | 0.09 |
| hydrogen cyanide | 0.12 | 0.13 | 0.08 | 0.08 | 0.06 | 0.06 |
| isocyanic acid | 0.03 | 0.03 | 0.03 | 0.03 | 0.02 | 0.02 |
| ethylene | 0.14 | 0.14 | 0.13 | 0.13 | 0.12 | 0.13 |
| formaldehyde | 0.47 | 0.48 | 0.18 | 0.18 | 0.19 | 0.20 |
| sulphur dioxide | 0.00 | 0.00 | 0.00 | 0.00 | 0.00 | 0.00 |
| acetaldehyde | 2.11 | 2.18 | 2.26 | 2.35 | 1.92 | 1.98 |
| formic acid | 0.25 | 0.26 | 0.15 | 0.16 | 0.22 | 0.23 |
| acetic acid | 2.22 | 2.30 | 1.92 | 1.99 | 1.71 | 1.76 |
| methanol | 0.50 | 0.52 | 0.45 | 0.47 | 0.47 | 0.49 |
| carbonyl sulfide | 0.00 | 0.00 | 0.03 | 0.04 | 0.02 | 0.02 |
| phenol | 0.81 | 0.84 | 0.85 | 0.88 | 0.48 | 0.50 |
| acetone | 0.57 | 0.59 | 0.51 | 0.53 | 0.41 | 0.43 |

**Table 3. Coconut shells pyrolysis yields for individual products**

| Sample | *Coconut shells* | | | | | |
|---|---|---|---|---|---|---|
| Sample mass, mg | 41.35 | | 43.62 | | 30.51 | |
| Heating rate, K/min | 10 | | 30 | | 100 | |
| Basis | a.r. | daf | a.r. | daf | a.r. | daf |
| Moisture | 5.20 | | 5.18 | | 5.39 | |
| ash | 0.05 | | 0.84 | | 0.27 | |
| volatiles (TG) | 71.92 | 75.91 | 73.98 | 78.72 | 72.90 | 77.27 |
| char (TG) | 22.83 | 24.09 | 20.00 | 21.28 | 21.44 | 22.73 |
| gas (FTIR) | 51.17 | 54.00 | 42.77 | 45.51 | 34.10 | 36.15 |
| tar (by difference) | 20.75 | 21.90 | 31.21 | 33.21 | 38.80 | 41.13 |
| pyrolytic water | 16.89 | 17.83 | 12.00 | 12.77 | 10.47 | 11.10 |
| carbon monoxide | 4.20 | 4.43 | 3.11 | 3.31 | 2.52 | 2.67 |
| carbon dioxide | 7.37 | 7.78 | 7.53 | 8.01 | 6.04 | 6.40 |
| methane | 0.75 | 0.79 | 0.61 | 0.65 | 0.46 | 0.49 |
| ammonia | 0.00 | 0.00 | 0.00 | 0.00 | 0.00 | 0.00 |
| hydrogen cyanide | 0.04 | 0.04 | 0.01 | 0.01 | 0.01 | 0.01 |
| isocyanic acid | 0.00 | 0.00 | 0.00 | 0.00 | 0.00 | 0.00 |
| ethylene | 0.34 | 0.36 | 0.08 | 0.09 | 0.06 | 0.06 |
| formaldehyde | 1.43 | 1.51 | 1.41 | 1.51 | 1.16 | 1.23 |
| sulphur dioxide | 0.00 | 0.00 | 0.00 | 0.00 | 0.00 | 0.00 |
| acetaldehyde | 5.38 | 5.68 | 5.71 | 6.08 | 0.96 | 1.01 |
| formic acid | 1.69 | 1.79 | 1.41 | 1.50 | 0.26 | 0.27 |
| acetic acid | 5.05 | 5.33 | 4.94 | 5.26 | 7.28 | 7.72 |
| methanol | 1.72 | 1.82 | 1.27 | 1.35 | 1.10 | 1.17 |
| carbonyl sulfide | 0.03 | 0.03 | 0.04 | 0.04 | 0.00 | 0.00 |
| phenol | 4.81 | 5.08 | 3.12 | 3.32 | 2.90 | 3.07 |
| acetone | 1.46 | 1.54 | 1.52 | 1.62 | 0.88 | 0.93 |

The results showed that for CNS and CcNS, respectively, the tar yields range from 34 to 39% and from 22 to 41% daf; pyrolytic water from 16 to 20% and from 11 to 18% daf; acetaldehyde from 2.0 to 2.4% and from 1.0 to 5.7% daf; acetic acid from 1.8 to 2.3 % and from 5.3 to 7.7% daf; and, phenol from 0.8 to 0.9% and from 3.1 to 5.1% daf.

Comparing the yields from CNS and those from CcNS, the following analysis can be done: i) CNS yielded more gases and more tars, in general, compared to CcNS; ii) CcNS yielded more char than and more combustible gases than CNS; iii) although the moisture yield is higher in CcNS, the total water yields (pyrolyitic water included) are higher in CNS; and as a consequence of their poor in nitrogen content, iv) CcNS present pyrolysis gases that are poor in N-species.

Although CcNS samples were richer in total carbon content than CNS, the high moisture and oxygen content in CcNS make this kind of biomass to be comparably the poorer in energy content, as seen in table 1.

In general, as the heating rate increased, the main pyrolysis products such as char, gases and pyrolytic water, tended to decrease while volatiles and tar, increased. This is consistent with cross-linking secondary reactions as well as with the devolatilization heating rate dependence as seen in previous works.

**Pyrolysis kinetics and Pools**

As discussed earlier, all the reaction rates were considered as obeying a parallel-first-order independent kinetics mechanism. This assumption is unanimously considered as the most acceptable approach for the biomass devolatilization process as indicated by Tsamba et al [4]. The same hypotheses were applied successfully by other authors in the same field [12],[14],[15]. Results obtained through these assumptions are given in Table 4 (CNS) and 5 (CcNS), for $A=2.2x10^{13}s^{-1}$, as previously suggested. The precursors were numbered according to their respective onset temperature sequence for each product species.

**Table 4. Pools and kinetic parameters from CNS pyrolysis (for $A= 2.2 \times 10^{13}\ s^{-1}$)[23]**

| Species | Pool No. | Yield (%w/w daf) | $E_0/R$ ($10^4$K) | σ/R (K) |
|---|---|---|---|---|
| Carbon Monoxide | 1 | 0.430 | 2.01 | 390 |
| | 2 | 1.080 | 2.25 | 520 |
| | 3 | 1.230 | 2.73 | 2300 |
| Carbon Dioxide | 1 | 2.600 | 1.74 | 450 |
| | 2 | 5.200 | 1.92 | 1280 |
| | 3 | 3.700 | 2.26 | 600 |
| | 4 | 2.900 | 2.61 | 2500 |
| Tars | 1 | 31.000 | 1.99 | 600 |
| | 2 | 6.300 | 2.28 | 100 |
| Water | 1 | 3.870 | 1.50 | 1000 |
| | 2 | 6.050 | 1.98 | 1500 |
| | 3 | 5.000 | 2.26 | 500 |
| | 4 | 4.650 | 2.60 | 3500 |
| Methane | 1 | 0.280 | 2.08 | 1980 |
| | 2 | 2.220 | 3.02 | 2800 |
| Ethylene | 1 | 0.134 | 2.77 | 2200 |
| Phenol | 1 | 0.120 | 2.05 | 800 |
| | 2 | 0.618 | 2.74 | 3900 |
| Acetone | 1 | 0.515 | 2.17 | 1800 |
| Methanol | 1 | 0.490 | 1.87 | 500 |
| Hydrogen Cyanide | 1 | 0.089 | 2.23 | 4200 |

| | | | | |
|---|---|---|---|---|
| Ammonia | 1 | 0.004 | 1.58 | 1100 |
| | 2 | 0.007 | 2.18 | 100 |
| | 3 | 0.060 | 2.42 | 2800 |
| | 4 | 0.030 | 3.39 | 2400 |
| Formaldehyde | 1 | 0.288 | 2.08 | 1200 |
| Formic Acid | 1 | 0.216 | 2.20 | 1000 |
| Acetic Acid | 1 | 1.100 | 2.05 | 600 |
| | 2 | 0.918 | 2.28 | 400 |
| Acetaldehyde | 1 | 0.470 | 2.09 | 1 |
| | 2 | 1.700 | 2.27 | 200 |
| Isocyanic Acid | 1 | 0.028 | 2.55 | 2200 |

**Table 5. Pools and kinetic parameters from CcNS pyrolysis (for A= 2.2 x $10^{13}$ $s^{-1}$)**

| Species | Pool No. | Yield (wt% daf) | Eo/R ($10^4$ K) | σ/R (K) |
|---|---|---|---|---|
| Carbon monoxide | 1 | 5.42E-03 | 2.10 | 390 |
| | 2 | 1.38E-02 | 2.32 | 120 |
| | 3 | 6.00E-03 | 2.60 | 2300 |
| | 4 | 1.10E-02 | 2.70 | 2630 |
| Carbon dioxide | 1 | 3.40E-03 | 1.84 | 1000 |
| | 2 | 2.00E-02 | 2.10 | 160 |
| | 3 | 4.00E-02 | 2.29 | 490 |
| | 4 | 1.00E-02 | 2.55 | 2000 |
| Tars | 1 | 9.90E-02 | 2.11 | 60 |
| | 2 | 2.25E-01 | 2.32 | 150 |
| Water | 1 | 4.40E-02 | 2.09 | 800 |
| | 2 | 4.00E-02 | 2.32 | 100 |
| | 3 | 6.80E-02 | 2.64 | 3500 |
| Methane | 1 | 3.40E-03 | 2.55 | 1250 |
| | 2 | 6.80E-03 | 3.10 | 3100 |
| Ethylene | 1 | 1.50E-03 | 2.79 | 3200 |
| Phenol | 1 | 3.00E-02 | 2.14 | 1000 |
| | 2 | 9.00E-03 | 2.49 | 1290 |
| Acetone | 1 | 1.10E-03 | 2.00 | 180 |
| | 2 | 1.58E-02 | 2.24 | 880 |
| Methanol | 1 | 3.30E-03 | 2.07 | 350 |
| | 2 | 1.14E-02 | 2.41 | 800 |
| Hydrogen Cyanide | 1 | 6.50E-05 | 1.99 | 1200 |

| | | | | |
|---|---|---|---|---|
| | 2 | 1.49E-04 | 2.50 | 1000 |
| **Formaldehyde** | 1 | 1.43E-02 | 2.16 | 1200 |
| Carbonyl Sulphide | 1 | 3.30E-04 | 2.20 | 2000 |
| **Formic acid** | 1 | 7.40E-03 | 2.07 | 300 |
| | 2 | 6.90E-03 | 2.31 | 1 |
| **Acetic acid** | 1 | 3.50E-02 | 2.07 | 250 |
| | 2 | 2.70E-02 | 2.22 | 490 |
| **Acetaldehyde** | 1 | 8.50E-03 | 2.09 | 1 |
| | 2 | 5.00E-02 | 2.30 | 200 |

As seen in the Tables above (4 and 5), the number of pools differs from one species to another. In both CNS and CcNS, carbon dioxide, carbon monoxide, water and ammonia are released from more than two precursors while formaldehyde and ethylene are released from only one precursor. An important difference between these two biomass samples is noticeable such as the difference in the number of pools for CO (4 in CcNS, 3 in CNS), water (3 in CcNS, 4 in CNS), acetone, HCN and methanol (2 in CcNS, 1 in CNS).

These differences in the number of pools precursors as well as the differences in the quality of evolved gases can be considered as a direct consequence of the difference in chemical composition between the biomass samples in study. However, the difficulties referred previously regarding the precision in the determination of $T_{max}$ may also have contributed to influence the results.

**Modelling Pyrolysis Evolved Gases**

The data obtained from this experiment (indicated in Tables 4 and 5), explicitly the kinetic parameters and the pool sizes, were used to generate input files for a DAEM code known as FG-Biomass. The code was the checked and adjusted by predicting the yields at the same heating rates and temperature programs as the experimental tests previously performed.

In general, the model agreed with the experimental results as it was possible to successfully replicate the location of the evolution peaks for individual pyrolysis product species. Yet, for a number of species, the model-predicted yields could not fit precisely the experimental yields at all heating rates.

These deviations are due to a different number of reasons such as the fact that i) the code still does not include the cross-linking competitive secondary reactions responsible for partial conversion of the tars into volatiles and char coking, and thus, influencing the yields of volatiles, char and tar; ii) the assumption of the reaction mechanism can be incompatible with this specific biomass samples and, iii) the sample mass might have influenced the transfer phenomena between the core and the surface of the sample, among other probable reasons.

Given these facts and the deviations found, the adjustment of the model could only be made by overpredicting or underpredicting the yields in one or another case (heating rate), and assuming a compromise to keep the deviation as lower as possible.

Following this approach, the following results were obtained (Figures 2 and 3).

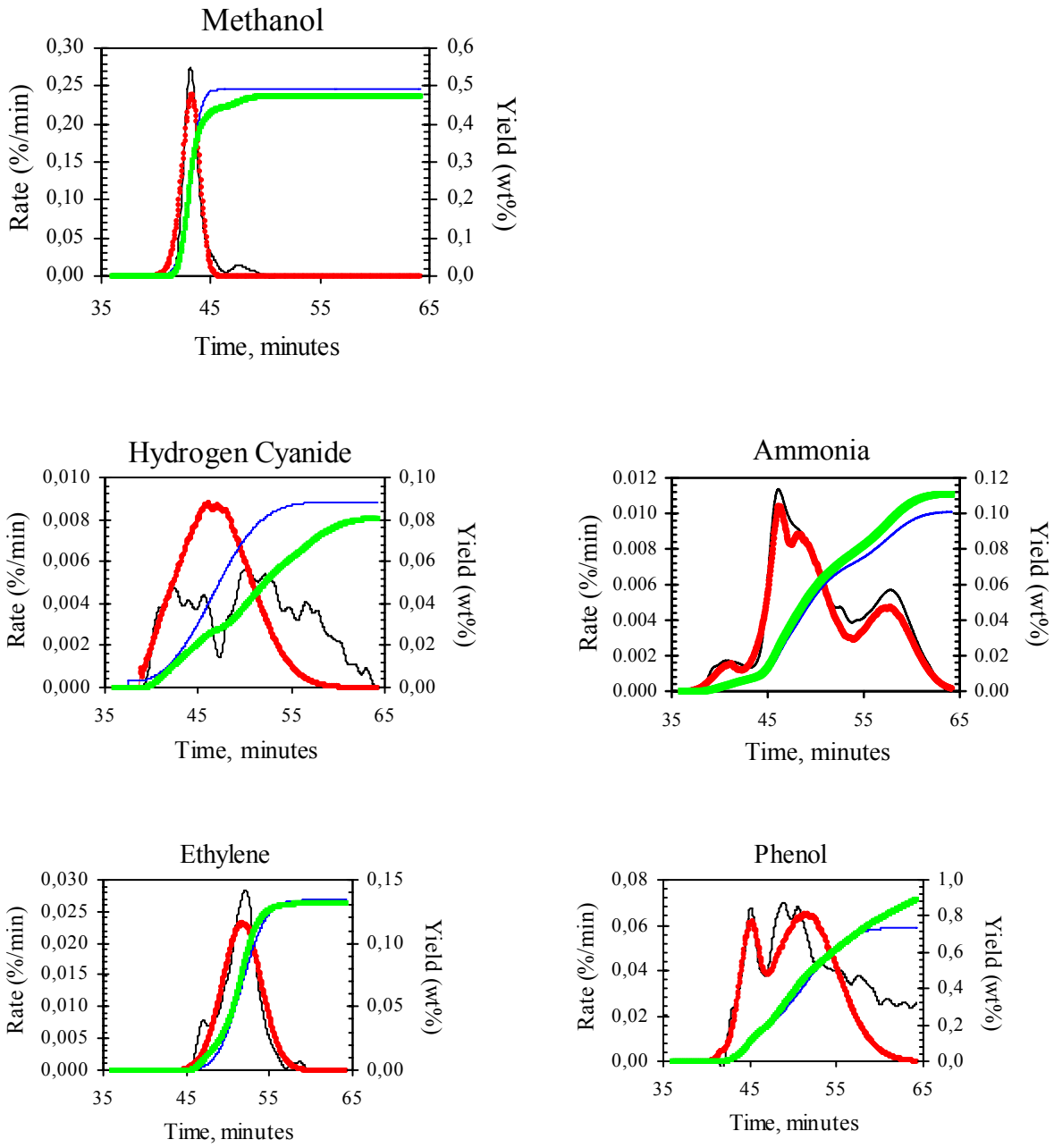


Fig. 2. Pyrolysis products yields and rates at 30 K/min (for CNS): black and blue curves are from TG-FTIR experimental results; green and blue curves are model-predicted curves [23]

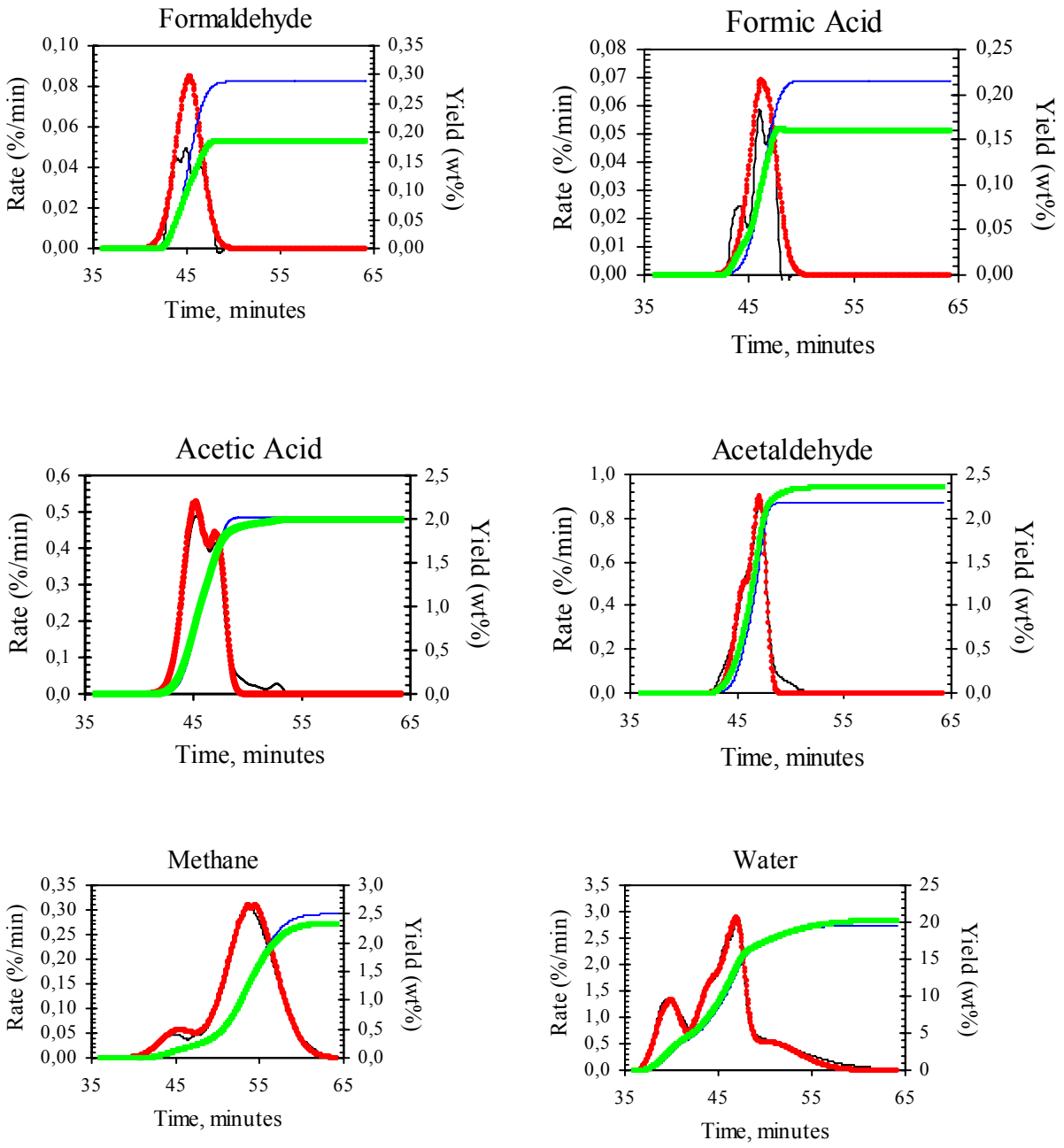


Fig. 2 (continued). Pyrolysis products yields and rates at 30 K/min (for CNS): black and blue curves are from TG-FTIR experimental results; green and blue curves are model-predicted curves[23]

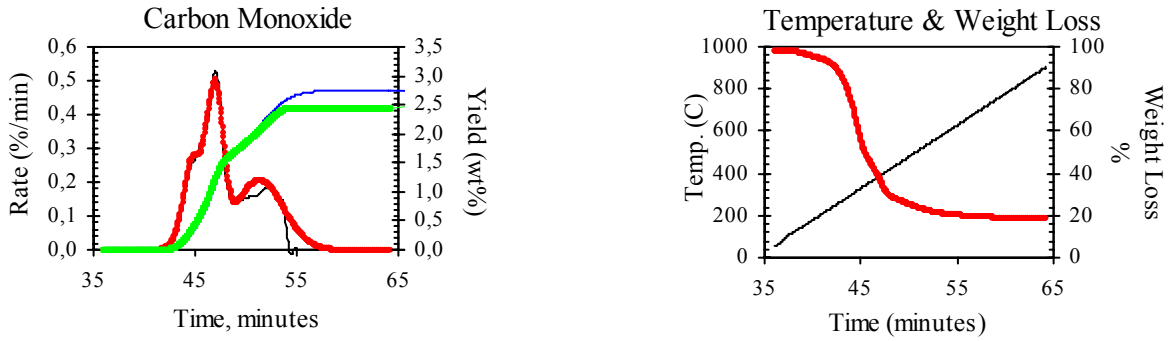


Fig. 2(continued). Pyrolysis products yields and rates at 30 K/min (for CNS): black and blue curves are from TG-FTIR experimental results; green and blue curves are model-predicted curves [23]

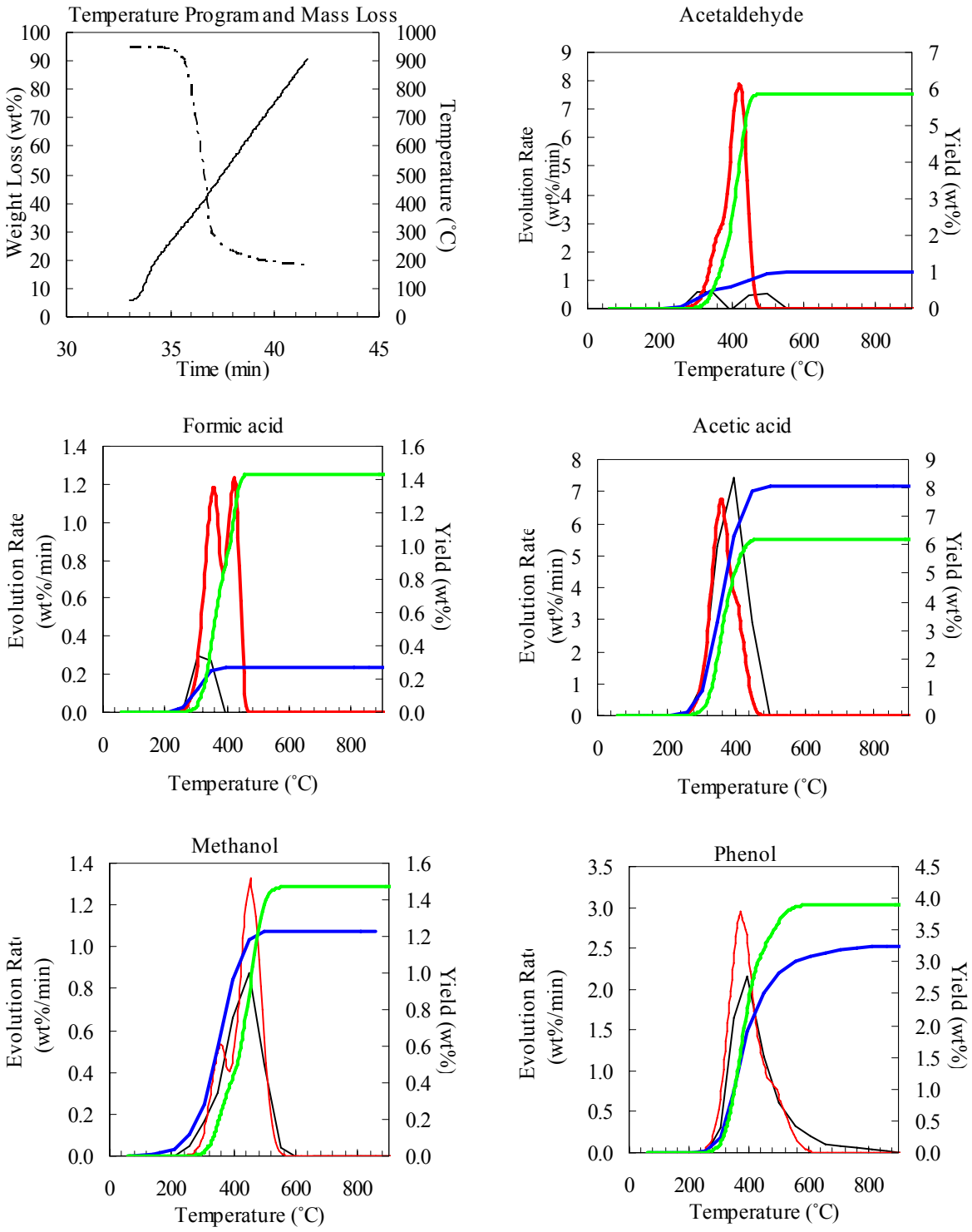


Fig. 3. Pyrolysis products yields and rates at 30 K/min (for CcNS): black and blue curves are from TG-FTIR experimental results; green and blue curves are model-predicted curves

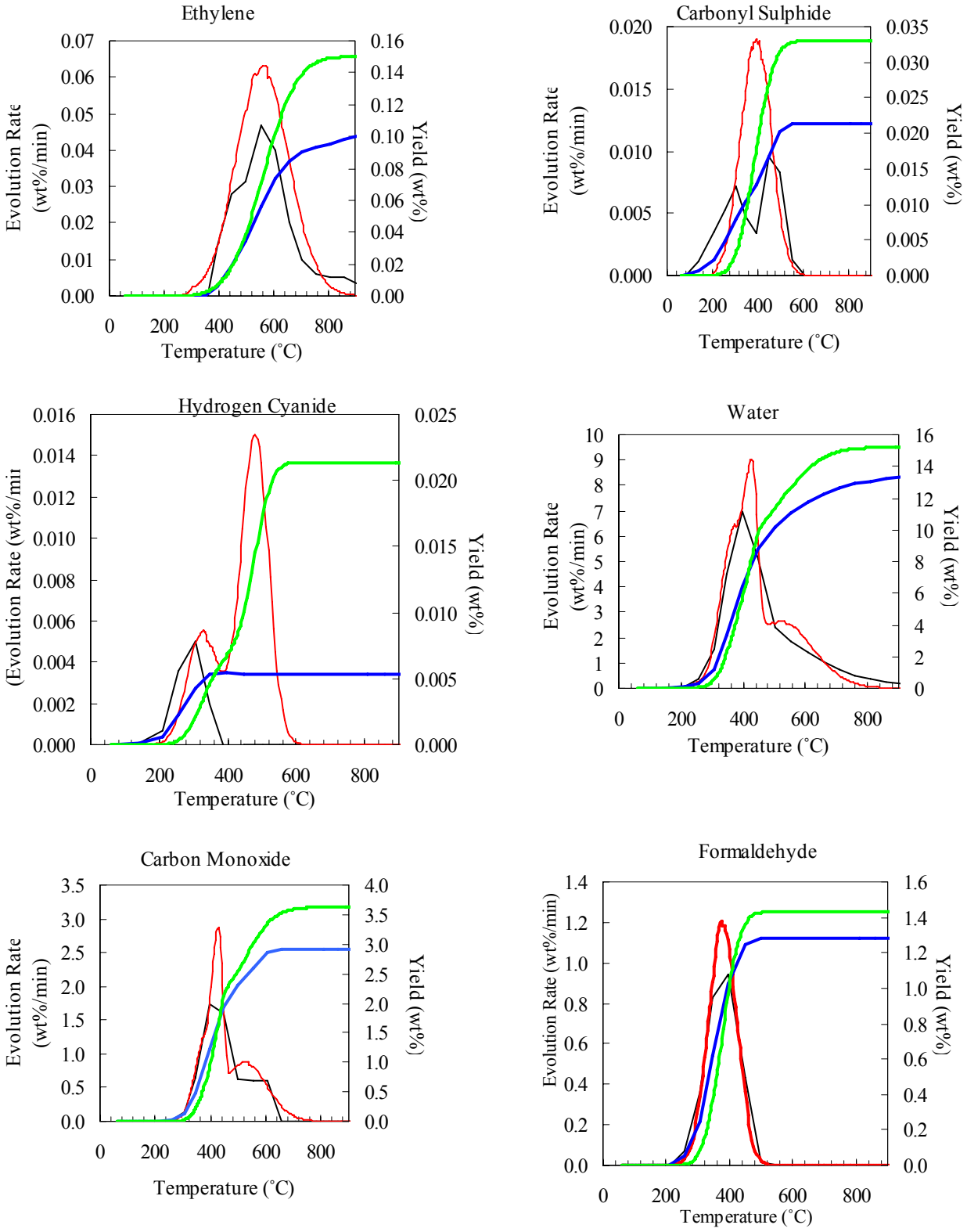


Fig. 3(continued). Pyrolysis products yields and rates at 100 K/min (for CcNS): black and blue curves are from TG-FTIR experimental results; green and blue curves are model-predicted curves

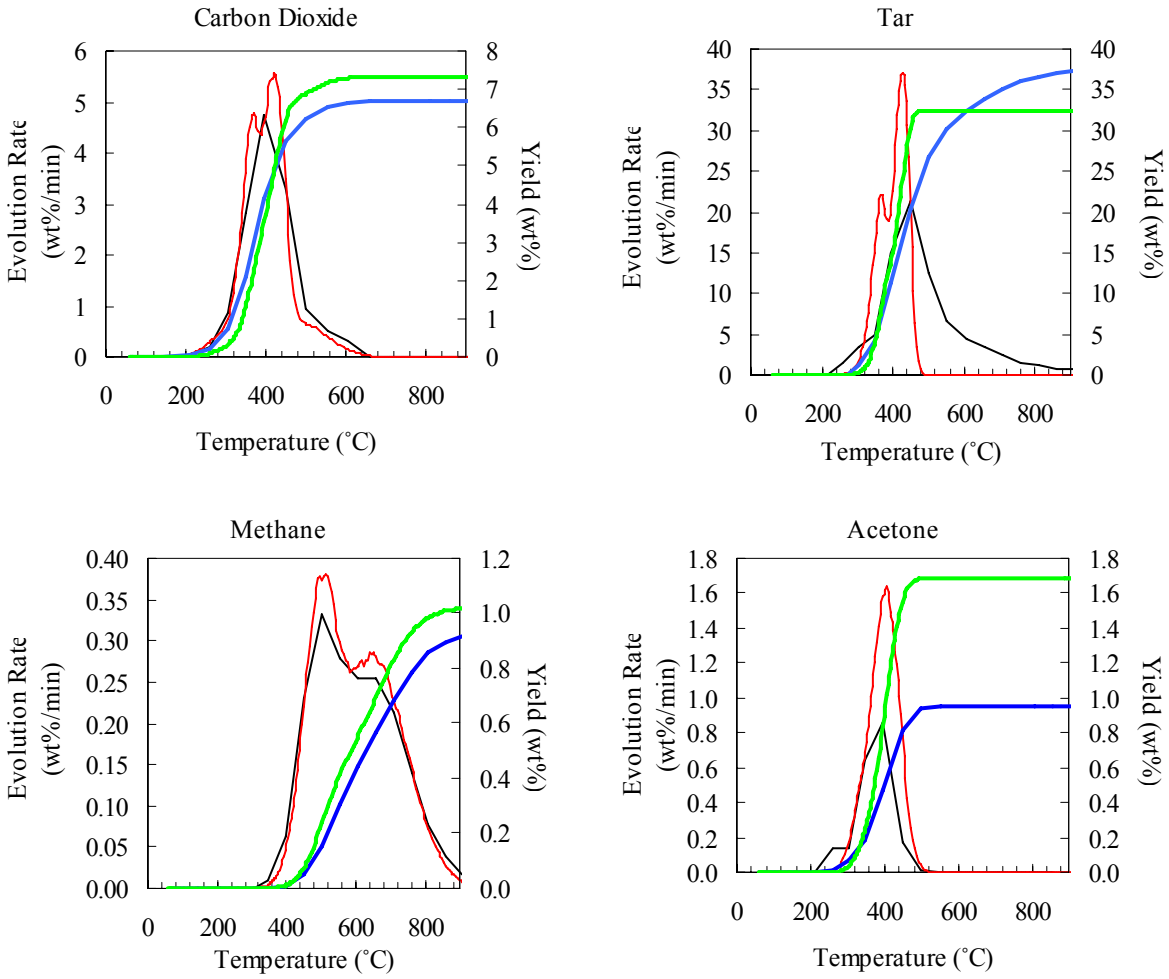


Fig. 3(continued). Pyrolysis products yields and rates at 100 K/min (for CcNS): black and blue curves are from TG-FTIR experimental results; green and blue curves are model-predicted curves

The figures above show clearly the deviations found by comparing the rate peaks and yields from experimental data and the same data obtained through modelling following the same temperature program.

As the input files obtained are made up of intrinsic kinetics and therefore independent of the heating rate, they can be applied for modelling at any heating rate.

Based in these input files, the code was then used to model the yields at very high heating rate such as 1,000 and 10,000K/s. The figures bellow are given just to illustrate the changes that are to be expected.

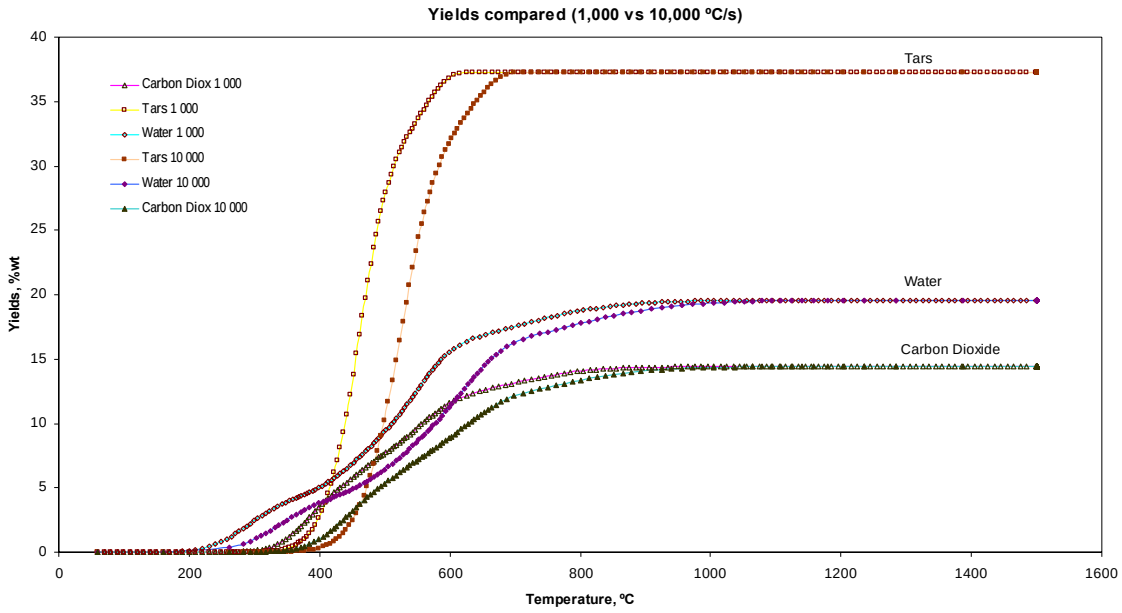


**Figure 3. Yields at high heating rates for $CO_2$, $H_2O$ and Tars from CNS**

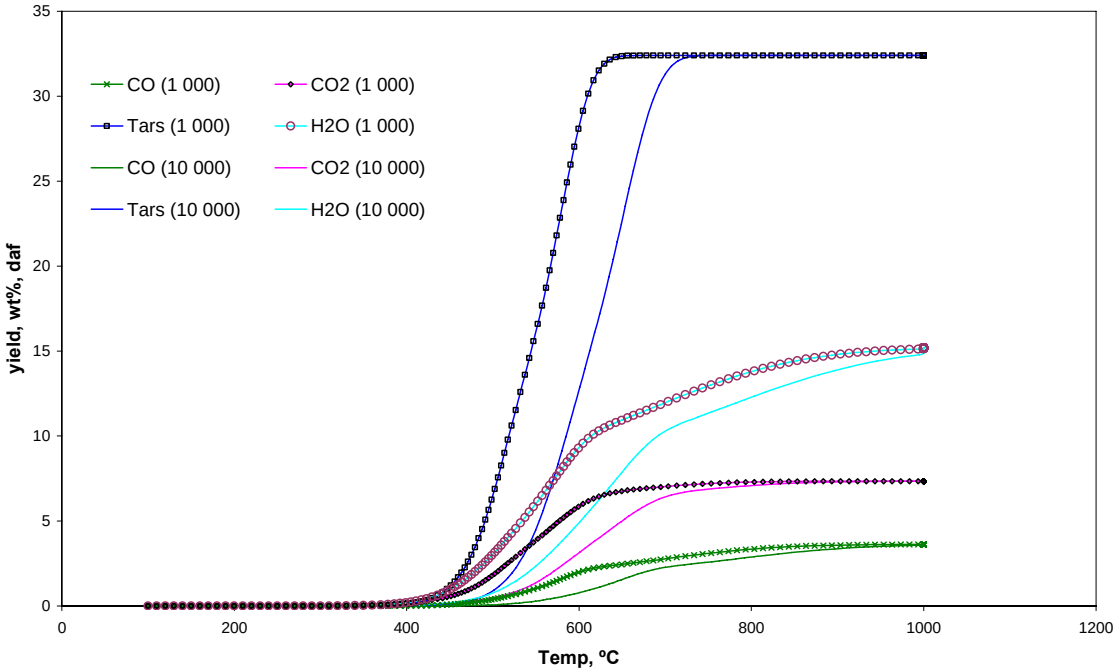


**Figure 4. Yields at high heating rates for $CO_2$, CO, $H_2O$ and Tars from CcNS**

From these figures, one can note that the yields do not change substantially. In fact, at high heating rate there is a delay in temperature level at which the maximum yield is achieved. On the contrary, in a time based comparison, the highest the heating rate, the lowest the time interval needed to achieve the maximum yield will be. This behaviour was noticed in all the remaining components. In order to maximise the yields, at very high heating rates, there may be necessary to keep the maximum temperature constant for some time, it is, to add a plateau to the temperature

program upon reaching the maximum temperature expected to give the maximum yield of a certain pyrolysis product.

**Conclusions**

TG-FTIR system was successfully used to determine and identify individual CNS and CcNS pyrolysis products and respective gas precursors (pools) at low heating rates (10, 30 and 100K/min) and to generate the respective intrinsic kinetics data, used as input files in a DAEM code to model pyrolysis yields and rates at different heating rates in a DAEM code.

By comparing the model predicted data with those generated experimentally, it was found that the model does simulate with acceptable fidelity the peaks location and the yields. However, as the model does not include the cross-linking competitive secondary reactions, the model-predicted yields presented deviations that may be resolved by improving the code. In fact, because of this fact, the main difference noticed at high heating rates is time and temperature shift at which a certain yield is achieved. Therefore, the change observed in volatiles, gases and tars yields that should accompany the heating rate increase, tend to be negligible.

# REFERENCES


[1]. YAMAN S.; Energy Conversion & Management 45 (2004) 651-671

[2]. HOQUE M.M. and BATTACHARYA S.C.; Energy 26 (2001) 101-110

[3]. RAVEENDRAN K., GANESH A and KHILAR K.; Fuel 75 (1995) 987-998

[4]. TSAMBA A.J., YANG W. and BLASIAK W.; Fuel Processing Technology, 2006; 87-6, 523-30

[5]. TSAMBA A.J., YANG W. and BLASIAK W.; Proceedings from the 8th International Conference on Energy for a Clean Air (CLEANAIR2005), Lisbon, Portugal, June 27-30th, 2005

[6]. TSAMBA A.J., YANG W., BLASIAK W. and WÓJTOWICZ, M.; 25th Incineration and Thermal Treatment Technologies International Conference (IT3'2006), Savannah, GA, May 15-19th, 2006

[7]. ROSTAMI A.A., HAJALIGOL M.R. and WRENN S.E.; Fuel, 2004, 83, 1519-1525

[8]. MAKI T., TAKATSUNO A. and MIURA K.; Energy & Fuels, 1997, 11, 972-977

[9]. ANTHONY D.B., HOWARD, J.B., HOTTEL, H.C. and MEISSNER, H.P. 15th Symposium (Int) on Combustion. The Combustion Institute, Pittsburg, 1975

[10]. SCOTT S.A., DENNIS J.S., DAVIDSON J.F. and HAYHURST A.N.; Fuel, 2006, 85, 1248-1253

[11]. GÜNES M. and GÜNES S.; Applied Mathematics and Computation, 2002, 130, 619-628

[12]. BASSILAKIS R., CARANGELO R.M. and WÓJTOWICZ M.A.; Fuel, 2001, 80, 1765-1786

[13]. WÓJTOWICZ M.A., BASSILAKIS R., SMITH W.W., CHEN Y. and CARANGELO R.M.; J. Anal. Appl. Pyrolysis, 2003, 66, 235-261

[14]. De JONG W., PIRONE A. and WÓJTOWICZ M.A.; Fuel, 2003, 82, 1139-1147

[15]. HOLSTEIN A., BASSILAKIS R. and WÓJTOWICZ M.A.; Proc. Combustion Institute, 2005, 30, 2177-2185

[16]. BAKER R.R., COBURN S., LIU C. and TETTEH J. J.; Anal. Appl. Pyrolysis, 2005, 74, 171-180

[17]. CARANGELO, R.M.; SOLOMON, P.R. and GERSON, D.J.; Fuel 66, 960 (1987)

[18]. WHELAN, J.K.; SOLOMON, P.R.; DESHPANDE, G.V. and CARANGELO, R.M.; Energy & Fuels 2, 65 (1988)

[19]. De JONG W., Di NOLA G., VENNEKER B.C.H., SPLIETHOFF H. and WÓJTOWICZ M.; Fuel, 2007, doi:10.106/j.fuel.2007.01.32 (article in press)

[20]. TENG, H., SERIO, M.A., WÓJTOWICZ, M.A., BASSILAKIS, R. and SOLOMON, P.R. Ind. Eng. Chem. Research. 1995; 34, 3102-11

[21]. KIM, S., PARK, J.K. and CHUN, H.D.; Journal Env. Engineering. July 1968; 507

[22]. Benson, S.W.; Thermochemical kinetics. John Willey & Sons. 1968

[23]. TSAMBA A.J., YANG W., BLASIAK W. and WÓJTOWICZ M.A.; Energy & Fuels, 2007, DOI:10.1021/ef0604792 (article in press)

Annex 6

# Cashew Nut Shells Char Reactivity and Combustion Kinetics

***Tsamba, A. J.***, *Yang, W., Blasiak, W. and Wójtowicz, M.A.*

Presented to
*International Conference on Incineration and Thermal Treatment Technologies (IT3'07)*
Phoenix, AZ (USA), May 14-18th, 2007


Royal Institute of Technology

School of Industrial Management and Engineering

Department of Materials Science and Engineering

Division of Energy and Furnace Technology

Brinellvägen 23

SE-100 44 Stockholm

SWEDEN

# CASHEW NUT SHELLS CHAR REACTIVITY AND COMBUSTION KINETICS

Tsamba, A.J.[©], Yang, W. and Blasiak, W.

ROYAL INSTITUTE OF TECHNOLOGY (KTH)
School of Industrial Engineering and Management,
Department of Materials Science and Engineering
Energy and Furnace Technology Division
Brinellvägen 23, SE-100 44 Stockholm, SWEDEN

## ABSTRACT

Combustion process is regarded as the most primitive and well-known chemical reaction. However, as the research on combustion increases, it becomes a fact that it is a very complex process with different parameters and features that cannot be studied at the same time and therefore, are not well known as such. In this study, cashew nut char, produced through pyrolysis at three different heating rates, is submitted to a combustion using a binary mixture of $O_2$ and He to study char reactivity and determine char combustion kinetic parameters. Reactivity is studied by using the critical temperature approach and peak separation software while kinetics is determined through the NETZSCH advanced software that allows the determination of the frequency factor, the activation energy and the reaction order. The results are compared to the similar data available from the literature for other biomasses. Cashew nut shells pyrolysis char was found to be more reactive than char from olive husks, grape residues and pine woods pyrolysis.

**Key words:** *char, combustion, reactivity, kinetics*

## INTRODUCTION

Climate change due to global warming is believed to be directly related to greenhouse effect mainly caused by anthropogenic emissions of the so called greenhouse gases. Among these gases, the most representative is carbon dioxide, which is by a large extent emitted from energy activities either from demand side or supply side. Contrasting with the biomass research boom in 70s, that was triggered by oil crisis, the massive increase in renewable energy sources like biomass, solar and wind research testified in the last two decades has to be attributed to the need of mitigating greenhouse gas effects and consequently reduce global warming. In fact, these energy sources, apart from being renewables, they are $CO_2$-neutral, meaning that they are environmentally friendly or their net emissions contribution to the greenhouse effect is nix.

[©] Corresponding author: ajtsamba@zebra.uem.mz (Alberto Júlio Tsamba)
Fax: +46 8 20 76 81 Ph: +46 8 790 6545

Solid biomass energy conversion forms are mainly based on thermochemical processes such as pyrolysis, gasification and combustion any of which requires a well designed technology to suit the uniqueness of a specified feedstock. In fact, biomass feedstocks differ from species to species and from place to place, according to the characteristics in which such feedstock is grown. The design of these technologies demands accurate thermal and chemical characteristic data of the feedstock.

As technical data, regarding tropical biomass as energy sources, is seldom available, this study, focusing on cashew nut shells char combustion, pretends to contribute to fill this gap as much as possible. It is part of a wide range of research studies in progress aiming at characterizing tropical biomass wastes by generating data to support proper technology design to accommodate different seasonal feedstocks conversion to energy without major changes, when switching from one to another.

Although combustion reaction (carbon-oxygen chemical interaction) is regarded as the most important and the oldest chemical reaction "known" by the human kind, it is still recognized as complex and made up of a number of diversified phenomena. Indeed, phenomena like mass and heat transfer along with various parallel and in series chemical reactions are present in this process, determining different behavior according to the conditions under which the process is being conducted. These complexities make combustion process a never-ending research field for different disciplines.

The focus of this study is the reactivity of cashew nut char and its combustion kinetics. Reactivity of biomass char is an important parameter that determines its promptness to react with oxygen, therefore, the whole reaction kinetics. On the other hand, reactivity of solids is related to their surface are and thus to their porosity. Indeed, evidences indicate that small char micropores might not be fully used during combustion [1].

Reactivity decreases while the char combustion proceeds due to the disappearance of highly reactive components and qualitative and quantitative negative changes in inorganics, which play a catalytic role in char combustion [2]. In general, chars from materials with high volatiles content tend to be most reactive.

Char combustion kinetics modeling is difficult given the complexity of the carbon-oxygen reaction mechanism that is greatly influenced by transient build up of surface oxides, the diffusion of these oxides, the inorganic catalysis and the heterogeneity of surface sites [3]. Indeed, char particle combustion may be controlled by chemical reaction or transport phenomena (intra-particle or extra-particle diffusion of gases).

These char combustion rate controlling parameters can be i) intrinsic kinetics of the reaction, ii) mass transfer through pores inside the particle, or iii) oxygen mass transfer to the exterior of the particle [4]. Intrinsic kinetics is the limiting parameter at temperatures up to 700-800 C, in a regime where heat and mass transfer become less significant. Intraparticle diffusion occurs when the burning is confined to the external surface of the particle resulting in the shrinkage of the char particle at a constant density. This regime is characterized by a limited diffusion of oxygen into the inside of the particle. As a

consequence, under these conditions, the reaction rate is proportional to the particle external surface area and the burn-off time is proportional to the particle initial size. When external mass transfer from inside the char particle is the rate-limiting factor, the char shrinks at constant density [4,5].

## Methodology

Cashew nut shells (CNS) chars obtained from pyrolysis in a thermogravimetric analyzer at three different heating (10, 30 and 100 K/min) is submitted to a process of combustion in the same device at 30 K/min, as shown in figure 1, using a binary mixture of oxygen (21%) and helium.

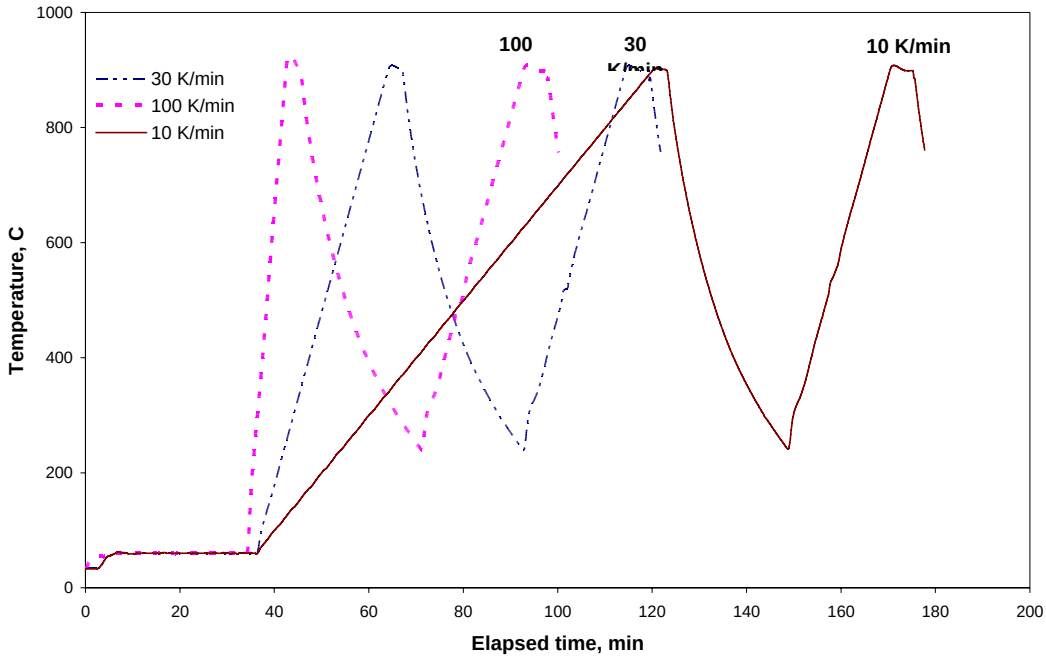


**Figure 1. Temperature Program (pyrolysis and combustion)**

For each analysis, approximately 64–78 mg of the sample material was heated in helium at 30K/mn, first to 60°C to dry the sample for 30 minutes, and then to 900 °C for pyrolysis. Upon reaching 900 °C and holding the temperature for 3 minutes, the sample was immediately cooled to about 250 °C over a 20-minute period. After cooling, a flow of the mixture of 21% $O_2$ and 79% He was switched to the thermobalance at 400 ml/mn, and the temperature was ramped to 900 °C at 30K/mn to combust the char. In these experiments, the carrier gas (He) was passed through oxygen trap to ensure an oxygen-free environment during pyrolysis. Mass change was taken every 30-40 seconds.

The mass changes obtained from the combustion experiments were used to determine the reactivity and the kinetics parameters of cashew nut char combustion process.

The determination of reactivity was performed using a simplified method successfully applied by *Wojtówicz et al* [6] that is based on the critical temperature ($T_{crit}$) concept. According to this simple approach, $T_{crit}$ can be defined as the temperature at which the rate of mass loss is 0.065/min, which is found to be high enough to be measured but low enough to ensure intrinsic kinetic-controlled regime. Thus, char reactivity index can be related to $1/T_{crit}$. This method is considered reproducible for any type of char.

The intrinsic kinetics parameters were determined using the NETZSCH Advanced Kinetics Model that allows the determination of the activation energy *(E)*, frequency factor *( A)* and reaction order *(m)* from thermogravimetric data.
The results obtained are compared to the data available in the literature for other kind of biomasses.

## Results and discussion

### *Char reactivity*

Figures 2-4 show the derivative thermograms for cashew nut shells char combustion. These curves show typically two peaks. The first peak, the major and most distinctive, occurs at lower temperatures while the second, clearly shown in Figs 3-4 for chars obtained at 30 and 100 K/min ($char^{(30)}$ and $char^{(100)}$), respectively[a].

Evidence found from this experiment is that char combustion takes place in two distinct stages, each one represented clearly by the respective peak. The second peak represents less than 10%mass loss during combustion and is less evident in the char obtained at 10 K/min. Based in Di Blasi et al study [2], the first peak represents the stage in which the combustion of aliphatic groups takes place while the second would be representing the combustion of aromatic groups.

Additionally, it can be found that the higher the pyrolysis heating rate, the higher the reactivity of the char obtained. In fact, this is obvious taking in account that at lower heating rates the reaction (residence) time is longer than at higher heating rates. Therefore, the devolatilisation process tends to be enhanced at the lowest heating rates. As the content of volatile components in the char contributes to its porosity and reactivity, chars that are poor in volatiles will, thus, be comparatively less reactive.

[a] Dot line represents experimental results while continuous lines represent peak separation redrawing.

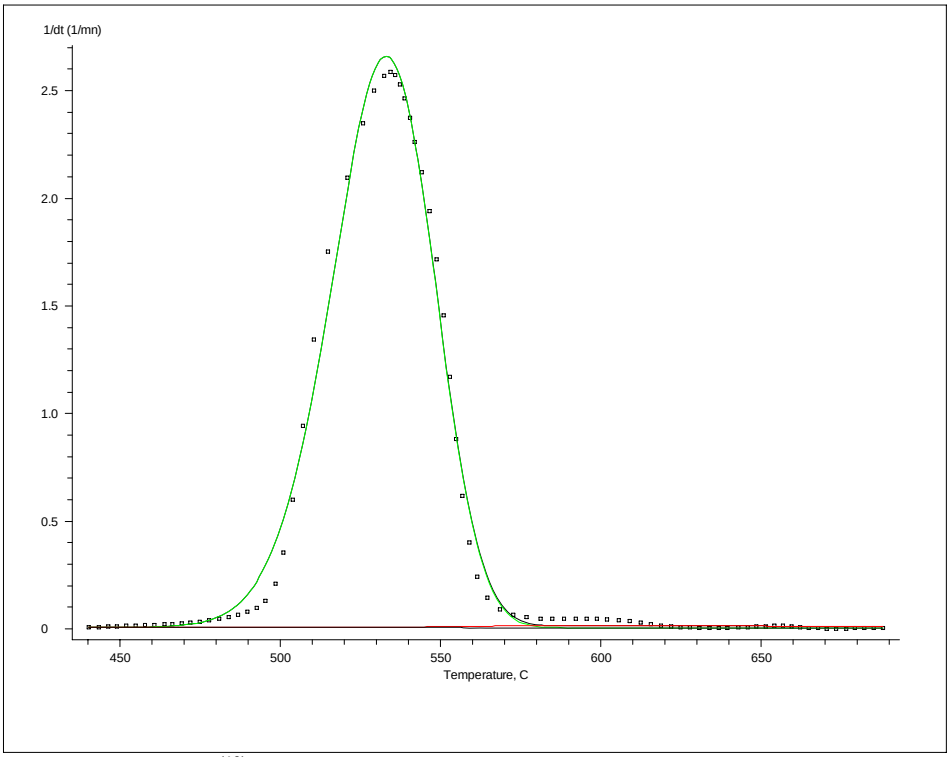


**Figure 2. DTG for char[10] combustion (dot-line is from the experiment; full line: prediction)**

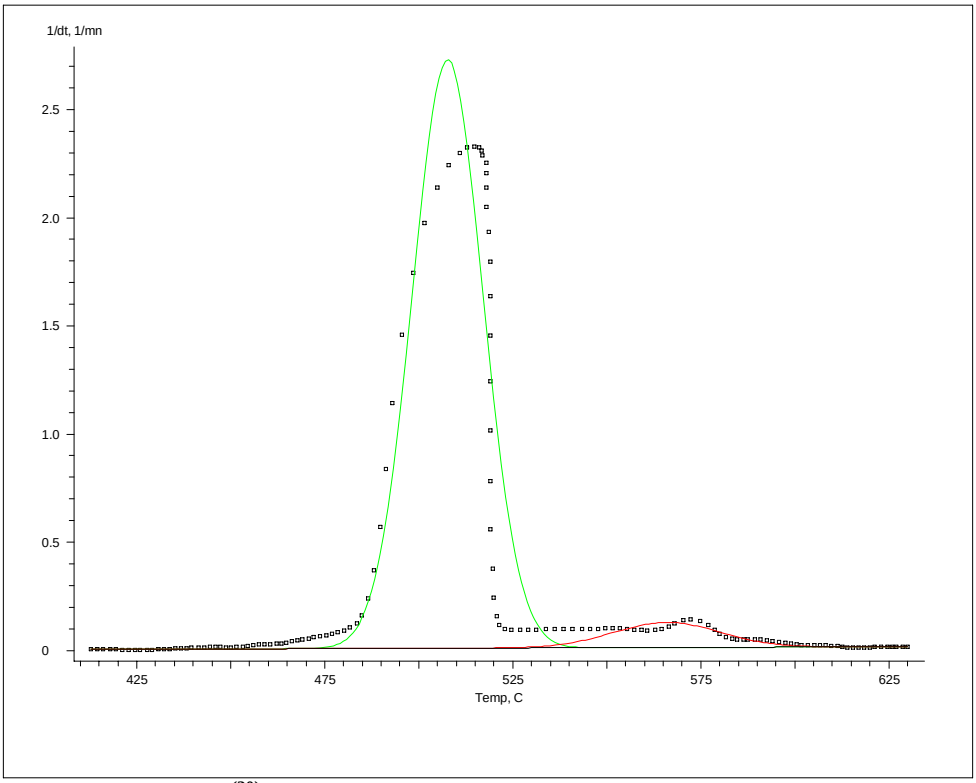


**Figure 3. DTG for char[30] combustion (dot-line is from the experiment; full line: prediction)**

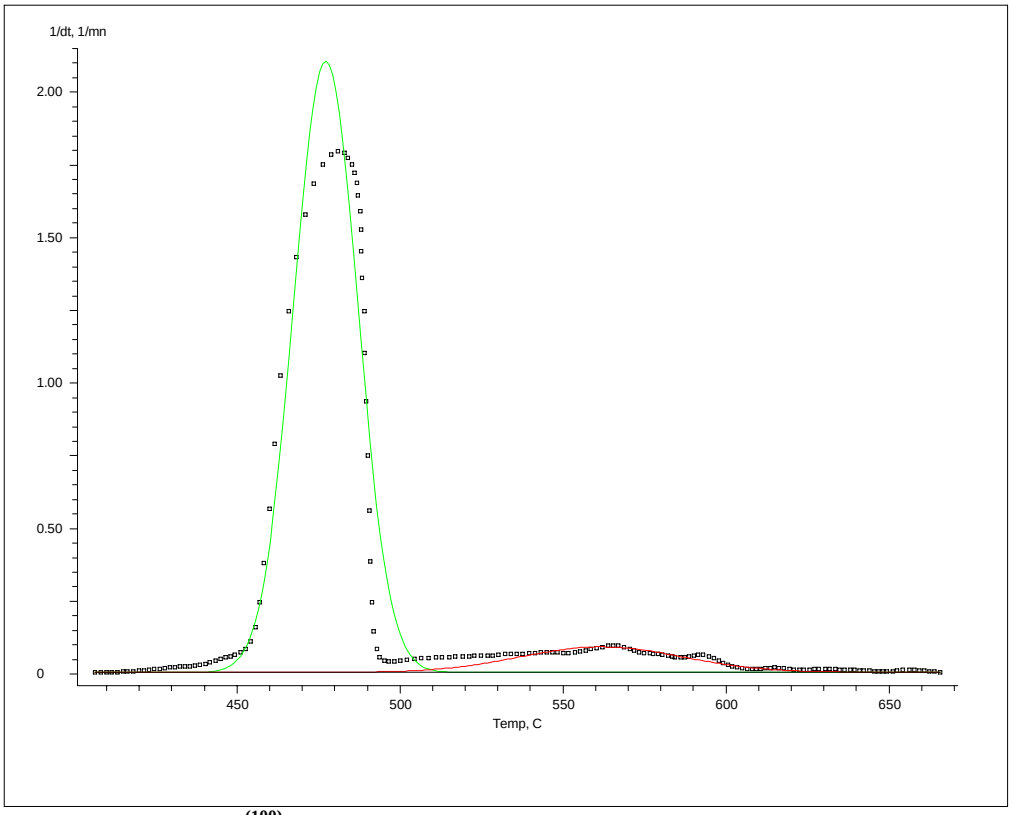


**Figure 4. DTG for char$^{(100)}$ combustion (dot-line is from the experiment; full-line: prediction)**

Additionally, NETZSCH peak separation software allowed separating and determining the contribution of each stage (peak) to the total mass loss reaction. This allowed the determination of the relative composition of cashew nut chars in aliphatic and aromatic groups. Based on this, it was found that aliphatic groups account for more than 90% wt of the CNS char mass.

The principal characteristics obtained from these results are summarized in table 1 and the trends are plotted in figure 5. In both the table and figure 5, $T_{on(set)}$ is the temperature at which the peak starts growing and represents the temperature at which the chemical reaction (or mass change) starts for a specific stage (represented by a particular peak); $T_{off(set)}$, represents the temperature at which a particular reaction ends; $T_{max}$ represents the temperature at which the reaction rate is the maximum for a particular stage; $DTG_{max}$ represents the magnitude of the maximum mass change (reaction) rate. $T_{crit}$ is the temperature at which the reaction rate equals 0.065g/g. min, as explained before. The fraction of the sample that reacts in a particular stage is represent in percentage that is determined from the respective peak area (%Area).

**Table 1. CNS combustion peaks' statistics summary**

| H-rate, K/min | Peak N°. | $T_{onset}$ (°C) | $T_{offset}$ (°C) | $T_{max}$ (°C) | $DTG_{max}$, $min^{-1}$ | %Area | $T_{crit}$ (°C) | 1/Tcrit $(°C^{-1})x10^{-3}$ |
|---|---|---|---|---|---|---|---|---|
| 10 | 1 | 450.5 | 564.6 | 535.8 | 2.582 | 97.67 | 478.2 | 2.09 |
| | 2 | 500.2 | (935.6) | 607.8 | 0.062 | 2.33 | | |
| 30 | 1 | 452.6 | 526.4 | 507.7 | 2.461 | 93.97 | 465.3 | 2.15 |
| | 2 | 536.2 | 593.8 | 564.6 | 0.192 | 6.03 | | |
| 100 | 1 | 455.6 | 492.7 | 477.2 | 1.965 | 90.42 | 450.1 | 2.22 |
| | 2 | 495.1 | 612.1 | 562.0 | 0.143 | 9.58 | | |

As it appears from these readings, the onset, offset and critical temperatures are almost in the same range for the three char samples. However, except the onset temperatures, the plots clearly show that the remaining reference temperatures (offset and maximum combustion rate) tend to decrease with the heating rate increase.

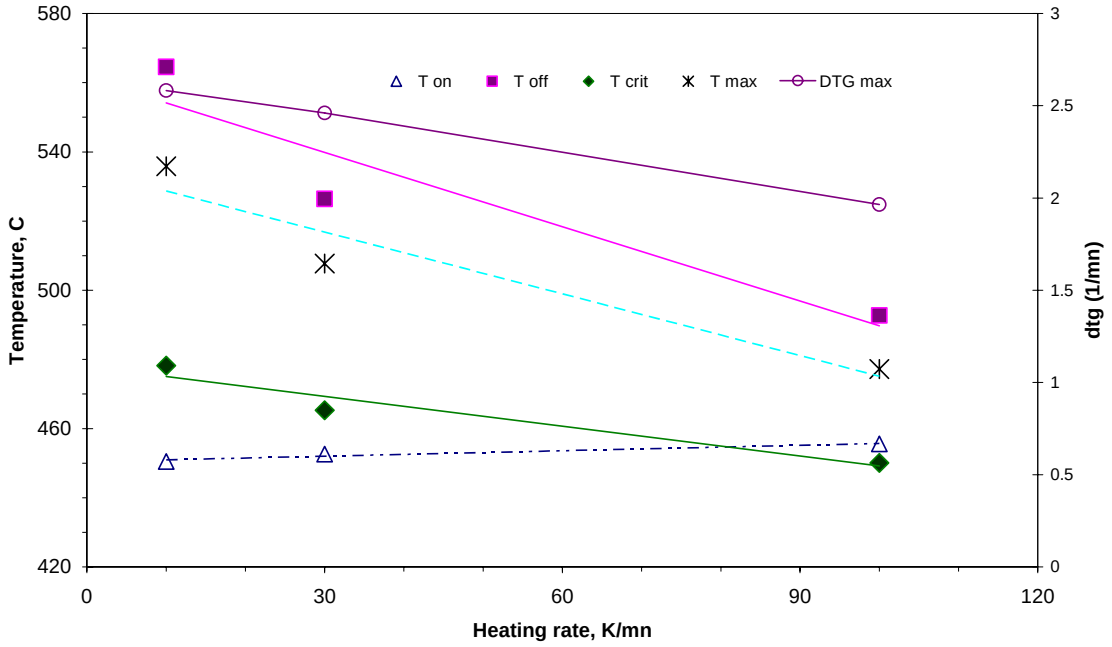


**Figure 5. Combustion peaks' statistics trends (peak 1)**

Using peak 1 as reference, and referring to the onset and critical temperature, and taking in account that the higher the temperature, the lower the reactivity, it can be confirmed that chars generated at lower heating rates are less reactive than those generated at high heating rate, which is in line with the explanation given elsewhere in this text. Nevertheless, the maximum reaction rate tends to decrease when the pyrolysis heating rate at which the char is generated increases. The opposite would be expected. The far right column in Table in table 1 also shows this trend through the inverse of $T_{crit}$ ($1/T_{crit}$). This can be derived from the fact that at high heating rates, the mass fraction combusted

in the first stage decreases as well in favor of the mass fraction being combusted in the second stage.

Comparing these results with other researchers' findings, such as Di Blasi et al [2], all obtained at 10 K/min (see figure 6), it can be concluded that cashew nut shells char exhibits values that are onset temperatures that are comparable to those of char from olive husks, grape residues, wheat straw and pine wood. However, the offset and maximum rate temperatures are lower in CNS char than in the biomass chars studied by Di Blasi et al [2]. In general, CNS char is much reactive than any of the chars presented by these researchers. It is important to note that in Di Blasi et al [2] study, autocatalysis effect is neither discussed nor determined. Therefore, this comparison is just indicative.

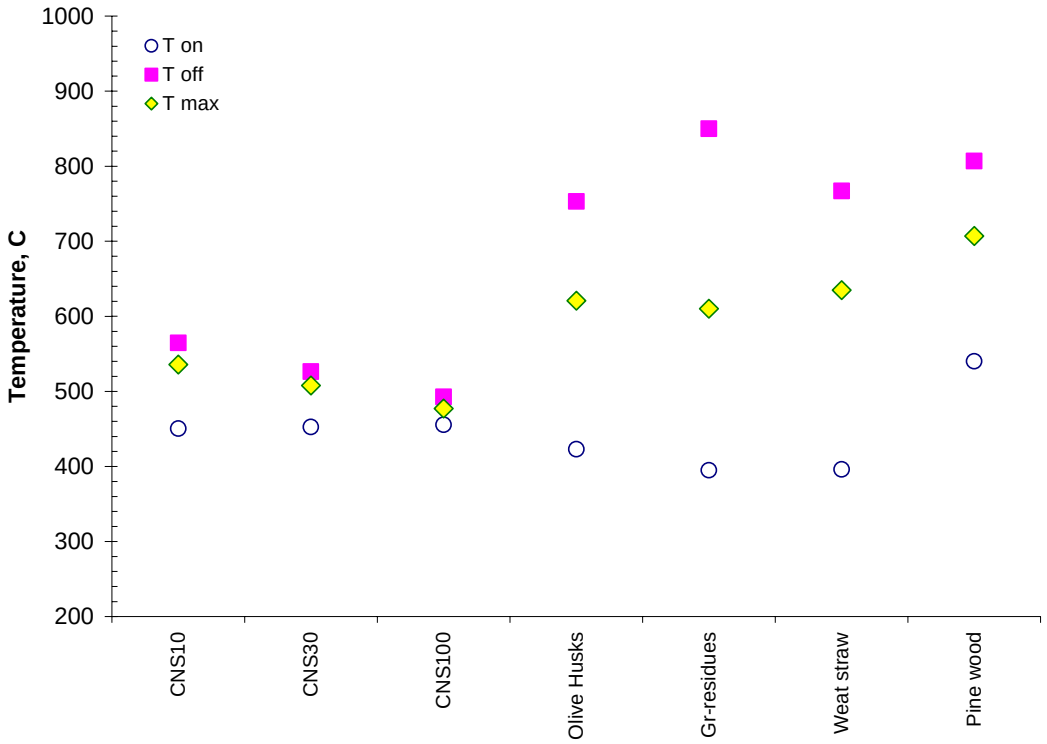


**Figure 6. Comparing reactivity (through $T_{on}$, $T_{off}$ and $T_{max}$) of CNS char and other biomass chars from literature**

***Char combustion kinetics***

The kinetic model adopted for this study is suggested by Di Blasi et al [2], as follows:

$$\frac{dY_s}{dt} = k\, P_{O2}^{n}\, Y_s^{m} \qquad (1)$$

$$k = A\exp\left(-E/RT\right) \qquad (2)$$

Where:

- $M_0$, is the initial mass sample;
- $M_a$, is the ash mass;
- k, is the Arrhenius constant;
- $P_{O2}$, is the oxygen partial pressure;
- $Y_s$, is the char mass fraction defined as $Y_s=(M_t-M_a)/(M_0-M_a)$;
- $M_t$, is the actual mass sample;
- E, is activation energy;
- R, ideal gas constant;
- T, absolute temperature;
- m, reaction power law.

As the oxygen pressure is constant, $P_{O2}$ is constant as well. Thus, the most important variables to be determined are E, A and m. According to Di Blasi et al[2] terminology, assuming m=1 leads to model N1 (only A and E are to be determined); model N2 stands for the case in which the three parameters are unknown.

Using NETZSCH advanced software for the determination of kinetics, the following results were obtained:

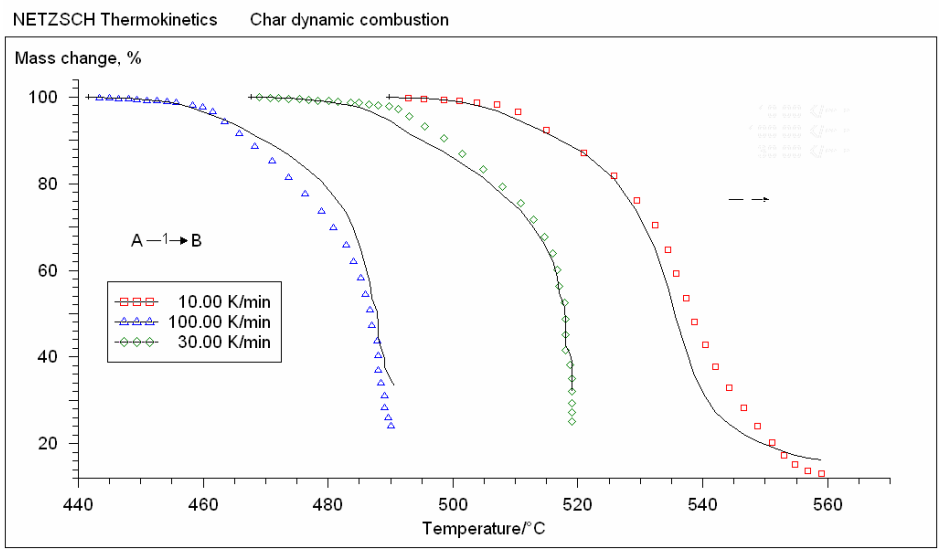


**Figure 7. Mass change during char combustion (1st stage/peak): experimental (dot line) and predicted (full line)**

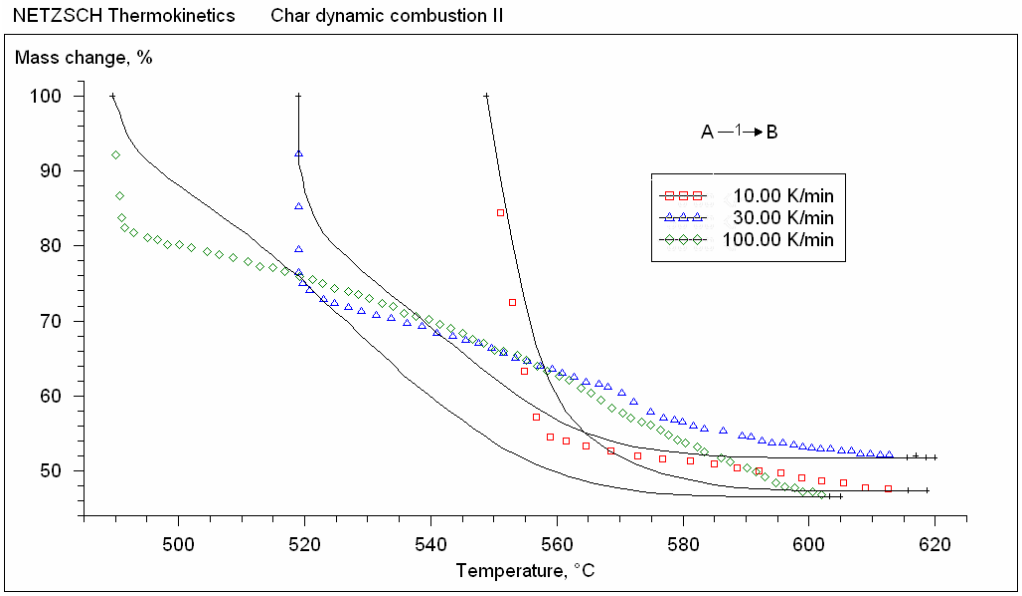


**Figure 8. Mass change during char combustion (2nd stage/peak): experimental (dot line) and predicted (continuous line) thermograms**

To run the NETZSCH advanced model, one has to assume, among other factors, the reaction model (mechanism) and define whether it is a single or multi-step reaction, with or without autocatalysis, diffusion mechanism, phase boundary diffusion mechanism involved or not and which regression to be taken (Gaussian, Frazier-Suzuki), among other characteristics, and the kind of experimental data to be used.

For these two stage reactions, the assumption was that any of them would follow an $n^{th}$ order with autocatalysis and phase-boundary diffusion involved.

Prediction by the model shows very good agreement for the first interval (fig. 5) and a fair agreement for the second interval (fig 6).

The results obtained from this experiment (1 and 2) are presented in Table 2 and figure 9 together with other biomass studied by Di Blasi [2].

**Table 2. CNS char combustion kinetics and results from other biomasses [2]**

| Sample | log A, 1/s | E act, kJ/mol | Log $k_{cat}$ | n | Obs. |
|---|---|---|---|---|---|
| CNS pk1 | 6.7901 | 135.138 | 0.3265 | 1.0000 | First peak |
| CNS pk2 | 5.4043 | 121.199 | 1.3785 | 1.8194 | Second peak |
| O-husks N1 | 5.0334 | 83.20 | | 1.000 | Model N1 |
| O-husks N2 | 5.0864 | 83.53 | | 1.103 | Model N2 |
| W-straw N1 | 4.1004 | 71.18 | | 1.000 | Model N1 |
| W-straw N2 | 4.2201 | 71.22 | | 1.478 | Model N2 |
| G-residues N1 | 4.0000 | 71.42 | | 1.000 | Model N1 |
| G-residues N2 | 4.8089 | 78.00 | | 2.000 | Model N2 |
| Pine wood N1 | 5.4871 | 100.40 | | 1.000 | Model N1 |
| Pine wood N2 | 6.1790 | 108.74 | | 1.229 | Model N2 |

Table 3 and figure 9 compare the results from Di Blasi et al [2] with the present study's results.

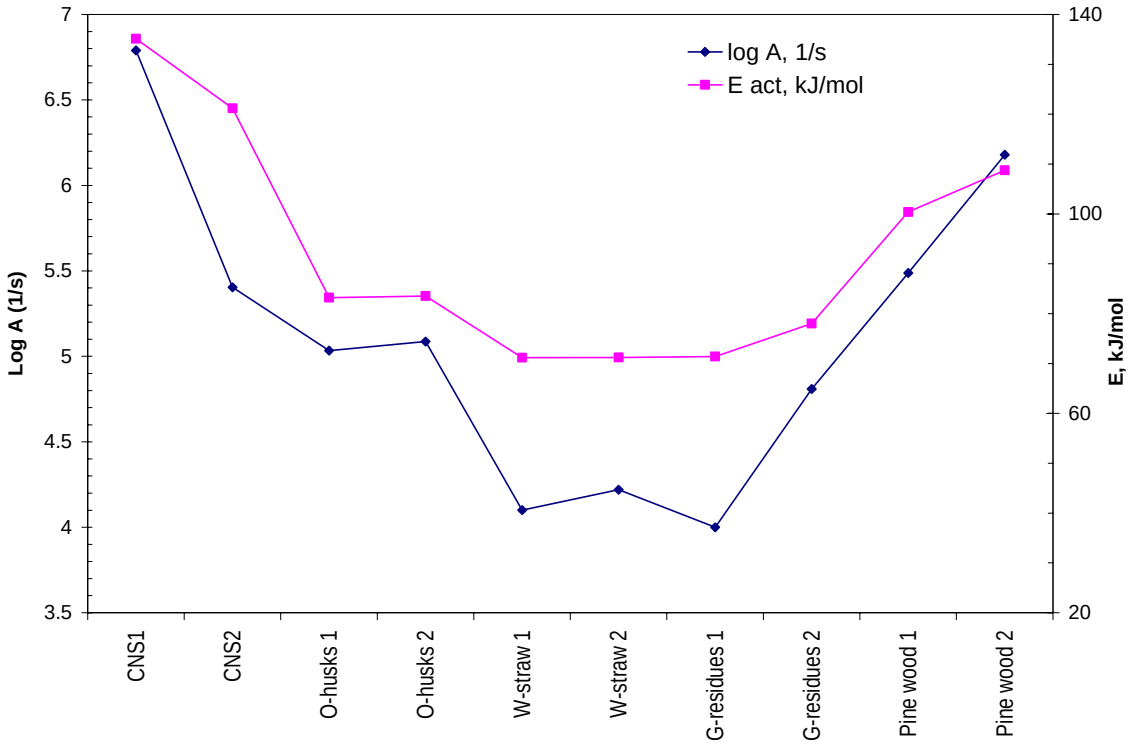


**Figure 9. Activation energies and frequency factors of different biomasses**

From this comparison, cashew nut char seems to be comparable to pinewood, despite the fact that Di Blasi et al[2] used a different methodology to assess the reactivity of the other biomass samples. The other biomasses exhibit lower values for both constants (E, A).

## CONCLUSIONS

Cashew nut char reactivity was determined using a very simple approach that relates reactivity to $1/T_{crit}$ to analyze data generated through combustion by a TG. By comparing the results with other biomass char reactivities it was found that CNS char is more reactive than olive husks, grape residues and pine wood chars. However, as expected, char reactivity is greatly influenced by the heating rate of the preceding pyrolysis process: the reactivity increases with the heating rate increase.

Char combustion kinetics were determined by using the NETZSCH advanced software which allows the pre-selection of key features of the reaction and gives the reaction order (m), the activation energy (E) and the frequency factor (A).

These data are of utmost importance in energy conversion technology design for tropical biomass wastes that are so far not well studied.

## REFERENCES

1. Kulaots, I; Hsu, A and Suuberg, EM; The role of porosity in char combustion; Proceedings of the Combustion Institute, 31 (2007) 1897-1903
2. Di Blasi, C; Buonanno, F and Branca, C; Reactivities of some biomass chars in air; Carbon 37(1999) 1227-38
3. Hurt, R and Calo, JM; Semi-global intrinsic kinetics for char combustion;Combustion and Flame, 125 (2001) 1138-49
4. Dennis, JS; Lambert, RJ; Milne, AJ; Scott, SA and Hayhurst, AN; The kinetics of chars derived from sludge; Fuel 84 (2005) 117-26
5. Henrich, E; Bürkle, S; Meza-Renken, ZI and Rumpel, S; Combustion and gasification kinetics of pyrolysis chars from waste and biomass; J. Analytical and Applied Pyrolysis, 49 (1999) 221-41
6. Wójtowicz, M; Bassilakis, R and Serio, MA; Char-oxidation reactivity at early and late stages of burn off; Proc. of 24th Biennal Conf. on Carbon; South Carolina, July 11-16, 1999; vol.I, pp 230-231.